

Experimental investigation and numerical modelling of biomechanical variation of
decomposed root: an application of vegetated slope stability



A Dissertation Submitted in Partial Fulfillment of the Requirements
for the Degree of Doctor of Philosophy in Civil Engineering

Department of Civil Engineering

FACULTY OF ENGINEERING

Chulalongkorn University

Academic Year 2021

Copyright of Chulalongkorn University

การทดสอบและแบบจำลองเชิงตัวเลขของการเปลี่ยนแปลงชีวกลศาสตร์ของรากที่ย่อยสลาย : การ
ประยุกต์กับงานเสถียรภาพของลาดดินที่ปกคลุมด้วยพืช



วิทยานิพนธ์นี้เป็นส่วนหนึ่งของการศึกษาตามหลักสูตรปริญญาวิศวกรรมศาสตรดุษฎีบัณฑิต
สาขาวิชาวิศวกรรมโยธา ภาควิชาวิศวกรรมโยธา
คณะวิศวกรรมศาสตร์ จุฬาลงกรณ์มหาวิทยาลัย
ปีการศึกษา 2564
ลิขสิทธิ์ของจุฬาลงกรณ์มหาวิทยาลัย

Thesis Title Experimental investigation and numerical modelling of
biomechanical variation of decomposed root: an
application of vegetated slope stability
By Mr. Trung Nghia Phan
Field of Study Civil Engineering
Thesis Advisor Professor SUCHED LIKITLERSUANG, D.Phil.

Accepted by the FACULTY OF ENGINEERING, Chulalongkorn University in
Partial Fulfillment of the Requirement for the Doctor of Philosophy

..... Dean of the FACULTY OF
ENGINEERING
(Professor SUPOT TEACHAVORASINSKUN, D.Eng.)

DISSERTATION COMMITTEE

..... Chairman
(Associate Professor Viroon Kamchoom, Ph.D.)
..... Thesis Advisor
(Professor SUCHED LIKITLERSUANG, D.Phil.)

..... Examiner
(Professor Boonchai Ukritchon, Sc.D.)

..... Examiner
(VEERAYUT KOMOVILAS, Ph.D.)

..... Examiner
(Associate Professor TIRAWAT BOONYATEE, D.Eng.)

..... External Examiner
(Associate Professor Anthony Kwan Leung, Ph.D.)

..... External Examiner
(Associate Professor Viroon Kamchoom, Ph.D.)

ตรัง เหงีย พาน : การทดสอบและแบบจำลองเชิงตัวเลขของการเปลี่ยนแปลงชีวกล
 ศาสตร์ของรากที่ย่อยสลาย : การประยุกต์กับงานเสถียรภาพของลาดดินที่ปกคลุมด้วย
 พืช. (Experimental investigation and numerical modelling of
 biomechanical variation of decomposed root: an application of vegetated
 slope stability) อ.ที่ปรึกษาหลัก : สุเชษฐ์ ลิขิตเลอสรวง

การเสริมกำลังของรากพืชในงานชีววิศวกรรมดินได้รับความสนใจเพิ่มขึ้น เนื่องจากเป็น
 วิธีการเพิ่มเสถียรภาพลาดดินที่ยั่งยืนและเป็นมิตรต่อสิ่งแวดล้อม นอกจากนี้ การหาค่าการ
 เปลี่ยนแปลงสมบัติชีวกลศาสตร์และการเสริมกำลังเชิงกลของรากต่อการย่อยสลายของรากยังเป็น
 สิ่งสำคัญในแง่การใช้งานในพื้นที่เกษตรกรรมที่ส่งผลต่อเสถียรภาพของลาดดิน อย่างไรก็ตาม การ
 เปลี่ยนแปลงสมบัติดังกล่าวในรากพืชตระกูลหญ้าโดยเฉพาะอย่างยิ่งที่ถูกทำให้ย่อยสลายด้วย
 สารเคมียังไม่ค่อยมีการศึกษามาก่อน การศึกษานี้มีวัตถุประสงค์ที่จะตรวจวัดสัญญาณ สมบัติชีว
 วิศวกรรม และค่าการเสริมกำลังในดิน ของรากหญ้าแฝกสองชนิดคือ หญ้าแฝกกลุ่ม และหญ้าแฝก
 ดอน นอกจากนี้ ยังศึกษาผลของการใช้สารเคมีที่ทำให้รากหญ้าเกิดการย่อยสลายต่อสมบัติชีว
 วิศวกรรมและการเสริมกำลังในดินด้วย ดำเนินการศึกษาด้วยชุดการทดสอบที่ประกอบไปด้วย การ
 สังเกตรากด้วยระบบโปรไซบลิค การทดสอบแรงดึงในแนวแกน และการทดสอบแรงเฉือน สารเคมี
 โพพานิลถูกนำมาใช้เพื่อกำหนดการย่อยสลายของรากหญ้าตามจำนวนวันคือ 7 28 56 และ 112
 วัน ประเมินค่าการเสริมกำลังของรากด้วยแบบจำลองของวงและแบบจำลองกลุ่มราก โดยค่าการ
 เสริมกำลังที่ได้จากแบบจำลองถูกนำไปใช้เป็นค่าพารามิเตอร์สำหรับการวิเคราะห์เสถียรภาพของ
 ลาดดินที่ปกคลุมด้วยพืช ผลการศึกษาพบว่าหญ้าแฝกดอนสามารถนำมาใช้เสริมกำลังในวิธีชีว
 วิศวกรรมดินได้เทียบเคียงกับการใช้หญ้าแฝกกลุ่ม การย่อยสลายของรากส่งผลต่อสมบัติชีววิศวกรรม
 ของรากหญ้า ได้แก่ กำลังรับแรงดึง ซีแคนท์โมดูลัส และความเครียดที่จุดขาด ตลอดจนค่าการ
 เสริมกำลังของราก ได้แก่ แรงเชื่อมประสานราก และค่าไคเลชัน ดังนั้นการย่อยสลายของรากย่อม
 ส่งผลต่อการเสื่อมประสิทธิภาพของการเสริมแรงของรากบนลาดดินที่ปกคลุมด้วยพืช

สาขาวิชา วิศวกรรมโยธา

ลายมือชื่อนิสิต

ปีการศึกษา 2564

ลายมือชื่อ อ.ที่ปรึกษาหลัก

6278303521 : MAJOR CIVIL ENGINEERING

KEYWORD: Root decomposition, vetiver grass, root biomechanical properties, root reinforcement, root orientation

Trung Nghia Phan : Experimental investigation and numerical modelling of biomechanical variation of decomposed root: an application of vegetated slope stability. Advisor: Prof. SUCHED LIKITLERSUANG, D.Phil.

Plant root reinforcement in soil bioengineering has gained increasing interest as a means of sustainable and environmentally friendly soil reinforcement and stabilization. In addition, quantifying evolutions of the biomechanical properties and mechanical root reinforcement to soil with the duration of root decomposition is important to agricultural land-use strategy and to soil stabilization purpose. However, the variations of these properties of the roots of herbaceous species, especially following herbicide application, have rarely been studied. This study aims to comprehensively measure the root morphological traits, root biomechanical properties, and root reinforcement of two contrasting vetiver species (*Chrysopogon nemoralis* and *Chrysopogon zizanioides*). In addition, the effects of root decomposition due to herbicide on the root biomechanical properties and root reinforcement of these two vetiver roots were investigated. A series of experiments, including root observation with a rhizobox system, uniaxial tensile test, and direct shear test, was performed. The herbicide (i.e., Propanil) was applied to four treatments of each species, considering four different durations of decomposition (7-, 28-, 56- and 112-days since herbicide application). In addition, the variation of root reinforcement was estimated using the existing root reinforcement models (i.e., Wu's model and the extended root bundle model). The estimated root reinforcement then was used as an input parameter in numerical modelling to evaluate the effect of root decomposition on vegetated slope stability. The results showed that *C. nemoralis* could be an alternative to *C. zizanioides* in soil bioengineering applications. In addition, root decomposition highlighted the significant influence on root biomechanical properties (i.e., tensile strength, secant modulus, and breakage strain) and root reinforcement (i.e., root cohesion and maximum dilatancy) of two vetiver species. Consequently, root decomposition resulted in the deterioration of the protective function of two vetiver species on vegetated slope stability.

Field of Study: Civil Engineering

Student's Signature

Academic Year: 2021

Advisor's Signature

ACKNOWLEDGEMENTS

First of all, I would like to express my gratitude to my supervisor, Prof. Suched Likitlersuang, who give me enthusiastic guidance, extraordinary support and effectual encouragement to keep me on the pathway towards the completion of my degree in Doctor of Philosophy.

Sincere appreciation extended to Asst. Prof. Viroon Kamchoon, Assoc. Prof. Anthony Kwan Leung, Prof. Boonchai Ukritchon, Assoc. Prof. Tirawat Boonyatee, and Dr. Veerayut Komovilas for their constructive critiques, serving and sharing time on my dissertation defence committee.

I also acknowledge the financial support from the Second Century Fund (C2F), Chulalongkorn University during my study in the Ph.D program at Chulalongkorn University.

Thanks to everyone who has directly or indirectly helped me over the three years. I also would like to express my sincere gratitude to all my Vietnamese friends for their help, warm friendship and encouragement. Especially, I would like to thanks Dr. Nguyen Thanh Son for his kind helping in my PhD research.

Finally, I would like to take this opportunity to express my deepest gratitude to my parents, and my sister for their love, support and continued encouragement.

จุฬาลงกรณ์มหาวิทยาลัย
CHULALONGKORN UNIVERSITY

Trung Nghia Phan

TABLE OF CONTENTS

	Page
.....	iii
ABSTRACT (THAI).....	iii
.....	iv
ABSTRACT (ENGLISH).....	iv
ACKNOWLEDGEMENTS.....	v
TABLE OF CONTENTS.....	vi
List of Tables.....	ix
List of Figures.....	xi
Chapter 1: Introduction.....	1
1. 1. Research background.....	1
1. 2. Objectives and scope of research.....	3
1.2.1. Research objectives.....	3
1.2.2. Scope of research.....	3
1. 3. Dissertation layout.....	4
Chapter 2: Literature review.....	6
2.1. Introduction.....	6
2.2. Introduction of vetiver species.....	6
2.3. Root morphological traits.....	7
2.4. Root biomechanical properties.....	9
2.5. Root mechanical reinforcement.....	10
2.6. Root decomposition.....	12

Chapter 3:	Laboratory testing program.....	15
3.1.	Introduction	15
3.2.	Test species and growth media.....	15
3.3.	Plantation procedures and plant treatment.....	17
3.1.	Plant preparation.....	17
3.2.	Plant growth condition.....	18
3.3.	Plant decomposition condition.....	20
3.4.	Measurement of root morphology	21
3.5.	Measurement of root biomechanical properties	23
3.6.	Measurement of root reinforcement.....	25
3.7.	Data analysis	26
3.8.	Test plan and schedule.....	27
Chapter 4:	Root biomechanical properties, mechanical reinforcement and morphological traits of <i>C. nemoralis</i> and <i>C. zizanioides</i> species.....	29
4.1.	Introduction	29
4.2.	Observed root morphological traits.....	29
4.3.	Biomechanical properties of <i>C. nemoralis</i> and <i>C. zizanioides</i> fresh roots	33
4.4.	The correlations between root diameter and root biomechanical properties .	37
4.5.	Root mechanical reinforcement – the contribution of roots to soil strength...	40
4.6.	Concluding remarks.....	46
Chapter 5:	The influence of root decomposition on root biomechanical properties and mechanical reinforcement.....	47
5.1.	Introduction	47
5.2.	Biomechanical properties of decomposing roots of <i>C. nemoralis</i> and <i>C. zizanioides</i> species.....	47

5.3. The influence of root decomposition on diameter-strength and diameter-modulus correlations of <i>C. nemoralis</i> and <i>C. zizanioides</i> species.....	51
5.4. Deterioration of mechanical reinforcement of decomposing roots of <i>C. nemoralis</i> and <i>C. zizanioides</i> species.....	55
5.5. Concluding remarks.....	65
Chapter 6: Root reinforcement estimation and stability analysis of slope reinforced by decomposing roots.....	67
6.1. Introduction.....	67
6.2. Root reinforcement estimation.....	67
6.2.1. Root reinforcement estimation procedure.....	67
6.2.2. Calibration of root parameters, Weibull survival function and root diameter distribution.....	70
6.2.3. Estimated reinforcement of decomposing roots.....	77
6.3. Numerical analysis to estimate the influence of root decomposition on vegetated slope stability.....	82
6.3.1. Theoretical framework.....	82
a. Unsaturated-saturated seepage analysis.....	82
b. Vegetated slope stability analysis.....	83
6.3.2. Geometry, boundary conditions and soil properties.....	84
6.3.3. Transient seepage analysis result.....	85
6.3.4. Influence of root decomposition on vegetated slope stability.....	86
6.4. Conclusive remarks.....	89
Chapter 7: Conclusion and recommendation.....	91
7.1. Conclusion.....	91
7.2. Recommendation.....	92

REFERENCES	94
APPENDIX.....	107
VITA.....	110



List of Tables

Table 2. 1. Summary of tensile strength of <i>C. zizanioides</i> species from the literature	10
Table 2. 2. Typical mechanical reinforcement of <i>C. zizanioides</i> roots	11
Table 3. 1. Physical and chemical properties of lateritic soil and rice husk ash.	16
Table 4. 1. Summary of orientation (Ω), diameter (d), $RAR_{5\%}$, and water content (w ; mean \pm standard error of the mean [SE]) of <i>C. nemoralis</i> and <i>C. zizanioides</i> species.	30
Table 4. 2. Summary of tensile strength (T_r), initial modulus (E_i), secant modulus (E_s) and breakage strain (ϵ_r ; mean \pm standard error of the mean [SE]) of <i>C. nemoralis</i> and <i>C. zizanioides</i> species.	36
Table 4. 3. Summary of the root volume ratio (RVR), root biomass per soil volume (ρ_r), and root number of the direct shear specimens.	42
Table 5. 1. Summary of tensile strength (T_r), initial modulus (E_i), secant modulus (E_r), and breakage strain (ϵ_r) (mean \pm standard error of mean (SEM)) of the <i>C. nemoralis</i> and <i>C. zizanioides</i> .	48
Table 5. 2. Summary of the fitting parameters (a and α), R^2 value and p-value of the power correlation ($T_r = a \cdot d_f^\alpha$) between tensile strength (T_r) and root diameter (d_f) of the <i>C. nemoralis</i> and <i>C. zizanioides</i> .	54
Table 5. 3. Summary of the fitting parameters (b and β), R^2 value and p-value of the power correlation ($E_s = b \cdot d_f^\beta$) between secant modulus (E_s) and root diameter (d_f) of the <i>C. nemoralis</i> and the <i>C. zizanioides</i> .	55
Table 5. 4. Summary of the results of the direct shear test for the fallow soil and soils reinforced by the <i>C. nemoralis</i> and the <i>C. zizanioides</i> .	61
Table 6. 1 Summary of scale (T_0 and E_0) and shape (α) factors of T_r - d , and E_s - d of <i>C. nemoralis</i> and <i>C. zizanioides</i> species.	72
Table 6. 2 Summary of shape (ω) and scale (λ) factors of Weibull survival function for <i>C. nemoralis</i> and <i>C. zizanioides</i> roots.	77

Table 6. 3. Simulated maximum displacement and maximum root reinforcement (mean and standard error (SE)) of <i>C. nemoralis</i> and <i>C. zizanioides</i> treatments using RBMw and Wu's model.....	80
Table 6. 4. Summary key properties of residual soil	84



List of Figures

Fig 3. 1. Bare root slips of (a) <i>C. nemoralis</i> and (b) <i>C. zizanioides</i> species	17
Fig 3. 2. Rhizobox component	19
Fig 3. 3. Vetiver grown in rhizobox system	19
Fig 3. 4. Typical container for tensile test	20
Fig 3. 5. Typical PVC column use for direct shear test	20
Fig 3. 6. Propanil (N-(3,4-Dichlorophenyl) propenamide)	21
Fig 3. 7. Digital camera system	22
Fig 3. 8. Flow chart of root image processing in ImageJ program	22
Fig 3. 9. L1 Force Measurement machine	23
Fig 3. 10. Digital camera system	23
Fig 3. 11. Root diameter measurement	24
Fig 3. 12. Trimmed specimen for direct shear test	26
Fig 3. 13. Direct shear machine	26
Fig 3. 14. Summary of test plant and schedule	28
Fig 4. 1. Time variations in the root growth rate (cm d^{-1}) <i>C. nemoralis</i> (blue line) and <i>C. zizanioides</i> species (red line) during the 11 weeks of planting. 32	32
Fig 4. 2. Depth variations in the morphological properties of <i>C. nemoralis</i> (blue line) and <i>C. zizanioides</i> species (red line). (a) Root area ratio “side” (RAR_s ; %), (b) root diameter (mm), and (c) root orientation ($^\circ$).....	33
Fig 4. 3. Boxplot of (a) tensile strength, (b) secant modulus and (c) initial modulus of <i>C. nemoralis</i> and <i>C. zizanioides</i> species	35
Fig 4. 4. Correlations between diameter and (a) tensile strength, (b) secant modulus and (c) initial modulus of <i>C. nemoralis</i> and <i>C. zizanioides</i> species	38
Fig 4. 5. Shear behaviour from direct shear tests on fallow soil (dash-dotted line) and soil reinforced with <i>C. nemoralis</i> (solid line) and <i>C. zizanioides</i> (dotted line) species	

under three normal stress levels: 11.3 kPa (Blue), 21.1 kPa (Red), and 40.8 kPa (Black).	43
Fig 4. 6. Root diameter distribution of (a) <i>C. nemoralis</i> and (b) <i>C. zizanioides</i> species presented in shearing specimens.....	44
Fig 4. 7. Derived Mohr–Coulomb failure envelope for the fallow soil (dark dash-dotted line) and the soils reinforced by <i>C. nemoralis</i> (blue solid line) and <i>C. zizanioides</i> (red solid line) species. The number indicates the root biomass per soil volume in the tested sample (ρ_r ; kg/m ³).	45
Fig 4. 8. Vertical displacement-horizontal displacement curves of fallow soil (dash-dotted line) and soil reinforced with <i>C. nemoralis</i> (solid line) and <i>C. zizanioides</i> (dotted line) species under three normal stress levels: 11.3 kPa (Blue), 21.1 kPa (Red), and 40.8 kPa (Black).	45
Fig 5. 1. The remained percentage of tensile strength, secant modulus, breakage strain, root diameter, unit root biomass per soil volume and root reinforcement of the (a) <i>C. nemoralis</i> and (b) <i>C. zizanioides</i> species with elapsed time since herbicide application. 49	
Fig 5. 2. The correlations between tensile strength (T_f) – diameter (d_f) of (a) <i>C. nemoralis</i> and (b) <i>C. zizanioides</i> subjected to different durations of root decomposition. The equation and R^2 of each fitting are summarised in Table 5. 2. ..	52
Fig 5. 3. The correlations between secant modulus (E_s) – diameter (d_f) of (a) <i>C. nemoralis</i> and (b) <i>C. zizanioides</i> subjected to different durations of root decomposition. The equation and R^2 of each fitting are summarised in Table 5. 3. ..	53
Fig 5. 4. Shear stress-displacement curves of fallow soil and soil reinforced by roots of <i>C. nemoralis</i> and <i>C. zizanioides</i> subjected to different durations of root decomposition under confining stress of (a) and (d) 11.3 kPa, (b) and (e) 21.1 kPa, (c) and (f) 40.8 kPa.	56
Fig 5. 5. Derived Mohr-Coulomb failure envelopes for the fallow soil and the soils reinforced by the roots of (a) <i>C. nemoralis</i> and (b) <i>C. zizanioides</i>	57

Fig 5. 6. Correlations between root cohesion and (a) root tensile strength, (b) secant modulus, (c) unit root biomass per soil volume of <i>C. nemoralis</i> and <i>C. zizanioides</i> species.	58
Fig 5. 7. Vertical displacement-horizontal displacement curves of fallow soil and soil reinforced by roots of <i>C. nemoralis</i> and <i>C. zizanioides</i> subjected to different durations of root decomposition under confining stress of (a) and (d) 11.3 kPa, (b) and (e) 21.1 kPa, (c) and (f) 40.8 kPa.	59
Fig 5. 8. Variation of root reinforcement during the decomposition	62
Fig 5. 9. Variation of maximum dilatancy of fallow soil and soil reinforced by <i>C. nemoralis</i> and <i>C. zizanioides</i> species subjected to different durations of root decomposition under confining stress of (a) and (d) 11.3 kPa, (b) and (e) 21.1 kPa, (c) and (f) 40.8 kPa	63
Fig 6. 1. Root reinforcement estimation workflow	69
Fig A. 1. The RGB and grey scale image of root system of (a) <i>C. nemoralis</i> and (b) <i>C. zizanioides</i> species	107
Fig A. 2. Failure surface after 24 hours of rainfall (the worst case) of slope reinforced by decomposed root of <i>C. nemoralis</i> species after (a) 7 days, (b) 28 days, (c) 56 days and (d) 112 days since herbicide application	108
Fig A. 3. Failure surface after 24 hours of rainfall (the worst case) of slope reinforced by decomposed root of <i>C. zizanioides</i> species after (a) 7 days, (b) 28 days, (c) 56 days and (d) 112 days since herbicide application	109

Chapter 1: Introduction

1. 1. Research background

Land-use conversion and deforestation in mountainous areas are becoming a part of the global trend, which is considered as the consequence of the growth of population and economy. In addition, agricultural land expansion is considered as one of the measures to archive the food security, which is the second Sustainable Development Goals (i.e., SDGs, proposed by United Nations). In the Southeast Asian countries, the agricultural land area increased 1,970,670 ha between 2010 and 2019 (FAO, 2021). The land-use conversion could be the cause of root decomposition, which influences the protective function of roots to slope stability. Consequently, the probability of landslide risk, slope instability, and soil erosion increase with time since root dying (Ammann et al., 2009; Bishop and Stevens, 1964; Johnson and Wilcock, 2002; Sidle et al., 2005).

The climate change phenomenon, such as intensive rainfall, has been considered a significant cause of landslides and soil erosion over the globe in the last decades. These natural disasters can cause severe damage to infrastructures and human life. In Thailand, a large slope failure event occurs every 3 to 5 years due to the intense rainfall, and the frequency of this serious problem has increased (Fowze et al., 2012; Soralump, 2010). In 2001, for instance, there were two significant landslide events occurred in Phare province, causing 40 deaths and in Phetchabun province (Komori et al., 2018). Another large event of landslide occurred in northern Thailand in 2006, destroying about 4,000 houses and more than 10,000 people had evacuated (Boonyanuphap, 2013). Thus, the combination of land conversion (i.e., human activity) and heavy rainfall (i.e., natural phenomenon) could induce natural disasters (i.e., landslides, flooding, soil erosion, etc.) more extreme. Indeed, Bishop and Stevens (1964) reported that landslides increased 4.5 times within ten years after logging in Southeast Alaska. While Johnson and Wilcock (2002) observed that landslides occurred about four times more often after large-scale dying off of yellow cedars (*Chamaecyparis nootkatensis* [D.Don] Spach).

Such weed clearance techniques in agricultural practices (i.e., cutting, burning, herbicide application, etc.) and deforestation (i.e., timber harvesting) are mostly used to convert forest and natural ecosystems to agricultural land (Clements et al., 1996; Kamchoom et al., 2021; Parish, 1990). However, due to the drawback of cutting (i.e., labour shortage) and burning (i.e., haze and smog from burning), herbicides have been widely used in Southeast Asian countries such as Thailand (Sapbamrer, 2018). Because of the wide use of herbicides for weed removal, some environmental problems and human health issues have arisen. For example, herbicides remain and contaminate soil, water, and air then damage surrounding ecosystems and human (Morin et al., 2021; Wongwichit et al., 2012). Moreover, plant death and the accompanying root decomposition caused by the herbicides would lead to the deterioration of the root biomechanical properties such as tensile strength that has implication to soil erosion and stability (Kamchoom et al., 2021). Indeed, plant has been used as a soil bioengineering means for effective and environmentally-friendly technique to prevent and mitigate soil erosion, shallow landslides (Grima et al., 2020; Kamchoom and Leung, 2018; Leknoi and Likitlersuang, 2020; Leung and Ng, 2013; Likitlersuang et al., 2017; Liu et al., 2019; Liu et al., 2014; Nguyen et al., 2020; Rey et al., 2019; Stokes et al., 2009; Zaïmes et al., 2019). Plant roots permeate the matrix of shallow soil and improve the soil stability through, broadly speaking, mechanical and hydrological reinforcements. The former refers to root 'entanglement' or reinforcement to the soil through the increase in cohesion (i.e. root cohesion) (Bordoni et al., 2019; Eab et al., 2015; Phan et al., 2021) and sometimes peak friction angle (e.g. Karimzadeh et al. (2021)), primarily depending on the root biomechanical properties (i.e., tensile strength, secant modulus) root quantity (i.e., root number, root biomass) (Pollen and Simon, 2005; Wu et al., 1979) as well as the relative orientation of the root distribution with respect to the direction of major principal stresses (Kamchoom et al., 2014; Karimzadeh et al., 2022; Karimzadeh et al., 2021). Investigation of the decline of root biomechanical properties, root quantity and root reinforcement due to different means of introducing root decomposition has been studied since the 1960s (Kitamura, 1968; O'loughlin and Watson, 1979; Ziemer, 1981). Despite of a large volume of studies available in the literature, data on the

deterioration of root biomechanical properties and root reinforcement to soil are scarce, especially for herbaceous species which share rather different root anatomy and growth mechanism from woody species that has been majorly focused in the literature. Thus, this study aimed to quantify the influence of root decomposition on the biomechanical properties of two contrasting vetiver species, including *Chrysopogon nemoralis* and *Chrysopogon zizanioides*, following herbicide application, and the changes of their ability to provide mechanical reinforcement to the soil. *C. zizanioides* can rapidly adapt to various adverse growth conditions and is mainly found in lowland and land areas with typically high water content (Wasino et al., 2019). Thus, it has been widely used for slope stabilization in soil bioengineering approaches, especially in Southeast Asian countries (Truong et al., 2008). By contrast, *C. nemoralis* is mainly distributed in mountainous areas (highland) and well-drained soils in Southeast Asian countries (Truong et al., 2008).

1. 2. Objectives and scope of research

1.2.1. Research objectives

The principal objectives of this study were:

- 1) To investigate the morphological traits, biomechanical properties, mechanical reinforcement of growing roots.
- 2) To investigate the influence of root decomposition on root biomechanical properties and mechanical reinforcement.
- 3) To estimate the root reinforcement from root biomechanical reinforcement using existing root reinforcement models.
- 4) To conduct the numerical modelling for investigating the effect of root decomposition on vegetated slope stability.

1.2.2. Scope of research

To clarify these aforementioned objectives, a series of laboratory experiments and numerical modelling were carried out. In the laboratory, a series of semi-controlled experiments was performed to investigate the morphological traits, biomechanical properties and mechanical reinforcement of two contrasting vetiver species. In

addition, the variation of root biomechanical properties and mechanical reinforcement over the root decomposition due to herbicide application was investigated in the laboratory. Besides that, existing root reinforcement models were adopted to estimate the root reinforcement from root biomechanical properties. In the numerical modelling, the influence of root decomposition followed by herbicide application on vegetated slope stability was investigated.

1. 3. Dissertation layout

This dissertation was presented in seven chapters and divided into three main parts namely, Part 1: Laboratory investigation of root morphological traits, biomechanical properties and mechanical properties of growing vetiver species; Part 2: Laboratory investigation of root biomechanical properties and mechanical reinforcement of the two vetiver species; Part 3: Root reinforcement estimation and numerical modelling. This chapter presented the research background, the main objectives and scope of study. The Chapter 2 presents the introduction of vetiver species and utilisation of vetiver species in soil bioengineering. It also includes the morphological traits, biomechanical properties and mechanical reinforcement of two vetiver species obtained in the previous studies. In addition, several studies in the literature related to influences of root decomposition on root biomechanical properties and mechanical reinforcement were summarised and reviewed. The Chapter 3 describes the laboratory testing program. It mainly explains and describes the laboratory program. The vegetation species, growth media properties and growth condition are also reported in this chapter. The plantation schedule, working principle and procedure of each testing are presented. The morphological traits, mechanical reinforcement, and biomechanical properties of growing root of the two vetiver species are reported and discussed in the Chapter 4. The chapter 5 presents and discusses the influence of root decomposition due to herbicide application on root biomechanical properties and mechanical reinforcement. The chapter 6 describes detail the estimation root reinforcement using the existing root reinforcement models. The estimated and measured results are compared and discussed in this chapter. In addition, the influence of root decomposition on vegetated slope stability is estimated by the numerical modelling using simulated root reinforcement in this

chapter. Finally, the major conclusions, contributions, recommendations, and further work are summarised in the Chapter 7.



Chapter 2: Literature review

2.1. Introduction

This chapter reviews and summarises previous studies investigating the effects of root decomposition on root characteristics, including biomechanical properties and mechanical reinforcement. It begins with introducing the vetiver species, the main studied species in this study. It is followed by literature on investigating morphological traits, biomechanical properties, and root reinforcement. The previous works from both field and laboratory investigation are included in this chapter.

2.2. Introduction of vetiver species

Vetiver grass is a perennial grass and widely distributed in the tropical regions in Asia, Australia, Africa, and other regions (Truong et al., 2008). In the “Vetiver System”, there are two types of vetiver species, that are commonly used for soil bioengineering namely, *C. nemoralis* A. Camus and *C. zizanioides* L. Nash (Truong et al., 2008; Wasino et al., 2019). In general, both the vetiver species can grow in various soil textures but seem not good efficient in clay (Truong et al., 2008). Furthermore, these two species have high tolerance to adverse soil conditions such as acidity, alkalinity, salinity (i.e., able to adapt to a wide range of pH from 3.3 to 12.5), and extreme water stresses such as drought and waterlogged (Truong et al., 2008). Council (1993) reported that the vetiver roots can grow very fast (e.g., 1 cm/day for *C. nemoralis* roots (Eab et al., 2015) and 2.2 cm/day for *C. zizanioides* roots). These two vetiver species are commonly found in the mainland of Southeast Asian countries, which are susceptible to natural disasters, such as soil erosion, landslides, and flooding because heavy rainfall occurs frequently (Kristo et al., 2017). In addition, the *C. nemoralis* and *C. zizanioides* species show some major differences not only in their growth conditions but also in the length and distribution of roots. For instance, *C. zizanioides* species can rapidly adapt to various environmental conditions and widely spread in lowland and moist plain areas (Wasino et al., 2019). The roots of *C. zizanioides* species are considered longer than those of *C. nemoralis* species. The *C. zizanioides* roots can penetrate down to 2–4 m depth with a mean tensile strength of up to 75 MPa (Kavian et al., 2018; Truong et al., 2008). As such, *C. zizanioides*

species have been widely and successfully used for soil erosion control and slope stabilisation over the world (Truong et al., 2008). Indeed, using *C. zizanioides* species can successfully reduce soil loss and runoff up to 76% and 69%, respectively (Truong and Loch, 2004). Furthermore, soil shear strength (i.e., in term of cohesion) can be increased 97% after 180 days *C. zizanioides* species was planted in an expansive soil (Wang et al., 2020). In contrast, the *C. nemoralis* species were found in mountainous areas or arid, well-drained areas (Leungvutiviroj et al., 2010). Recently, this species has been utilised to stabilise dikes in rice fields by farmers in the Central Highland and some coastal provinces in Vietnam (Truong et al., 2008) and prevent runoff and soil loss in Thailand (Donjadee et al., 2010). While there were several studies demonstrated the ability of *C. zizanioides* species for soil stability by performing the intensive investigation for its biomechanical properties, morphological traits, and root reinforcement (Fahlen, 2002; Leknoi and Likitlersuang, 2020; Mickovski and Van Beek, 2009; Wu et al., 2021). These properties of the roots of *C. nemoralis* species have not been extensively studied. Therefore, the biomechanical properties and effects of soil reinforcement between these two species should be comprehensively investigated and compared. Furthermore, the potential of these two species (i.e., especially *C. nemoralis* species) in soil bioengineering can be explicitly evaluated.

2.3. Root morphological traits

Root morphological traits (i.e., root diameter, number of roots, and root orientation) are considered as the important factors that influence the root mechanical reinforcement. Indeed, the amount of roots presented in soil matrix, which represented by either root area ratio (RAR), “side” root area ratio (RAR_s), or root diameter distribution, were used as an important input factor in such root reinforcement model (e.g., Wu’s model (Wu et al., 1979) and Root Bundel Model (Schwarz et al., 2013)). By contrast, the effect of root orientation on the mechanical reinforcement of plant roots has been rarely explored. However, some previous studies revealed that the different orientations of roots may influence on their contribution to soil reinforcement (Gray and Ohashi, 1983; Thomas and Pollen-Bankhead, 2010). For instance, Gray and Ohashi (1983) found that the shear reinforcement of sand is the greatest when fibers are oriented at 60° with respect to

the shear direction rather than at 90° as assumed by [Wu et al. \(1979\)](#). In addition, [Gray and Ohashi \(1983\)](#) revealed that shear strength of sand decreases in the presence of fibers oriented at 120°. However, in most well-known root reinforcement models, root fibers are assumed to be either perpendicular to a shear plane ([Wu et al., 1979](#)) or parallel to the pull direction ([Cohen et al., 2011](#); [Schwarz et al., 2010](#)). In addition, root fibers are assumed oriented parallel to one another within a root bundle because of the lack of information and understanding of the individual root orientation; as such, root reinforcement may be overestimated or underestimated ([Cohen et al., 2011](#); [Pollen and Simon, 2005](#); [Schwarz et al., 2010](#)).

Several approaches, including non-destructive and destructive, have been applied in-situ, laboratory and greenhouse base to investigate root morphological traits. The most traditional method is field excavation, which has been used for a long time to extract the complete root system ([Böhm, 2012](#); [Fiorani and Schurr, 2013](#); [Pagès and Pellerin, 1994](#)). However, the disturbance of soil around the root system, heavy machines required, time consumption and breakage of root connections are the major disadvantage of this method ([Wu and Guo, 2014](#)). Over the past decade, researchers have developed alternative ways to handle the significant challenge in the root morphology investigation, which is the opacity of soil media. Several methods have been performed to image root morphology of individual plants grown both in soil and non-soil media. Digital cameras, flat-bed scanners, and laser scanners ([Ammann et al., 2009](#); [Fang et al., 2009](#)) have been applied to obtain the image of root morphology in non-soil media. On the other hand, to image the root morphology in soil media, X-ray micro-computed tomography (CT) ([Flavel et al., 2012](#)) and magnetic resonance imaging ([Rascher et al., 2011](#)) have been used. However, the high cost is seen as a disadvantage of these methods. Root system images obtained from these methods can be analysed using image processing or root programs such as EZ-RHIZO ([Armengaud et al., 2009](#)), RootReader ([Clark et al., 2011](#)), WinRHIZO ([Wu and Guo, 2014](#)), ImageJ ([Flavel et al., 2012](#)), and CRootBox ([Schnepf et al., 2018](#)) to quantify root morphological traits. In this study, the rhizoboxes system coupled with image processing using ImageJ software (i.e., an open-source software

for image analysing), was adopted to investigate the root morphological traits (root diameter, RAR_s , root orientation), their variation by depth and root growth rate.

2.4. Root biomechanical properties

The root biomechanical properties, including tensile strength, modulus and breakage strain, are considered the main factors that govern roots' contribution to soil shear strength (Simon and Collison, 2002; Wu et al., 1979; Wu et al., 2021). The root biomechanical properties can be obtained in either the laboratory or field. Although the root biomechanical properties have been investigated for a long time, no standard method or guideline is followed for performing a root tensile and pull-out test (Wu et al., 2021). In the most studies, roots were applied uniaxial tension until it breaks to record the peak stress at the failure (Wu et al., 2021). In this study, the root biomechanical properties of the two vetiver species were measured using uniaxial tensile test in the laboratory. The detail of the tensile test was described detail in the Chapter 3.

The root tensile strength is the most investigated and reported root biomechanical property. The tensile strength of roots are normally defined as the ratio of peak tensile force and either mean root area (De Baets et al., 2008; Wu et al., 2021) or area of root at failure point (Mickovski and Van Beek, 2009). However, the mean root area is not the reliable factor to determine root tensile strength of the species, which have root barks (Karrenberg et al., 2003). Thus, the cross-sectional area of roots at failure was used to define root tensile strength in this study. In addition, it is noteworthy that the root tensile strength significantly varies among species or even in the same species. Indeed, Coppin and Richards (1990) reported that the root tensile strength varied from 3.7 MPa (*Campanula trachelium* species) to 86.5 MPa (*Medicago sativa* species). In the same species, the root tensile strength of *C. zizanioides* species, for instance, varied from 1.8 MPa to 88.52 MPa (refers to Table 2.1). The variability in root tensile strength could be explained by the differences in root age, cellulose and lignin content, root water content (Wu et al., 2021). In general, root tensile strength correlated with root diameter following the negative power law trend (Bischetti et al., 2005; De Baets et al., 2008; Tosi, 2007). This means that fine roots are stronger than coarse roots. Thus, the roots of grass species, which

mainly consist of fine roots, could contribute more strength to soil than roots of woody species.

Table 2. 1. Summary of tensile strength of C. zizanioides species from the literature

Reference	Tensile strength (MPa)
Teerawattanasuk et al. (2014)	4.31 – 57.93
Mickovski and Van Beek (2009)	1.8 - 17
Hengchaovanich (1998)	75
Islam and Badhon (2020)	27
Noorasyikin and Zainab (2016)	12.61 – 88.52
Zegeye et al. (2018)	25.9

Most of previous studies mainly paid attention to the root tensile strength and omitted information about root modulus and breakage strain. However, the important of root modulus and breakage strain which define the stiffness and brittleness of roots, to root mechanical reinforcement, recently were recognised and received more attention (Wu et al., 2021). Wu et al. (2021) reported that the Young's modulus and breakage strain of *C. zizanioides* roots were 527.213 ± 4.26 MPa and 0.201 ± 0.006 mm/mm, respectively. In this study, the comprehensive investigation of root biomechanical properties, including the tensile strength, modulus and breakage strain of growing and decomposing roots of both vetiver species was performed.

2.5. Root mechanical reinforcement

Root mechanical reinforcement is one of the critical indicators in selecting vegetation species for the soil bioengineering approach. Root reinforcement is commonly measured by the direct shear test in the field or the laboratory (Docker and Hubble, 2008; Eab et al., 2015; Mickovski and Van Beek, 2009). In this way, the root reinforcement is defined as the difference in shear strength of fallow and vegetated soil. However, soil and roots in the soil matrix reach their peak strength at different displacements (Pollen et al., 2004). Thus this method could lead to the overestimation of root reinforcement (Cohen et al., 2011).

Table 2. 2. Typical mechanical reinforcement of *C. zizanioides* roots

Reference	Root reinforcement (kPa)
Eab et al. (2015)	6 – 6.8
Islam et al. (2010)	10.8 – 13.3
Mickovski and Van Beek (2009)	2.1 – 3.7
Jotisankasa et al. (2015)	0.4 – 8.1
Islam et al. (2016)	0.94 – 1.4
Badhon et al. (2021)	2.6 - 15
Voottipruex et al. (2008)	9.81

Similar to root biomechanical properties, root reinforcement obtained from direct shear tests widely varies among different species and even in the same species. Indeed, different species' typical root mechanical reinforcement varies from 1 to 94.3 kPa (Chok et al., 2015). The root mechanical reinforcement of *C. zizanioides* species were summarised in Table 2. 2. It is noteworthy that the root reinforcement of *C. nemoralis* was not found in the literature.

Another method to quantify the root reinforcement is using the prediction model. The root reinforcement model estimates the contribution of roots to soil strength from the root morphological traits (i.e., root diameter, root quantity) and root biomechanical properties (i.e., root tensile strength and modulus). One of the earliest root reinforcement models is Wu's model, which Wu et al. (1979) proposed. In this model, root reinforcement is quantified as the additional cohesion (i.e., root cohesion) alongside soil cohesion in the Mohr-Coulomb failure framework (Eq. 2.1) Wu et al. (1979) assumed that all roots are perpendicular to the shear plane and break simultaneously. Thus, Wu's model generally highlighted the overestimation of root cohesion (Meijer et al., 2018; Preti, 2013). However, Wu's model, so far, is still extensively used to estimate root reinforcement due to its simplicity.

$$\tau_f = c' + \sigma' \tan \phi' + C_r \quad (2.1)$$

where τ_f and σ' are shear and effective normal stress at shear surface, ϕ' is effective friction angle of soil and C_r is root cohesion which is defined as follow:

$$C_r = 1.2 \times \sum_1^N T_{r_i} \left(\frac{A_{r_i}}{A_s} \right) \quad (2.2)$$

where N is root number in the bundle, T_{r_i} and A_{r_i} are tensile strength and area of i^{th} root, and A_s is soil area. To remedy the remaining shortages in Wu's model, [Pollen and Simon \(2005\)](#) introduced fibre bundle model (FBM), assumed that roots in the soil matrix will be broken progressively under an increasing of load, which was introduced firstly by [Waldron \(1977\)](#). In this model, the total load distributes to the remaining intact roots follow either local load sharing (LLS) or global load sharing (GLS) mechanism. However, FBM model do not provide complete force and displacement curve, which is important to estimate residual tensile force. Moreover, the influences of root geometry, root diameter distribution, root mechanical properties on root reinforcement were not took into account in this model. To deal with these drawbacks in FBM, [Schwarz et al. \(2010\)](#) proposed new model for lateral root reinforcement estimation called as Root Bundle Model (RBM). In this model, the strain loading step was applied instead of stress loading step in FBM. Moreover, spatial distribution of root-size (dimensions and number of roots), root geometry (diameter-length relationship, tortuosity, branching factors), root mechanical properties (tensile strength and Young's modulus) as well as root-soil friction were considered in this model to provide more accuracy root reinforcement contribution. The FBM, therefore, can provide complete pull-out force and displacement curve. Although RBM is considered as an explicit model to estimate the reinforcement of the root bundle, this model is difficult to apply due to its complicated and some parameters in this model is hard to measure. More recently, [Schwarz et al. \(2013\)](#) enhanced the RBM by adopting the Weibull survival function in RBM to capture the variability of root biomechanical properties (i.e., tensile strength, modulus).

2.6. Root decomposition

Investigation of the decline of root biomechanical properties, root quantity and root reinforcement due to different means of introducing root decomposition has been studied since the 1960s ([Kitamura, 1968](#); [O'loughlin and Watson, 1979](#); [Ziemer, 1981](#)). For instance, [Ziemer and Swanston \(1977\)](#) reported that Hemlock and Sitka Spruce species were lose one-half of their tensile strength after logging 4-6 years. More

recently, [Ammann et al. \(2009\)](#) highlighted the tensile strength of *Picea abies* species reduced by 70% after 12 years since falling. Despite of a large volume of studies available in the literature, data on the deterioration of root biomechanical properties and root reinforcement to soil are scarce, especially for herbaceous species which share rather different root anatomy and growth mechanism from woody species that has been majorly focused in the literature. More recently, [Kamchoom et al. \(2021\)](#) reported the tensile strength of *C. dactylon* reduced by 30% (from 24.64 ± 1.99 MPa to 17.27 ± 1.83 MPa) and 40% (from 24.64 ± 1.99 MPa to 14.87 ± 1.32 MPa) after 360 days of burning and 60 days of herbicide application, respectively. Most of the existing studies focused on specifically the deterioration of root tensile strength and decomposition rate of vegetation root system during decomposition due to stem cutting and wild fire ([Ammann et al., 2009](#); [O'loughlin and Watson, 1979](#); [Vergani et al., 2014](#); [Watson et al., 1999](#); [Wu et al., 1979](#); [Zhu et al., 2019](#)). The reduction of decomposed roots followed by herbicide application, which is one of the most weed clearance techniques in agricultural practices. In addition, [Kamchoom et al. \(2021\)](#) demonstrated that the tensile strength of decomposed roots due to herbicide application declined at a rate that was faster than those of roots decomposed by burning. Thus, this study aimed to measure the variations of the biomechanical properties of decomposing roots of two contrasting vetiver species, including *C. nemoralis* and *C. zizanioides*, following herbicide application, and the changes of their ability to provide mechanical reinforcement to the soil.

Furthermore, the reduction in the root reinforcement as the root decomposed also gained attention in previous studies. Most of existing studies used prediction models ([Vergani et al., 2014](#); [Watson et al., 1999](#)) and direct shear test ([Zhu et al., 2019](#); [Ziemer, 1981](#)) to estimate the decline of root reinforcement over time since plant was died. For instance, the direct shear test results presented by [Zhu et al. \(2019\)](#) observed a loss of the reinforcement of the roots of *Symplocos setchuensis* by 85.9% after 12 months since stem cutting. By using Fibre Bundle Model (FBM), [Vergani et al. \(2014\)](#) reported that the reinforcement of mixed Silver Fir-Norway Spruce (i.e., *Abies alba* Mill. *Picea abies* (L.) Karst.) remained only 34% in the third year after felling. By using either direct shear test or prediction models, the decline in

root tensile strength, Young's modulus and root density were considered as the main factors that lead to the reduction of root reinforcement (Vergani et al., 2014; Zhu et al., 2019). However, the maximum dilatancy, which is considered as an important factor that governs the peak shear strength of reinforced soil, received less attention. More recently, the maximum dilatancy of reinforced soil has been investigated in Yildiz et al. (2018). Yet, the variation of dilatancy of reinforced soil due to root decomposition is not reported in the literature.



Chapter 3: Laboratory testing program

3.1. Introduction

The laboratory program consists of three main testing including root morphology investigation, root biomechanical properties measurement and root reinforcement measurement. These testing are semi-controlled experiments, where the growth media conditions, nutrient and water supply are well controlled. All of treatments were placed either in open greenhouse or outdoor, where daily temperature, relative humidity and daylight ranged from 24 to 37 °C, 37% to 98%, 9.3 to 12.1h, respectively. All the tests were conducted in the Civil Engineering building, Faculty of Engineering, Chulalongkorn University, Thailand. In addition, the statistical analysis on experiment data was performed using IBM SPSS statistics 22nd edition. The plant conditions, growth media properties were presented. The experimental setup, test plan and procedures were described in detail.

3.2. Test species and growth media

The two vetiver species, namely, *C. nemoralis* A. Camus and *C. zizanioides* L. Nash, were investigated. The *C. zizanioides* species is commonly found in the tropical regions worldwide (Truong et al., 2008). *C. zizanioides* can rapidly adapt to adverse growth conditions and is mainly found in lowland and areas with typically high-water content (Wasino et al., 2019). By contrast, *C. nemoralis* is mainly distributed in mountainous areas (highland) and well-drained soils (Truong et al., 2008).

Soil and rice husk ash were used as growth media in this study. Soil was collected from Chachoengsao Province, Thailand, and it was used to grow the two vetiver species for studying root reinforcement via direct shear tests. Soil samples were collected using a shovel at a depth ranging between 0.15 and 0.25 m. The field soil was then brought to the laboratory. To eliminate the size effect on direct shear test, the soil was sieved through the sieve No. 10 (2 mm opening) before use for transplanting. Rice husk ash was utilised to grow the two vetiver species in rhizoboxes and containers for measuring morphological traits and root biomechanical properties, respectively. Ash is a by-product of rice husk after electrically generated combustion, and it is known to contain substantial amount of residual nutrients that

could be recycled to support plant growth (Priyadharshini and Seran, 2010). The ash is observed to be hydrophilic. The rice ash and soil can be classified as poorly graded sand (SP) in accordance with the Unified Soil Classification System (ASTM-2487, 2011) or silt loam in accordance with the classification by the United States Department of Agriculture (USDA, 1951). The physical properties and the available nutrients in these growth media are summarized in Table 3. 1.

Table 3. 1. Physical and chemical properties of lateritic soil and rice husk ash.

Parameter	Growth media		Reference
	Lateritic soil	Rice husk ash	
Specific gravity, G_s	2.66	2.11	Specific Gravity test (ASTM D854)
Dry density (g/cm^3)	1.28	0.95	
Void ratio, e	1.08	1.22	Standard compaction test
Porosity, n	0.52	0.55	(ASTM D698)
D60 (mm)	1.7	1.5	Sieve analysis
D30 (mm)	0.5	1	(ASTM D2487)
D10 (mm)	0.15	0.3	
Texture	Poorly graded sand	Poorly graded sand	
pH	6.9	6.5	Standard buffer solution
Phosphorous, P (ppm)	30.82	1465	
Potassium, K (ppm)	395	7338	
Nitrogen, N (ppm)	190	1300	

3.3. Plantation procedures and plant treatment

3.1. Plant preparation

Two ecotypes of *C. nemoralis* and *C. zizanioides* species, namely, Huai Kha Khaeng and Songkhla 3, from Prachin Buri Province, Thailand, were selected for testing, respectively (Fig 3. 1). The parent vetiver clumps in the site were carefully removed from the soil. To obtain bare root slips (approximately 20 cm for tillers and 5 cm for roots in length) which consist of both tillers and roots, mature tillers from the clumps were split apart, and the soil attached to the roots was rinsed gently. The bare root slips were then stored in sealed plastic bags and transferred to the laboratory (Fig 3. 1).



Fig 3. 1. Bare root slips of (a) *C. nemoralis* and (b) *C. zizanioides* species

The propagation method, which [Truong et al. \(2008\)](#) proposed, was applied to grow two vetiver species under three different conditions (i.e., in rhizoboxes with rice husk ash, PVC containers with rice-husk ash, and PVC pipes with soil). First, mother vetiver clumps were split into slips, which contained at least two to three tillers (20 cm length) with a part of the vetiver crown. Afterward, root slips were dipped in tap

water and kept outdoor until the growth of new roots. Lastly, the slips were transplanted in rhizoboxes, drainage containers, and PVC pipes.

3.2. Plant growth condition

In order to investigate the root morphological traits, the two vetiver species were planted in the rhizoboxes (125 cm x 45 cm x 4 cm) for 77 days (Fig 3. 2). The rhizoboxes have been widely used to investigate the root architecture (Mašková and Klimeš, 2020). The rice husk ash was used as growth media in this measurement. Rice husk ash is black which contrasts with the root colour (white), which made the measurement of root architecture using image processing easier. The ash was mixed with water to an optimum moisture of 8% by mass. Afterward, the rhizoboxes were filled with rice husk ash at 650 kg/m^3 density and placed in an open greenhouse. In addition, the rhizoboxes were placed at 45° in an open greenhouse and composed of several drainage holes that created a drainage condition similar to that found in natural slopes (Fig 3. 3).

Similarly, *C. nemoralis* and *C. zizanioides* species were grown in rice husk ash for measuring root biomechanical properties. 10 polyvinyl chloride (PVC) containers (75 cm diameter, 100 cm height) were prepared to grow the two vetiver species (i.e., 5 containers for each species). Some drainage holes were made at the bottom of both containers, allowing for free water drainage, to closely mimic the growth conditions of a natural slope in a laboratory. These containers were placed outdoor and filled with moist rice husk ash (i.e., water content of 8% by mass) at a dry density of 650 kg/m^3 . The two vetiver species were planted in the containers for 49 days (Fig 3. 4).

For determining the root reinforcement provided by the two vetiver species, 10 PVC columns (15 cm inner diameter, 100 cm height) were used (Fig 3. 5). These columns were designed to be composed of eight species of half-split PVC tubes in order to minimise the disturbance of the sampling of rooted soils after planting. These pipes were divided into four layers (25 cm height in each). In the first layer, the upper 10 cm is a free space used for adding water and fertiliser, and the underlying layer (15 cm) was filled with rice husk ash to minimise water evaporation and support the initial root growth. The moist soil (i.e., water content of 12.8% by mass) was compacted in three bottom layers to the target dry density at 1100 kg/m^3 . A fallow

column of soil compacted to the same dry density (i.e., 1100 kg/m^3) was produced as control. Both *C. nemoralis* and *C. zizanioides* species were planted in these column (i.e., placed outdoor) for 91 days.

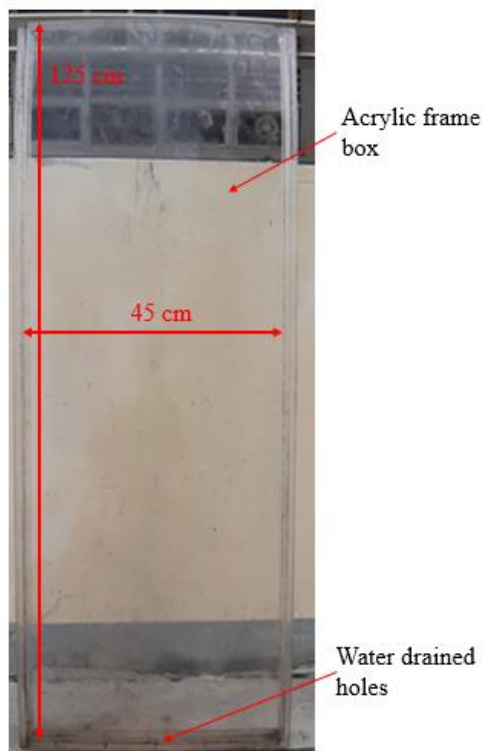


Fig 3. 2. Rhizobox component



Fig 3. 3. Vetiver grown in rhizobox system

All treatments were irrigated and supplied with nutrient (i.e., KNO_3 , $\text{Ca}(\text{NO}_3)_2$, $\text{MgSO}_4 \cdot 7\text{H}_2\text{O}$, KH_2PO_4 , Ferric Ethylenediamine Tetraacetic acid (Fe-EDTA) at 0.1% (by volume), and micronutrient at 0.025% (by volume) every day for the first 14 days and then every two days for the next 14 days. Both water and nutrient were not supplied for the rest of the planting period. Its noteworthy that growth period of the two vetiver species were different among three measurements. Different growth periods were considered because roots grown in soil have found to be weaker (i.e., smaller tensile strength) than those grown in rice husk ash by a previous study on the same vetiver species (Likitlersuang et al., 2022).



Fig 3. 4. Typical container for tensile test

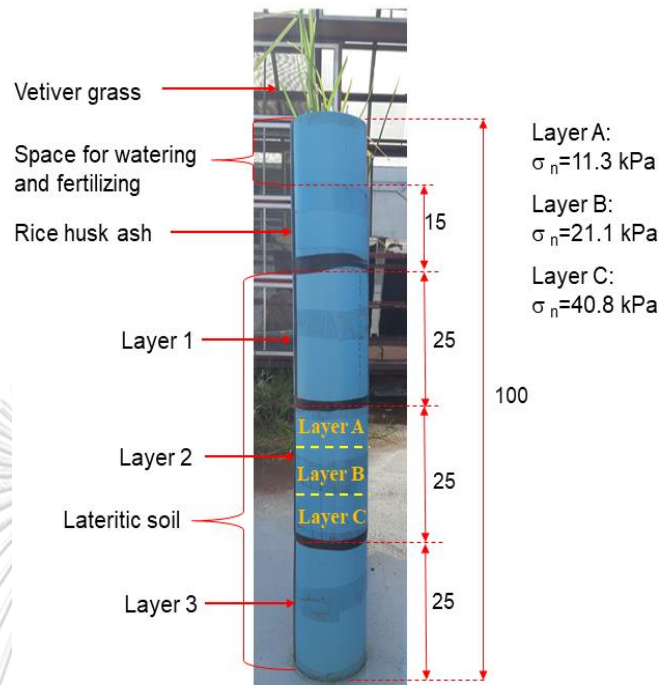


Fig 3. 5. Typical PVC column use for direct shear test

3.3. Plant decomposition condition

After planting for 49 days (i.e., for roots biomechanical properties measurement) and 91 days (i.e., for root reinforcement measurement), the containers and columns were treated by herbicide to introduce root decomposition. It is noted that herbicide was not applied for the rhizoboxes (i.e., root morphological traits observation). The eight containers and eight columns were applied with Propanil (N-(3,4-Dichlorophenyl) propanamide) at 36% (weight/volume) in water. Propanil is a legal herbicide, which has been widely used in Thailand and other southeast Asian countries for land clearance and weed control (Fig 3. 6). All these columns and containers were then left for root decomposition for 7, 28, 56 and 112 days (denoted as treatments D-7, D-28, D-56 and D-112, respectively). Both vetiver species were subjected to the same four treatments. The remaining two columns and two containers were reserved as control (i.e., no herbicide application; denoted as D-0). All 10 columns and 10 containers were irrigated every week since the 3rd week after herbicide application. At each of the designated durations of root decomposition, the columns and containers

were sent for testing the root biomechanical properties and root reinforcement, respectively.



Fig 3. 6. Propanil (*N*-(3,4-Dichlorophenyl) propenamide)

3.4. Measurement of root morphology

The root morphological traits of the *C. nemoralis* and *C. zizanioides* species were measured by using a rhizobox system via image analysis. The entire root system in all the treatments was imaged weekly by using a digital camera with a resolution of 5184 x 3456 pixels plus two 50 W light emitting diode (LED) floodlights since the third week of planting (Fig 3. 7). The captured root system images were analysed with ImageJ to measure the root morphological traits of the two vetiver species at 10 cm depth interval. The procedure of image processing is illustrated in the Fig 3. 8. Firstly, the Red-Green-Blue (RGB) root images were scaled and cropped to obtain the measured area. Afterward, a grey scale image (8 bits image type) was created in pre-processing step Fig A. 1.



Fig 3. 7. Digital camera system

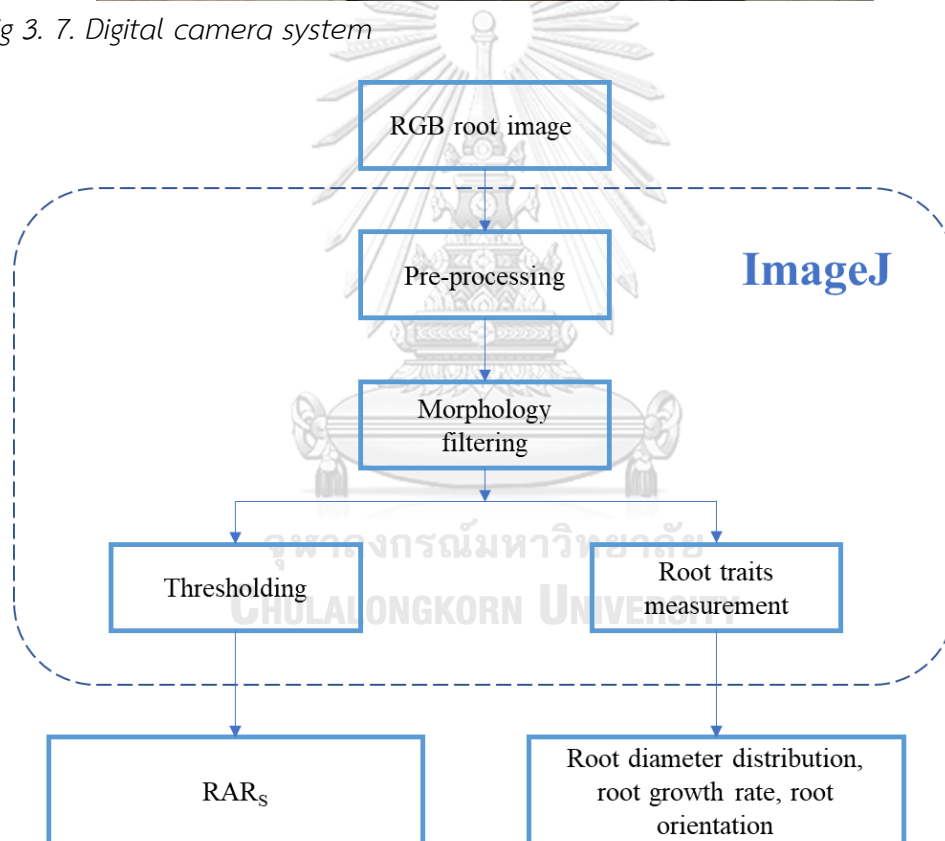


Fig 3. 8. Flow chart of root image processing in ImageJ program

These grey images then were divided into 10 images (45 cm x 10 cm) in order to measure root morphological traits at 10 cm interval in depth. The processed images then were filtered by using Fast Fourier Transform (FFT) bandpass filter and MorphoLibJ to reduce white noise in initial root images which influences on measurement results. The following morphological traits were measured: (1) RAR_s

(i.e., defined as the ratio between total pixel areas occupied by the roots and the total surface area of the rhizobox); (2) root orientation (Ω) (i.e., the angle between the horizontal plane and root direction and assumed to vary from 0° to 90°); (3) root diameter of individual root segments and (4) root growth rate (i.e., defined as the ratio of the total root length per day).

3.5. Measurement of root biomechanical properties

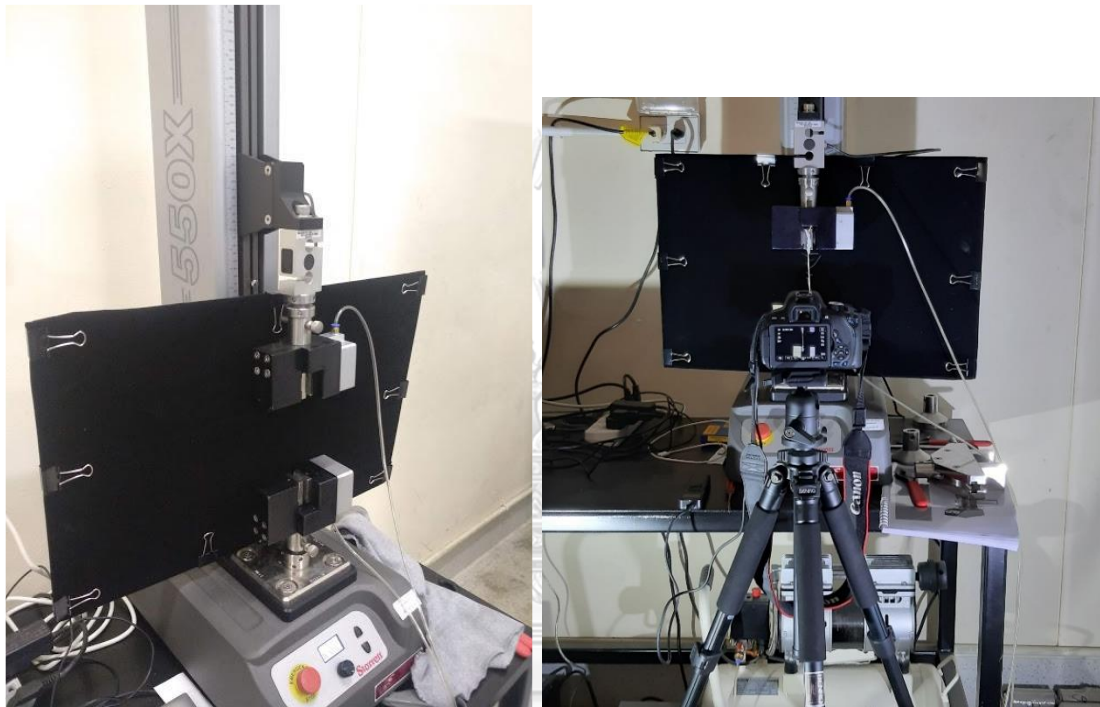


Fig 3. 9. L1 Force Measurement machine Fig 3. 10. Digital camera system

After 49 days of planting, 60 root segments from each replicate per species were collected to measure the tensile strength and Young's modulus of the roots. Individual root segments of 200 mm long were cut from the fresh root system and then stored in sealed plastic bags in a fridge at 5°C . Previous studies (e.g., [Boldrin et al. \(2018\)](#)) demonstrated that the root moisture content can significantly influence the biomechanical properties of roots. Furthermore, slope failure often occurs under wet conditions, so the root segments were soaked prior to testing to obtain conservative values of their biomechanical properties.

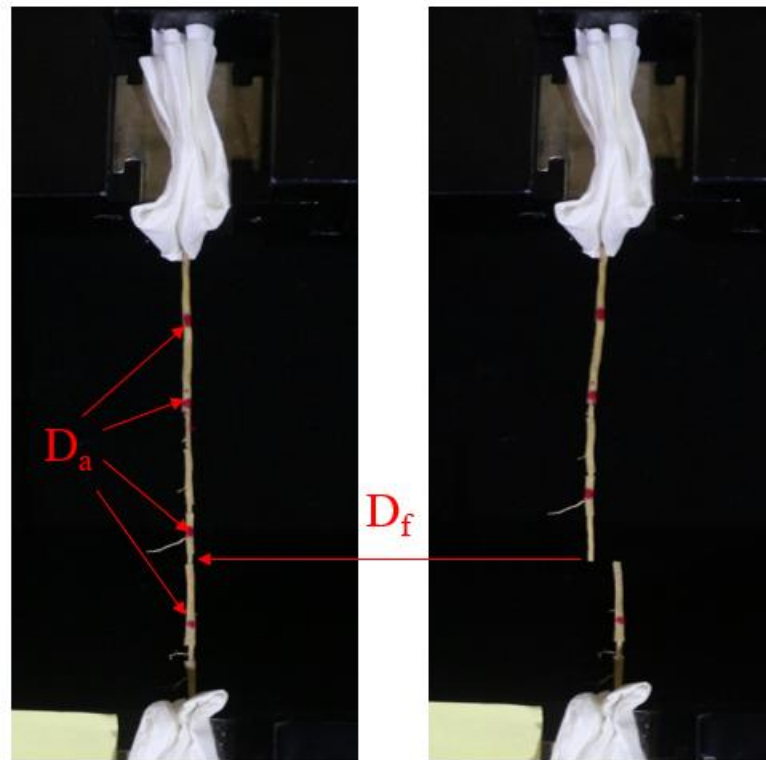


Fig 3. 11. Root diameter measurement

Each root segment was subjected to a uniaxial tensile test by using a universal testing machine (model: L1-550X Digital Force Tester; Starrett) in our laboratory (Fig 3. 9). A thin layer of soft paper was used to pad the clamps at both ends of each root segment. The gauge length (i.e., the length between the top and bottom clamps) was fixed at 100 mm. A constant loading speed of 5 mm/min was applied to each root segment. During tensioning, root straining was captured with a digital camera system (Fig 3. 10). Hence, any change in the diameter of each root segment could be determined through image analysis. The camera was also used to capture the moments when the root segments broke. Then, these images were utilised to determine the root diameter at the failure point (Fig 3. 11). A test was deemed invalid when the roots were broken at or near a clamping position.

The measured tensile stress-strain curve was used to determine the root tensile strength (T_r), breakage strain (ϵ_r), and secant modulus (E_s) as follow:

$$T_r = \frac{F_f}{\pi \left(\frac{d_f}{4} \right)^2} \quad (3.1)$$

$$\varepsilon_r = \frac{\Delta L_f}{L_0} \quad (3.2)$$

$$E_s = \frac{T_r}{\varepsilon_r} \quad (3.3)$$

where F_f is the force at root breakage and d_f is the root diameter at failure, ΔL_f is the elongation at breakage and L_0 is the gauge length (i.e., 100 mm). In addition, the Young's modulus (E_i) was also determined as the gradient of initial linear part of the stress-strain curve. The water content (w) of all root segments was also calculated using Eq. (3.4):

$$w = \frac{m_0 - m_d}{m_d} \quad (3.4)$$

where m_0 (mg) is weight of soaked root measured before testing and m_d (mg) is the weight of root after dried in the oven for 24 hours.

3.6. Measurement of root reinforcement

Soil samples at 50 to 75 cm depths (i.e., 15 cm long) of each column were used for testing. This depth range was chosen because there was sufficient root amount to effectively determine the root reinforcement effect and the sample was free from the overlying ash. Each of these 15 cm long soil samples was divided into three specimens (i.e., 5 cm thick each), which was then trimmed to fit into a direct shear box (Fig 3. 12). Noted the maximum of root diameter is 3 mm, which has no effect from the size of direct shear box (ASTM-D3080/D3080M, 2011). The procedures of direct-shear test outlined in ASTM-D3080/D3080M (2011) were adopted for testing. Each sample was first consolidated at three different confining stresses of 11.3, 21.1 and 40.8 kPa (Fig 3. 13). At equilibrium (i.e., when the vertical soil displacement was negligible), the samples were sheared to a horizontal displacement of 10 mm. The direct shear tests were conducted under unsaturated conditions. The moisture content of the samples varied from 16.7% to 17.3%. The test results were used to determine the shear strength parameters, including cohesion and friction angle, following the Mohr-Coulomb failure envelop. In addition, the maximum dilatancy which is defined as the initial gradient of vertical displacement-horizontal displacement curve (i.e., negative value presents the contraction) was determined.

Each sample was weighted before and after each shearing test and eventually oven-dried (after root removal; see below) to determine the initial and final water content (by mass).



Fig 3. 12. Trimmed specimen for direct shear test



Fig 3. 13. Direct shear machine

After each shearing test, the roots were separated from the soil sample by washing through a sieve #60 (i.e., with an opening size of 0.25 mm) by tap water. The number and diameter of all root segments exhumed were recorded before oven-dried for 24 hours to determine the dry root weight (W_r). Hence, the unit root biomass per soil volume, ρ_r , can be determined by Eq. (3.5),

$$\rho_r = \frac{W_r}{nV_s} \quad (3.5)$$

where n is root number, V_s is the soil volume after consolidation but before shearing.

3.7. Data analysis

The test data was analysed by performing both statistical and regression analyses. The significant differences in terms of root tensile strength, Young's modulus, secant modulus and root breakage strain among different treatments of root decomposition were tested by the analysis of one-way variance (ANOVA), followed by the post-hoc Tukey's test. Significance of any root tensile strength – diameter, root secant modulus – diameter, root cohesion-tensile strength, root cohesion-secant modulus and root cohesion-root biomass correlations were quantified by nonlinear or linear regressions. Results were considered statistically significant when the probability value (i.e., p -value) ≤ 0.05 .

3.8. Test plan and schedule

In this study, the test was started with vetiver growing since July 2020, which is the rainy season in Thailand. After the planting period (each measurement has the specific planting duration), the morphological traits, biomechanical properties and reinforcement of fresh roots (D-0) were tested. Afterward, the herbicide was applied to introduce the root decomposition. At the given period (i.e., 7, 28, 56 and 112 days; denoted D-7, D-28, D-56 and D-112, respectively) after herbicide application, the biomechanical properties and root reinforcement of *C. nemoralis* and *C. zizanioides* were tested. The tests were end in the mid-February 2021. The test plan and schedule are summarized in the Fig 3. 14.



		Jul-20	Aug-20	Sep-20	Oct-20	Nov-20	Dec-20	Jan-21	Feb-21
Measurement	Treatment	W-1 W-2 W-3 W-4	W-1 W-2 W-3 W-4	W-1 W-2 W-3 W-4	W-1 W-2 W-3 W-4	W-2 W-3 W-4 W-1	W-2 W-3 W-4 W-1	W-2 W-3 W-4 W-1 W-2 W-3 W-4 W-1	W-2
Root morphological traits	Growth		Planting		Testing (D-0)				
	Herbicide application								
Root biomechanical properties	Growth		Planting		Testing (D-0)				
	Herbicide application				Herbicide application				
Root mechanical reinforcement	Growth		Planting		Testing (D-0)				
	Herbicide application				Herbicide application				

Fig 3. 14. Summary of test plant and schedule

Chapter 4: Root biomechanical properties, mechanical reinforcement and morphological traits of *C. nemoralis* and *C. zizanioides* species.

4.1. Introduction

In the test series, the biomechanical properties, mechanical reinforcement and root morphological traits of fresh roots (D-0) of both *C. nemoralis* and *C. zizanioides* species under the semi-controlled conditions were investigated. In this chapter, the observed and measured properties of the fresh roots are presented and discussed. In addition, the correlations among these root properties are also presented.

4.2. Observed root morphological traits

The following morphological traits of the roots of the *C. nemoralis* and *C. zizanioides* species are summarised in Table 4. 1: orientation, diameter, and RAR₅ obtained through rhizobox system analysis (363 and 444 root segments of the *C. nemoralis* and *C. zizanioides* species, respectively), and root water content obtained from the tensile strength measurement (37 and 40 root segments of *C. nemoralis* and *C. zizanioides* species, respectively). Under the same growth conditions (i.e., water and nutrient supply, planting period and growth media), the diameter of the roots of the *C. nemoralis* and *C. zizanioides* species was significant difference (p-value < 0.05). The roots of *C. nemoralis* (from 0.3 to 2.57 mm) were significantly thicker than the *C. zizanioides* roots (from 0.52 to 2.2 mm) (p-value<0.05). However, [Truong et al. \(2008\)](#) obtained opposite findings from genetic perspectives. The growth and properties of root systems are controlled by not only genes but also growth conditions ([McMichael and Quisenberry, 1993](#)). Therefore, the inconsistency between our study and that of [Truong et al. \(2008\)](#) might be caused by the influence of growth conditions on root diameter. Indeed, the shortage of water and nutrient supply from the fifth week of planting could be the stress factor influencing the *C. zizanioides* roots, which were favourable to moist soil conditions; by contrast, arid soil is more suitable for the growth of *C. nemoralis* roots ([Truong et al., 2008](#)). In addition, fine roots (<2 mm) constituted most of the root systems of the *C. nemoralis* and *C. zizanioides* species, and they accounted for 90.1% and 98.4% of the total root number, respectively. The root diameter of the *C. zizanioides* species (0.52–2.2 mm)

was similar to those reported in the literature. For instance, [Truong et al. \(2008\)](#) and [Mickovski and Van Beek \(2009\)](#) reported that the root diameter of *C. zizanioides* species varies from 0.2 mm to 2.4 mm and from 0.2 to 2.2 mm, respectively. Consistent with previous results, this finding implied that the roots of *C. zizanioides* species could grow in their particular diameter range even under different climate conditions, such as the tropics ([Truong et al., 2008](#)) and the Mediterranean ([Mickovski and Van Beek, 2009](#)).

Table 4. 1. Summary of orientation (Ω), diameter (d), RAR_S , and water content (w ; mean \pm standard error of the mean [SE]) of *C. nemoralis* and *C. zizanioides* species.

Species	<i>C. nemoralis</i>	<i>C. zizanioides</i>
Root orientation (°)	49.78 \pm 1.57	50.62 \pm 1.27
Diameter (mm)	1.3 \pm 0.03	1.09 \pm 0.02
RAR_S (%)	5.15 \pm 0.51	4.05 \pm 0.39
Water content (mg/mg)	3.4 \pm 0.22	4.23 \pm 0.22

In contrast to root diameter, no significant differences in the water content, RAR_S , and root orientation were found between the two species (p -value > 0.05). Indeed, the average water contents of the *C. nemoralis* and *C. zizanioides* species were 3.4 \pm 0.22 and 4.23 \pm 0.22 mg/mg, respectively. The two tested species had mean RAR_S of 5.15% \pm 0.51% and 4.05% \pm 0.39%, respectively. The average orientations were 49.78 $^\circ \pm$ 1.57 $^\circ$ and 50.62 $^\circ \pm$ 1.27 $^\circ$, respectively. Particularly, RAR_S of the *zizanioides* species in this study (4.05% \pm 0.39%) was about two times greater than that reported in [Mahannopkul and Jotisankasa \(2019b\)](#) (1.87% \pm 0.22%). This observed difference in RAR_S could be explained by the effect of soil density on root growth. Indeed, the bulk density (1350 kg/m³) of clayey sand ([Mahannopkul and Jotisankasa, 2019b](#)) were higher than that of rice husk ash (650 kg/m³) tested in this study. Thus, the roots in our case were expected to experience less mechanical impedance to root growth ([Houlbrooke et al., 1997](#)). The information about RAR_S of the *C. nemoralis* species and the root orientation of the two species are unavailable in the literature

for comparison and discussion. Therefore, this study is the first to present the comprehensive data on root morphological traits of *C. nemoralis* and *C. zizanioides* species.

The significant correlation between root orientation and root diameter were found in this study for both vetiver species (p -value<0.05). The linear relationship between them in the *C. nemoralis* and *C. zizanioides* roots is displayed in Eqs. 4.1 and 4.2, respectively.

$$\Omega = 38.962 * d; (p - value < 0.05; R^2 = 0.85; N = 363) \quad (4.1)$$

$$\Omega = 46.07 * d; (p - value < 0.05; R^2 = 0.89; N = 444) \quad (4.2)$$

where Ω is root orientation ($^{\circ}$), d is root diameter (mm). This finding indicated that thicker roots tended to grow vertically (i.e., high values of orientation), whereas thinner roots grew horizontally. Indeed, the root system of the *C. nemoralis* and *C. zizanioides* species is classified as a fibrous root system, which mainly consists of primary and lateral roots (Truong and Loch, 2004). In general, primary roots are thicker, grow from stems, and penetrate downward to deep layers due to gravity. On the contrary, lateral roots are thinner, and they grow from primary roots and allow the radial expansion of lateral roots (Waidmann et al., 2020). Root orientation is also considered an important factor that influences root reinforcement (Gray and Leiser, 1983; Thomas and Pollen-Bankhead, 2010). However, most existing root reinforcement models assume that roots are oriented either perpendicular to the shear plane (Wu et al., 1979) or parallel to the pull-out direction (Cohen et al., 2011; Pollen and Simon, 2005; Schwarz et al., 2010). Thus, the correlation between root orientation and diameter derived from this study provided new information to incorporate the effects of root orientation on the improvement of existing root reinforcement models more accurately in the future.

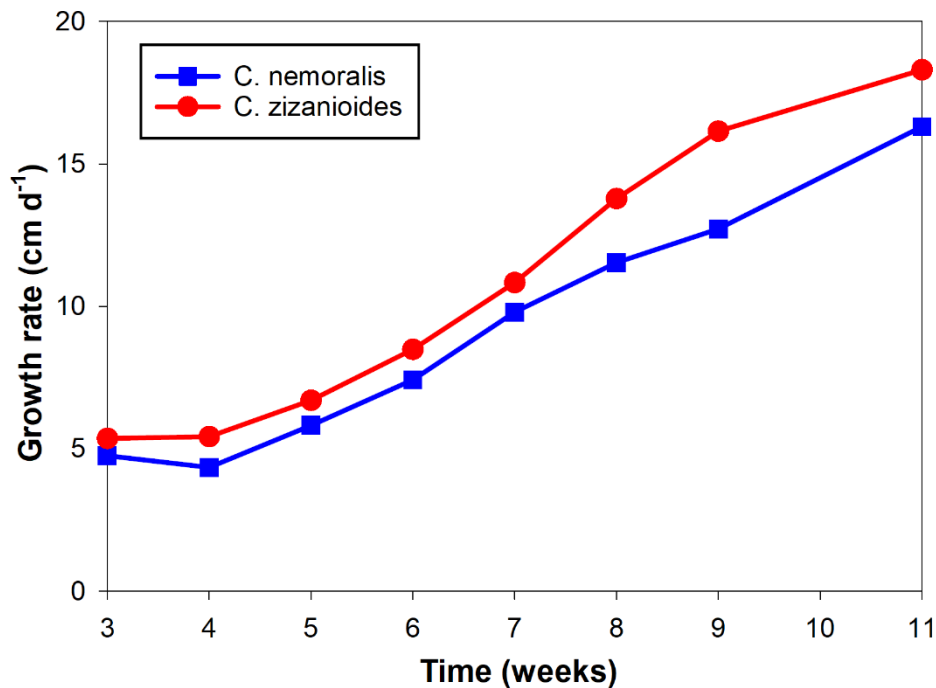


Fig 4. 1. Time variations in the root growth rate (cm d^{-1}) *C. nemoralis* (blue line) and *C. zizanioides* species (red line) during the 11 weeks of planting.

The growth rates of the roots of both species increased significantly over the planting period of 11 weeks ($p\text{-value} < 0.05$). The growth rates of the two species were significantly different ($p\text{-value} < 0.05$; Fig 4. 1). The *C. zizanioides* roots ($10.63 \pm 1.76 \text{ cm d}^{-1}$) grew faster than the *C. nemoralis* roots ($9.09 \pm 1.5 \text{ cm/d}$; $p\text{-value} < 0.05$). This finding might be attributed to the ability of the *C. zizanioides* species to adapt to various growth conditions more quickly than the *C. nemoralis* species (Truong et al., 2008). Moreover, the growth rates of the roots in this study were generally higher than those reported in the literature. For instance, the average growth rate of a *C. nemoralis* roots is 1 cm/d (Eab et al., 2015). The different growth rates could be attributed to the various measurement methods and growth conditions, such as media, density, and nutrient supply, among these existing studies. Indeed, in Eab et al. (2015), the growth rate of root was measured as the extension of the longest individual root per time of planting, which was different from the present study where the total root length was used to determine the root growth rate. In addition, Eab et al. (2015) planted *C. nemoralis* species under hydroponic conditions, quickly releasing nutrients for plant uptake (Likitlersuang et al., 2022); thus, the roots in their

case did not need to elongate to search for nutrients and were shorter than those planted in soil or rice-husk ash as in the present study.

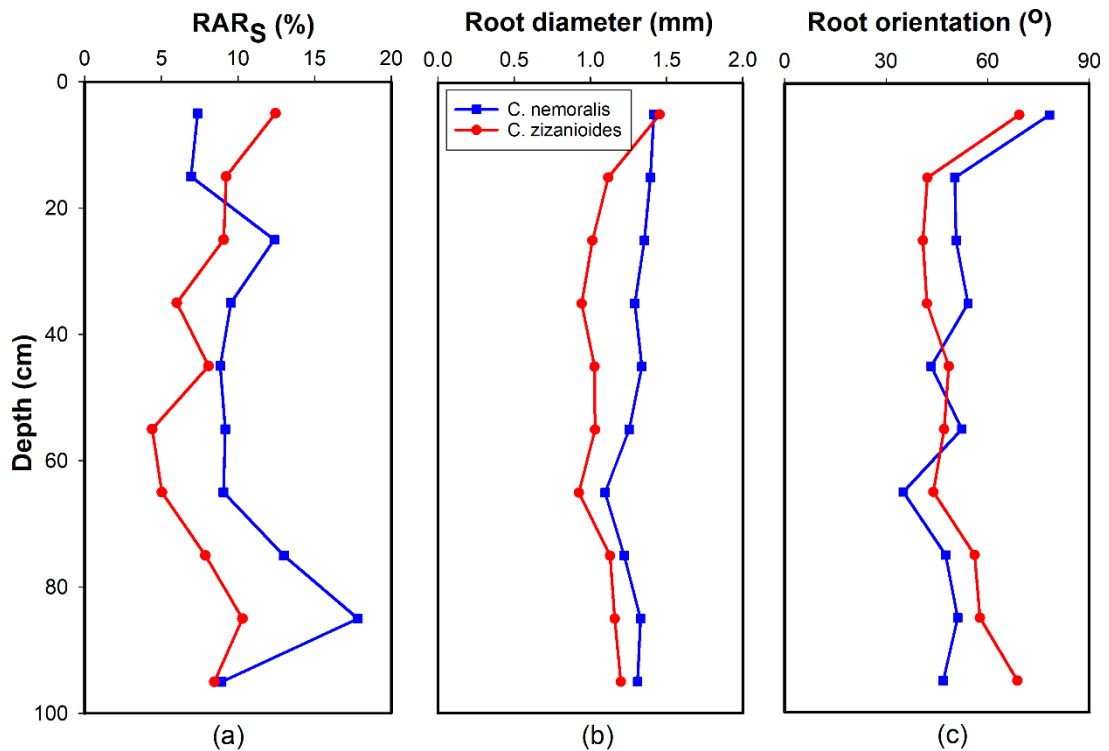


Fig 4. 2. Depth variations in the morphological properties of *C. nemoralis* (blue line) and *C. zizanioides* species (red line). (a) Root area ratio "side" (RAR_S; %), (b) root diameter (mm), and (c) root orientation (°).

The depth variations in RAR_S, orientation, and diameter of the roots of the two species are shown in Fig 4. 2. No significant variations in these root morphological properties over a 1 m observation depth were detected between the two species (p -value > 0.05). These findings were in agreement with those reported in the literature. For instance, Mahannopkul and Jotisankasa (2019b) used a minirhizotron to determine RAR_S in a field and revealed that RAR_S of *C. zizanioides* species does not significantly vary with depth in sandy soil. A similar trend for RAR_S was also observed in the case of rice-husk ash in our study.

4.3. Biomechanical properties of *C. nemoralis* and *C. zizanioides* fresh roots

The boxplots of the tensile strength (T_r), initial modulus (E_i) and secant modulus (E_s) of *C. nemoralis* and *C. zizanioides* fresh roots are given in the Fig 4. 3. The average tensile strength was 47.49 ± 3.13 MPa (*C. nemoralis* roots; for a diameter of 0.35–1.14

mm) and 41.23 ± 2.75 MPa (*C. zizanioides* roots; for a diameter of 0.44–1 mm). The tensile strength of the two vetiver species was generally different from those reported in the literature. For instance, [Mickovski and Van Beek \(2009\)](#) and [Wu et al. \(2021\)](#) observed that the tensile strength of *C. zizanioides* roots varies from 2 to 17 MPa and from 7.34 to 58.41 MPa at the corresponding diameter ranging from 0.3 to 1.4 mm and from 0.16 to 1.57 mm, respectively, which were lower than those recorded in this study (13.28–84.18 MPa). By contrast, the tensile strength of the *C. zizanioides* roots reported by [Mahannopkul and Jotisankasa \(2019a\)](#) is 117 ± 2.13 MPa, which was higher than that observed in this study. The variability of tensile strength could be explained by the difference in the measurement of root diameter, which is used to determine tensile strength ([Wu et al., 2021](#)). Indeed, the average diameter of the root segments was utilised to determine the tensile strength in previous studies ([Mickovski and Van Beek, 2009](#); [Wu et al., 2021](#)), whereas the root diameter at the failure point was adopted in the present study. Furthermore, the average diameter was almost two times higher than that at the failure point of both vetiver species (p -value < 0.05). As a result, the strength increased with decreasing of diameter as described in Eqs. 4.3 and 4.4. In addition, root age is a factor that can influence tensile strength; in general, young roots are considered to be weaker than mature roots ([Dumlao et al., 2015](#)). For example, our *C. zizanioides* species (2 months old) was younger than that tested by [Mahannopkul and Jotisankasa \(2019a\)](#) (12 months old), which resulted in the lower strength.

There was no significant difference in term of tensile strength between *C. nemoralis* and *C. zizanioides* species (p -value > 0.05). Indeed, the variation in the strength of the *C. nemoralis* roots (14.2–89.75 MPa) was comparable with that of the *C. zizanioides* roots (13.28–84.18 MPa). This finding implied that the mechanical contribution of the *C. nemoralis* species to soil reinforcement was comparable with that of the *C. zizanioides* species. Therefore, selecting species for slope stabilisation would depend on the geographical location of the concerned slopes. For instance, *C. nemoralis* species might be a better option than *C. zizanioides* species in mountainous areas where the former could be more adaptive to survive and grow.

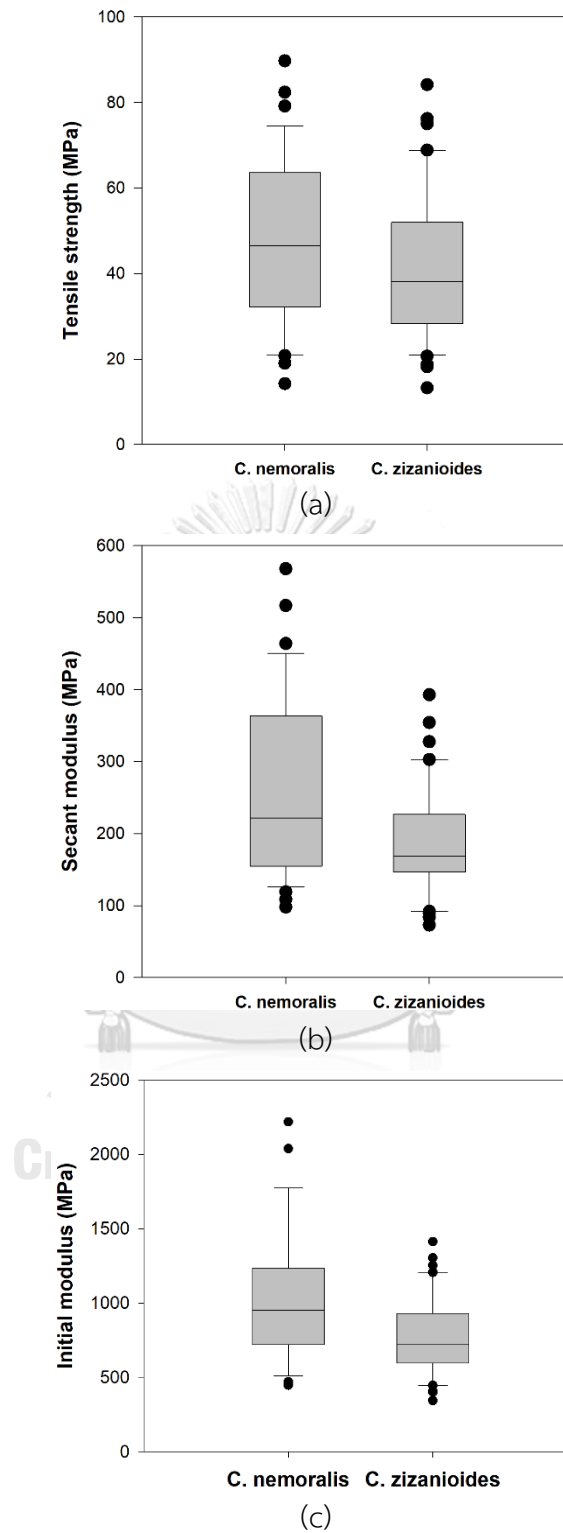


Fig 4. 3. Boxplot of (a) tensile strength, (b) secant modulus and (c) initial modulus of *C. nemoralis* and *C. zizanioides* species

Table 4. 2. Summary of tensile strength (T_r), initial modulus (E_i), secant modulus (E_s) and breakage strain (ϵ_b ; mean \pm standard error of the mean [SE]) of *C. nemoralis* and *C. zizanioides* species.

Species	<i>C. nemoralis</i>	<i>C. zizanioides</i>
Tensile strength (MPa)	47.49 \pm 3.13	41.23 \pm 2.75
Initial modulus (MPa)	1056.45 \pm 77.36	770.26 \pm 41.65
Secant modulus (MPa)	257.66 \pm 20.72	189.25 \pm 11.89
Breakage strain (mm/mm)	0.2 \pm 0.009	0.22 \pm 0.004

Unlike tensile strength, initial and secant modulus significantly differed between the two species (p -value < 0.05). Indeed, the average initial and secant modulus of the *C. nemoralis* species (1056.45 \pm 77.36 MPa and 257.66 \pm 20.72 MPa) were higher than that of the *C. zizanioides* species (770.26 \pm 41.65 MPa and 189.25 \pm 11.89 MPa), respectively. Thus, the stress in the *C. nemoralis* roots could be mobilised to a greater degree than that in the *C. zizanioides* roots by the same amount of strain, and the *C. nemoralis* roots might be broken at the smaller strain than that of *C. zizanioides* roots. Indeed, the breakage strain of *C. nemoralis* (0.2 \pm 0.009 mm/mm) was significantly smaller than that of *C. zizanioides* roots (0.22 \pm 0.004 mm/mm) (Table 4. 2; p -value $<$ 0.05). It also means that the soil reinforced by *C. nemoralis* roots might reach the peak strength at a smaller displacement during shearing. Indeed, the *C. nemoralis* roots provided more shear resistance to soil than the *C. zizanioides* roots over 10 mm displacement under the normal stresses of 21.1 and 40.8 kPa (Fig 4. 5). So far, most studies have measured the tensile strength of vetiver roots. However, the importance of root modulus and breakage strain, which measure the stiffness and brittleness of roots, respectively, has been recently considered in understanding root-soil interaction and the pre-failure mechanism of the vegetated slope (Wu et al., 2021). Thus, the future studies should pay more attention to modulus and breakage strain of roots along with the tensile strength.

4.4. The correlations between root diameter and root biomechanical properties

This study highlighted the significant correlations of diameter-tensile strength, diameter-secant modulus and diameter-initial modulus, which followed the negative power law for both *C. nemoralis* and *C. zizanioides* roots (p -value<0.05) as follow:

$$T_r = 26.1 \times d_f^{-1.129}; (p\text{-value} < 0.05; R^2 = 0.56; N = 37) \quad (4.3)$$

$$T_r = 20.09 \times d_f^{-1.577}; (p\text{-value} < 0.05; R^2 = 0.55; N = 40) \quad (4.4)$$

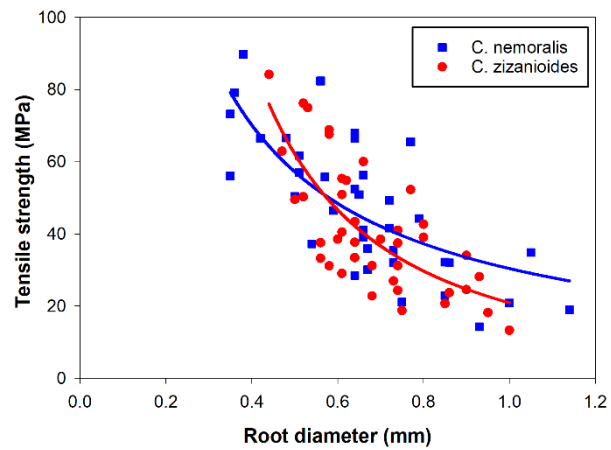
$$E_i = 581.81 \times d_f^{-1.121}; (p\text{-value} < 0.05; R^2 = 0.6; N = 37) \quad (4.5)$$

$$E_i = 447.95 \times d_f^{-1.212}; (p\text{-value} < 0.05; R^2 = 0.51; N = 40) \quad (4.6)$$

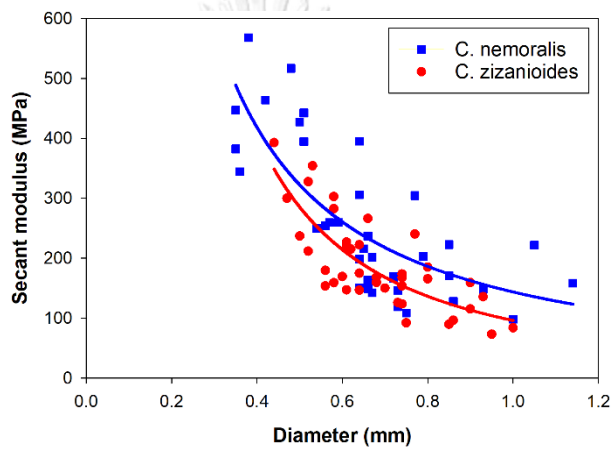
$$E_s = 133.41 \times d_f^{-1.21}; (p\text{-value} < 0.05; R^2 = 0.6; N = 37) \quad (4.7)$$

$$E_s = 94.59 \times d_f^{-1.54}; (p\text{-value} < 0.05; R^2 = 0.61; N = 40) \quad (4.8)$$

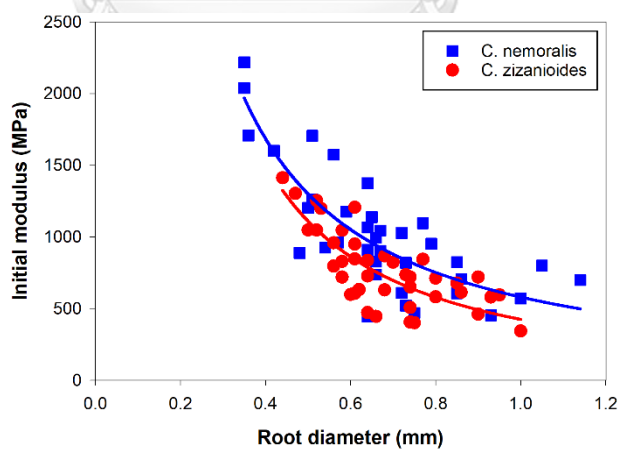
These correlations of two vetiver species are shown in the Fig 4. 4. This trend has been widely used to describe the correlation between the tensile strength and diameter of roots of several vegetation species (Bischetti et al., 2005; Tosi, 2007). The negative correlation identified that the thinner roots are stronger and stiffer. The negative correlation identified in this study was consistent with previous findings on *C. zizanioides* species (e.g., in (Mickovski and Van Beek, 2009); Wu et al. (2021) for strength-diameter and Mahannopkul and Jotisankasa (2019a) for modulus-diameter correlation). The negative correlation could be contributed to the cellulose and lignin content (Genet et al., 2005; Zhang et al., 2014); root moisture (Boldrin et al., 2018), and root anatomy (Chimungu et al., 2015). Also, this trend could be explained by the influence of the root water content on the tensile strength and modulus of herbaceous species (Mahannopkul and Jotisankasa, 2019a; Wu et al., 2021). Indeed, the root water content



(a)



(b)



(c)

Fig 4. 4. Correlations between diameter and (a) tensile strength, (b) secant modulus and (c) initial modulus of *C. nemoralis* and *C. zizanioides* species

(w) of *C. nemoralis* and *C. zizanioides* species was positively correlated with strength, initial and secant modulus as follows:

$$w = 0.02 \times T_r + 2.28; (p\text{-value} < 0.05, R^2 = 0.11, N = 37) \quad (4.9)$$

$$w = 0.03 \times T_r + 3.03; (p\text{-value} < 0.05, R^2 = 0.13, N = 40) \quad (4.10)$$

$$w = 0.001 \times E_i + 1.92; (p\text{-value} < 0.05, R^2 = 0.24, N = 37) \quad (4.11)$$

$$w = 0.002 \times E_i + 2.87; (p\text{-value} < 0.05, R^2 = 0.11, N = 40) \quad (4.12)$$

$$w = 0.004 \times E_s + 2.32; (p\text{-value} < 0.05, R^2 = 0.15, N = 37) \quad (4.13)$$

$$w = 0.007 \times E_s + 2.84; (p\text{-value} < 0.05, R^2 = 0.15, N = 40) \quad (4.14).$$

In addition, negative correlation between water content and diameter of *C. nemoralis* and *C. zizanioides* root were found as presented in Eqs. 4.15 and 4.16, respectively.

$$w = -3.46 \times d_f + 5.7; (p\text{-value} < 0.05, R^2 = 0.23, N = 37) \quad (4.15)$$

$$w = -5.43 \times d_f + 7.94; (p\text{-value} < 0.05, R^2 = 0.29, N = 40) \quad (4.16)$$

These observations explained why the strength increased as the diameter decreased. Furthermore, the tensile strength of the *C. nemoralis* and *C. zizanioides* species was significantly correlated with the corresponding initial modulus (p-value < 0.05, R² up to 94% and 92%, respectively). The linear relationship between strength and modulus of *C. nemoralis* and *C. zizanioides* species are presented in Eqs. 4.17 and 4.18:

$$E_i = 21.92 \times T_r; (p\text{-value} < 0.05, R^2 = 0.94, N = 37) \quad (4.17)$$

$$E_i = 17.42 \times T_r; (p\text{-value} < 0.05, R^2 = 0.92, N = 40) \quad (4.18)$$

This observation agreed with that reported by [Boldrin et al. \(2017\)](#). The tensile strength of roots is considered the fundamental parameter in most existing root reinforcement models ([Pollen and Simon, 2005](#); [Wu et al., 1979](#)). In addition, influence of root modulus on root-soil mechanical activation and their shear strength at different strains was highlighted by [Boldrin et al. \(2017\)](#) and [Mickovski and Van Beek \(2009\)](#). Thus, modulus (i.e., both initial and secant) of roots has been considered in some root reinforcement models to estimate the mechanical contribution of root systems on soil stability ([Cohen et al., 2011](#); [Schwarz et al., 2010](#); [Schwarz et al., 2013](#)). However, data on the correlation between modulus and diameter are lacking in terms of any meaningful comparison and discussion.

4.5. Root mechanical reinforcement – the contribution of roots to soil strength

Fig 4. 5 Fig 4. 5 shows the shear stress-shear displacement curves for fallow soil and soil reinforced by the *C. nemoralis* and *C. zizanioides* fresh roots at three confining pressure levels of 11.3, 21.1, and 40.8 kPa. As expected, the presence of *C. nemoralis* and *C. zizanioides* fresh roots (D-0) increased the shear strength of the soil under any confining pressure. However, at the confining pressure levels of 21.1 and 40.8 kPa, the *C. nemoralis* roots provided more shear resistance to soil than that of the *C. zizanioides* roots over 10 mm displacement (p -value < 0.05). The shear behaviour of the rooted soil could be affected by tensile strength and root diameter distribution (Pollen and Simon, 2005; Schwarz et al., 2013). However, this study revealed that the tensile strength had no significant differences between the *C. nemoralis* and *C. zizanioides* species (refers to section 4.3; p -value > 0.05). In addition, Fig 4. 6 shows that the soil reinforced by the *C. zizanioides* species (i.e., subjected 21.1 and 40.8 kPa) mainly consisted of small roots (i.e., <1 mm in diameter; i.e., more than 71%). Conversely, thicker roots (i.e., >1 mm in diameter) were mainly found in the soil reinforced by the *C. nemoralis* species (i.e., more than 50%). In addition, thinner roots require less force to break than thicker roots, potentially causing a progressive failure mechanism (Pollen and Simon, 2005). In addition, there was the significant difference in term of the root number, dry root biomass per soil volume (ρ_r) (Table 4. 3; p -value < 0.05). Indeed, the average root number, and ρ_r of the *C. nemoralis* roots (34 ± 1.73 , and $0.86 \pm 0.03 \text{ kg m}^{-3}$, respectively) were much higher than those of the *C. zizanioides* roots (24.33 ± 0.33 , and $0.71 \pm 0.003 \text{ kg m}^{-3}$, respectively; p -value < 0.05). These parameters represent the amount of root in the soil specimens. Therefore, the difference in the root diameter distribution and the amount of root between the two species may explain the variation in the effects of shear behaviour and soil reinforcement.

Both fallow and reinforced soils exhibited a strain-hardening behaviour at three different confining pressure levels. Under small (i.e., 11.3 kPa and moderate (i.e., 21.1 kPa)) confinements, the fallow soil reached the peak stress (i.e., plateau) at a smaller

displacement than the soils reinforced by the two species. Moreover, under these stress regimes, the initial stiffness of the reinforced soil cases was greater than that of the fallow case, meaning a quicker mobilisation of shear strength at smaller shear displacement. This phenomenon however vanished at the high confinement (40.8 kPa). After 10 mm displacement was achieved by shearing, the shear stress of the fallow and rooted soils increased continuously at any stress level and did not reach a maximum value. Therefore, the shear stresses at 10 mm displacement were used to evaluate the shear strength properties of the bare and root-reinforced soils. Fig 4.7 relates the ultimate shear stress with the corresponding confining pressure of both the fallow and reinforced soils, forming the Mohr-Coulomb failure envelopes. The roots of either *C. nemoralis* or *C. zizanioides* greatly affected the cohesion of the soil. The presence of the fresh roots of *C. nemoralis* and *C. zizanioides* increased the cohesion by 4.9 kPa and 4.4 kPa (i.e., known as root cohesion; Cr). The root reinforcement of *C. nemoralis* species obtained in the present study (4.9 kPa) was lower than that reported by [Eab et al. \(2015\)](#) (6.8 kPa). In contrast, the *C. zizanioides* roots in this study provided more reinforcement (4.4 kPa) to soil than those in the study of [Teerawattanasuk et al. \(2014\)](#) (3.58 kPa) and [Mickovski and Van Beek \(2009\)](#) (2.7 kPa). These differences could be partially explained by the variations in soil conditions and root age among these studies and could cause the biomechanical properties and reinforcement of roots to vary ([Mickovski and Van Beek, 2009](#)). Indeed, the tensile strengths of the *C. zizanioides* species planted in weathered clay ([Teerawattanasuk et al. \(2014\)](#); 4.31–57.93 MPa) and in clayey soil ([Mickovski and Van Beek \(2009\)](#); 2–17 MPa) were smaller than that planted in rice husk ash in the present study (13.28–84.18 MPa). In addition, [Dumlao et al. \(2015\)](#) revealed that the root age significantly influences root strength (i.e., young roots are weaker than mature ones). Therefore, the examined *C. nemoralis* roots in our study (13 weeks old) were weaker than those in the study of [Eab et al. \(2015\)](#) (16 weeks old). By contrast, the presence of roots of two vetiver species introduced only a minimal change in the peak friction angle. Indeed, the peak friction angle was increased marginally by 3.8° and 2.5° (by 14.4% and 9.5% compared to fallow soil). These values agreed with those reported in other studies. For instance, [Maffra et al. \(2019\)](#)

reported that the friction angle of clayey soil increased by 14.4% in the presence of Atlantic Forest native species. [Ali and Osman \(2008\)](#) found that the friction angle does not significantly change because of the presence of vegetation roots. The effects of roots on friction angle greatly depend on the relative direction between the major principal stress in soil and the predominant direction of root orientation; in principle, friction angle would be significantly affected if root segments were aligned with the direction of the major principal stress ([Karimzadeh et al., 2021](#)). In the case of direct shearing, root segments were likely to be oriented almost perpendicularly to the shear plane, which might not be a favourable orientation to fully mobilise the root tensile properties of resistance. Therefore, no significant change in root friction angle was found in the case of direct shearing as in this study. By contrast, [Karimzadeh et al. \(2021\)](#) showed that the friction angle of sand reinforced by vetiver grass significantly increases when a sample is subject to a triaxial extension loading; the direction of the major principal stress is perpendicular to the predominant direction of the vetiver roots. Thus, most of the mechanical strength of roots to resist soil shearing is mobilised.

Table 4. 3. Summary of the root volume ratio (RVR), root biomass per soil volume (ρ_r), and root number of the direct shear specimens.

Normal stress (kPa)	Depth (cm)	<i>C. nemoralis</i>			<i>C. zizanioides</i>		
		RVR (%)	ρ_r (kg/m ³)	Root number	RVR (%)	ρ_r (kg/m ³)	Root number
11.3	55	0.9	0.85	34	0.31	0.71	25
21.1	65	0.66	0.92	37	0.25	0.7	24
40.8	75	0.69	0.8	31	0.21	0.71	24

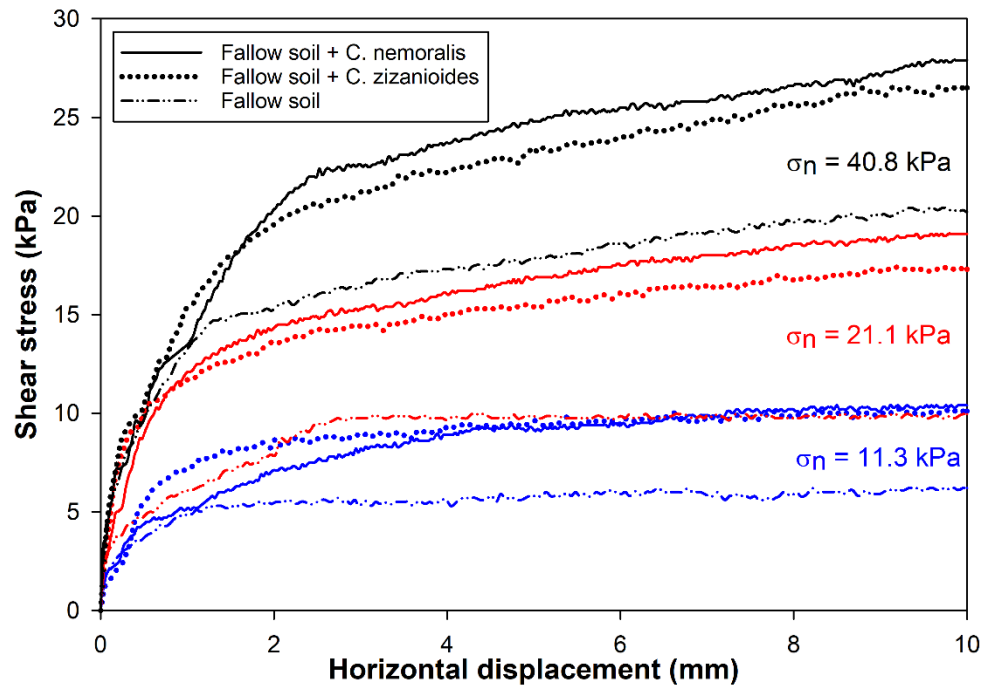


Fig 4. 5. Shear behaviour from direct shear tests on fallow soil (dash-dotted line) and soil reinforced with *C. nemoralis* (solid line) and *C. zizanioides* (dotted line) species under three normal stress levels: 11.3 kPa (Blue), 21.1 kPa (Red), and 40.8 kPa (Black).

Fig 4. 8 depicts the corresponding vertical displacement-horizontal displacement curves. As expected, following the strain-hardening behaviour, both the fallow and reinforced soils under all treatments displayed a volumetric contractive behaviour, as indicated by the soil settlement. Importantly, the presence of either *C. nemoralis* or *C. zizanioides* fresh roots (D-0) made the soil volumetrically more dilative (or less contractive), indicated by the increase of the maximum dilatancy in all cases. For instance, the maximum dilatancy of soil reinforced by *C. nemoralis* and *C. zizanioides* roots were -0.16 mm/mm and -0.32 mm/mm, which are higher than that of fallow soil (-0.67 mm/mm) in case of 40.8 kPa confining regime. This phenomenon could be explained by the occupation of growing roots in soil pore space, which makes the soil become denser. The similar hypothesis can be found in case of fibres (Diambra et al., 2010; Wood et al., 2016). The root-induced change in dilatancy was found for various species as woody species (e.g., Yildiz et al. (2018) and vetiver species (e.g., Mahannopkul and Jotisankasa (2019a) and Karimzadeh et al. (2021)). It is noted that the influence of roots on soil maximum dilatancy could be governed by

various factors including saturation degree (Mahannopkul and Jotisankasa, 2019a), root biomass (Yildiz et al., 2018) and the confining pressure (Karimzadeh et al., 2021).

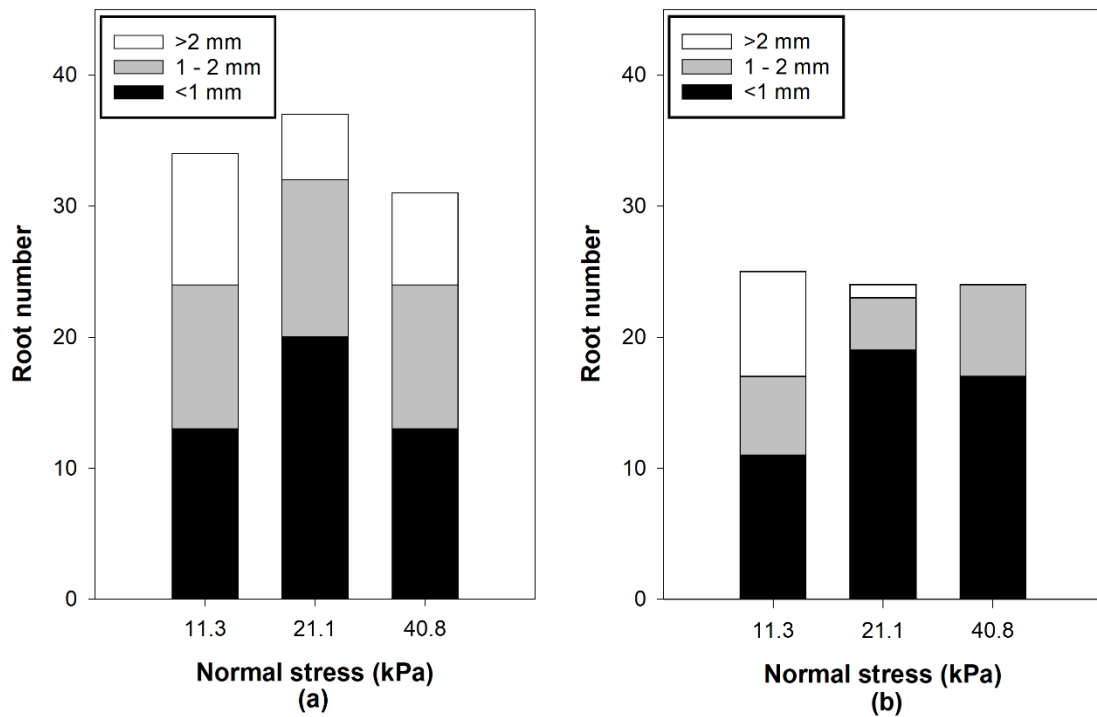


Fig 4. 6. Root diameter distribution of (a) *C. nemoralis* and (b) *C. zizanioides* species presented in shearing specimens.

It is noteworthy that the presence of the roots of both vetiver species caused an increase in soil shear strength even at a small shear displacement of 10 mm. The contribution of the *C. nemoralis* species to soil shear strength was comparable with that of the *C. zizanioides* species (only 0.5 kPa and 1.27° different between *C. nemoralis* and *C. zizanioides* species in terms of cohesion and friction angle, respectively). The *C. nemoralis* roots were shorter than the *C. zizanioides* roots, which have been widely used for slope stabilisation (Truong et al., 2008). However, the root systems of the *C. nemoralis* and *C. zizanioides* species were investigated up to 1 m depth in the present study. Therefore, we suggested the potential use of an alternative *C. nemoralis* species for shallow slope stabilisation and soil erosion control.

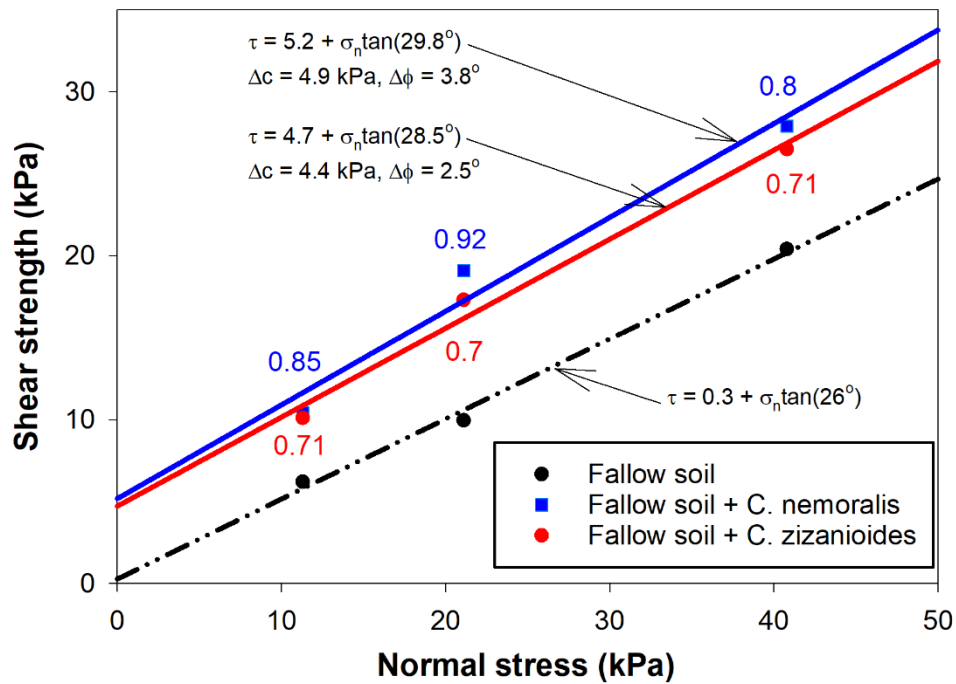


Fig 4. 7. Derived Mohr-Coulomb failure envelope for the fallow soil (dark dash-dotted line) and the soils reinforced by *C. nemoralis* (blue solid line) and *C. zizanioides* (red solid line) species. The number indicates the root biomass per soil volume in the tested sample (ρ_r ; kg/m^3).

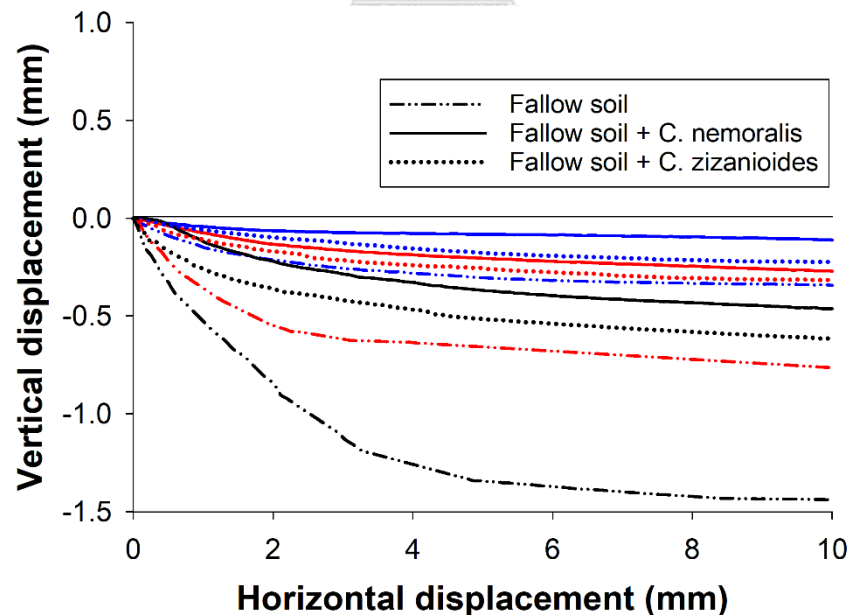


Fig 4. 8. Vertical displacement-horizontal displacement curves of fallow soil (dash-dotted line) and soil reinforced with *C. nemoralis* (solid line) and *C. zizanioides* (dotted line) species under three normal stress levels: 11.3 kPa (Blue), 21.1 kPa (Red), and 40.8 kPa (Black).

4.6. Concluding remarks

The series of laboratory experiments were conducted to investigate the biomechanical properties (tensile strength and initial and secant modulus of roots, and breakage strain), morphological traits (RAR_s , diameter, and root orientation), and root mechanical reinforcement of two contrasting vetiver species, namely, *C. nemoralis* and *C. zizanioides* species. The following conclusions could be drawn:

The comprehensive datasets of the biomechanical properties (tensile strength and initial and secant modulus of roots, and breakage strain), morphological traits (RAR_s , root diameter, and root orientation), and mechanical reinforcement of the roots of *C. nemoralis* and *C. zizanioides* are presented. The root properties of the two vetiver species (i.e., tensile strength–diameter, initial modulus–diameter, secant modulus–diameter, tensile strength–Young’s modulus, and root orientation–diameter) have significant correlations ($p < 0.05$). This study is the first to use a rhizobox for observing root morphological traits and to identify a correlation between root orientation and diameter. This finding provides new insights into root orientation, which is an important yet often overlooked parameter in the evaluation of existing root reinforcement models.

Under the same growth conditions, the presence of roots, either from *C. nemoralis* or *C. zizanioides* species, greatly enhances the soil shear strength in terms of cohesion, but the increase in cohesion between the two species is similar. The friction angle obtained from the soil reinforced by either the *C. nemoralis* or *C. zizanioides* roots has no significant difference. Thus, it is suggested that the *C. nemoralis* species shares similar soil reinforcement effects to the *C. zizanioides* species, which has been widely used in soil bioengineering practice. Furthermore, this study is expected to be a milestone for promoting vetiver species (i.e., especially *C. nemoralis* species) for soil bioengineering in Southeast Asian countries, which are greatly impacted by global climate change.

Chapter 5: The influence of root decomposition on root biomechanical properties and mechanical reinforcement

5.1. Introduction

Using uniaxial tensile test and direct shear test, this study investigated the influence of root decomposition due to herbicide application on root biomechanical properties and root reinforcement provided by *C. nemoralis* and *C. zizanioides* species. In this chapter, the evolution of root biomechanical properties, including tensile strength, breakage strain, secant and initial modulus of two vetiver species with increasing duration of decomposition (i.e., at 7, 28, 56 and 112 days after herbicide application) are presented. Also, the variations of root reinforcement in terms of root cohesion and maximum dilatancy due to root decomposition are presented and discussed.

5.2. Biomechanical properties of decomposing roots of *C. nemoralis* and *C. zizanioides* species

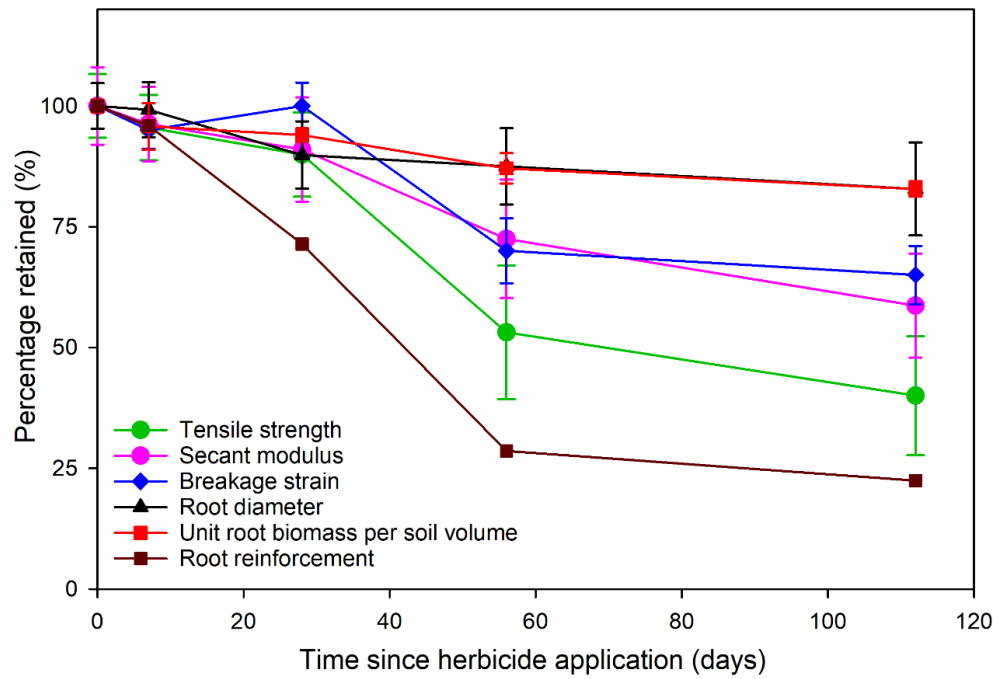
The mean \pm standard error (SE) of mean of the tensile strength, Young's modulus, secant modulus and breakage strain of different decomposition duration of the two species are summarised in Table 5. 1. The root decomposition has significant effects on the root biomechanical properties (i.e., tensile strength, secant modulus and breakage strain) of both *C. nemoralis* and *C. zizanioides* (p -value < 0.05), especially in the later stage (i.e., after 56 days since herbicide application) of the root decomposition. After 28 days of root decomposition, there were no significant changes in the tensile strength, secant modulus and breakage strain of the two species (p -value > 0.05). Significant decline of tensile strength and breakage strain was found after 56 days of root decomposition (p -value < 0.05). Meanwhile, the secant modulus of both species highlighted a significant difference after 112 days since herbicide application.

Particularly, as shown in Fig 5. 1, there was an evident exponential reduction of strength during 112 days of root decomposition. At the end of the tests, only 40.0% and 51.9% of the initial root tensile strength of the fresh roots of *C. nemoralis* and *C. zizanioides* (D-0) were left (Fig 5. 1), respectively.

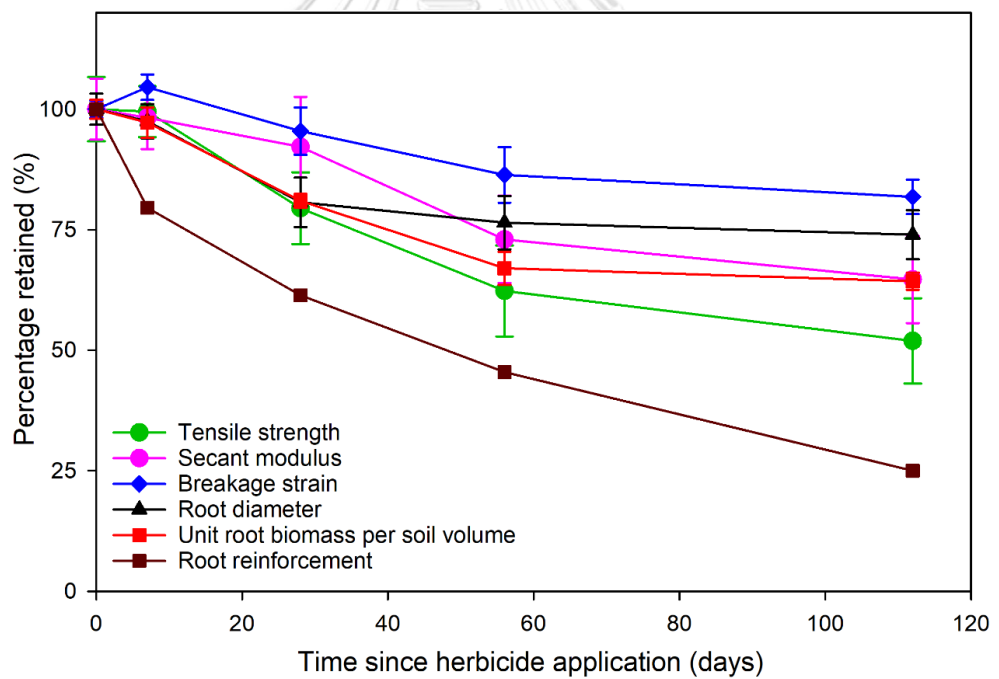
Table 5. 1. Summary of tensile strength (T_r), initial modulus (E_i), secant modulus (E_s), and breakage strain (ϵ_r) (mean \pm standard error of mean (SEM)) of the *C. nemoralis* and *C. zizanioides*.

Species	Treatment	T_r (MPa)	E_i (MPa)	E_s (MPa)	ϵ_r (mm/mm)
<i>C. nemoralis</i>	D-0	47.49 \pm 3.13 ^a	1056.45 \pm 77.36 ^a	257.66 \pm 20.72 ^a	0.2 \pm 0.009 ^d
	D-7	45.37 \pm 3.07 ^a	1176.73 \pm 59.42 ^a	248.09 \pm 19.16 ^{ab}	0.19 \pm 0.007 ^{de}
	D-28	42.71 \pm 3.72 ^a	1027.46 \pm 91.06 ^a	234.42 \pm 25.26 ^{ac}	0.2 \pm 0.01 ^{cde}
	D-56	25.23 \pm 3.49 ^b	1030.09 \pm 86.82 ^a	186.77 \pm 22.93 ^{ae}	0.14 \pm 0.009 ^s
	D-112	19.01 \pm 2.34 ^b	1068.41 \pm 77.66 ^a	151.09 \pm 16.29 ^e	0.13 \pm 0.008 ^s
<i>C. zizanioides</i>	D-0	41.23 \pm 2.75 ^a	770.26 \pm 41.65 ^b	189.25 \pm 11.89 ^d	0.22 \pm 0.004 ^{ab}
	D-7	41.02 \pm 2.17 ^a	698.26 \pm 49.29 ^b	185.88 \pm 12.09 ^d	0.23 \pm 0.006 ^a
	D-28	32.76 \pm 2.44 ^{ab}	817.13 \pm 78.1 ^b	174.46 \pm 18.07 ^d	0.21 \pm 0.01 ^{abc}
	D-56	25.68 \pm 2.43 ^{bc}	757.76 \pm 79.31 ^b	138.13 \pm 12.53 ^{df}	0.19 \pm 0.01 ^{bcd}
	D-112	21.4 \pm 1.89 ^c	820.44 \pm 75.06 ^b	122.37 \pm 11.09 ^f	0.18 \pm 0.006 ^{cf}

The rate of strength reduction of *C. zizanioides* roots (i.e., reduced by 37.7% after 56 days since herbicide application) was similar to that of the roots of another herbaceous species, *C. dactylon*, reported by Kamchoom et al. (2021), who also applied the same herbicide agent and the same concentration to introduce root decomposition and observed a strength reduction of 40% after 60 days since herbicide application. However, the rate of strength drop for herbaceous species, in general, was faster than other woody species reported in the literature.



(a)



(b)

Fig 5. 1. The remained percentage of tensile strength, secant modulus, breakage strain, root diameter, unit root biomass per soil volume and root reinforcement of the (a) *C. nemoralis* and (b) *C. zizanioides* species with elapsed time since herbicide application.

For examples, O'loughlin and Watson (1979) and Preti (2013) reported that the tensile strength of the roots of *Pinus radiata* and *Fagus sylvatica* L. species lost 50% of its initial value after 20 months and 4.5 years after stem cutting, respectively. More recently, Zhu et al. (2019) reported that the mean tensile strength of *Symplocos setchuensis* reduced only 17.9% of their original strength after 12 months since stem cutting. The observed differences among the literature and the present study can be partially explained by the difference in the diameter of fibrous and woody roots. For example, the diameter of the fibrous roots we tested was less than 2 mm, which was at the low end of the range of woody roots reported in the literature (e.g., varying widely from 1 to 10 mm in Preti (2013), Vergani et al. (2014) and Zhu et al. (2019). Given a higher ratio of surface area per volume contacted to detritivores and bacteria, which cause of organic matter decomposition, thinner roots are more prone to decomposition (Silver and Miya, 2001). The mortality cause is also a possible reason that attributes to the difference in the decline rate of root strength between the present and past studies (Vergani et al., 2017). While the cause of root mortality in our study was by herbicide application, root decomposition in most of the literature on woody species was introduced by timber harvesting or wildfires. In addition, Kamchoom et al. (2021) demonstrated that the tensile strength of decomposed roots due to herbicide application declined at a rate that was faster than those of roots decomposed by burning.

By contrast, the Young's modulus of the two tested species has no significant difference over the entire root decomposition periods (i.e., 112 days; Table 5. 1; p -value >0.05). Similar findings were reported by O'loughlin and Watson (1979), Watson et al. (1999) and Ammann et al. (2009) for decomposing roots of *Pinus radiata* and *Picea abies* species due to stem cutting and felling, respectively. We note that the estimation of Young's modulus could be subjective because of the difficulties to objectively identify a linear portion of a tensile stress-strain curve which is often curved at small strains (Boldrin et al., 2018; Kamchoom et al., 2021; Wu et al., 2021). However, at large tensile strain (e.g., at the breakage strain), significant reduction of root secant modulus (E_s) due to root decomposition was found (Table 5. 1 and Fig 5. 1; p -value <0.05), as expected following the reduction of both root strength and

breakage strain (Eq. 3.3). Indeed, after 112 days since herbicide application, when compared with the control (i.e., D-0), the mean secant modulus reduced by 41.4% (for *C. nemoralis* species) and by 35.3% (for *C. zizanioides* species), respectively. The root secant modulus has been recognised as an indispensable input parameter (compared with Young's modulus) for limited root reinforcement models available in the literature (e.g., Schwarz et al. (2013)). The fact that both the root strength and secant modulus reduced with decomposition duration implied drops of soil reinforcement and slope stability. Despite the important role of root modulus, the corresponding data (both initial and secant modulus) are scarce, compared with the root strength. More investigation on the changes in root modulus (in addition to root strength) upon decomposition are needed to inform the formulation of root reinforcement models and then to improve the predictability of soil stability.

We also found a significant decline of breakage strain due to the root decomposition (p -value <0.05 ; Table 5. 1). After 112 days of root decomposition (D-112), the root breakage strain of *C. nemoralis* and *C. zizanioides* dropped by 35% and 18.2% of their original value obtained at the fresh state (D-0), respectively (Fig 5. 1). The decline of root breakage strain (or increased brittleness) was also reported for *S. setchuensis* (Zhu et al., 2019), again explained by the change of both the cellulose and lignin contents. Recently, the root breakage strain, which indicates the root brittleness, is recognised to play an important role in pre-failure kinematics and mobility of vegetated soils (Wu et al., 2021). The greater the root brittleness, the smaller the tensile strain required to fully mobilise the root tensile strength and also the smaller shear strain needed to fully mobilise the shear strength of root-reinforced soils, especially at low confinements.

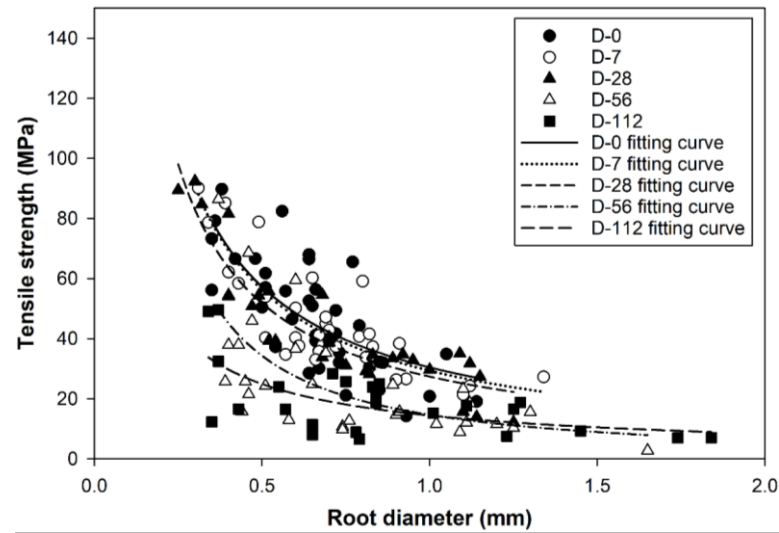
5.3. The influence of root decomposition on diameter-strength and diameter-modulus correlations of *C. nemoralis* and *C. zizanioides* species

Similar to the fresh root (D-0), both root tensile strength and secant modulus of decomposing roots of the two species significantly decreased with root diameter at failure (d_f) (p -value <0.05) (Fig 5. 2 and Fig 5. 3). Negative power correlations were identified, expressed by Eqs. 5.1 and 5.2:

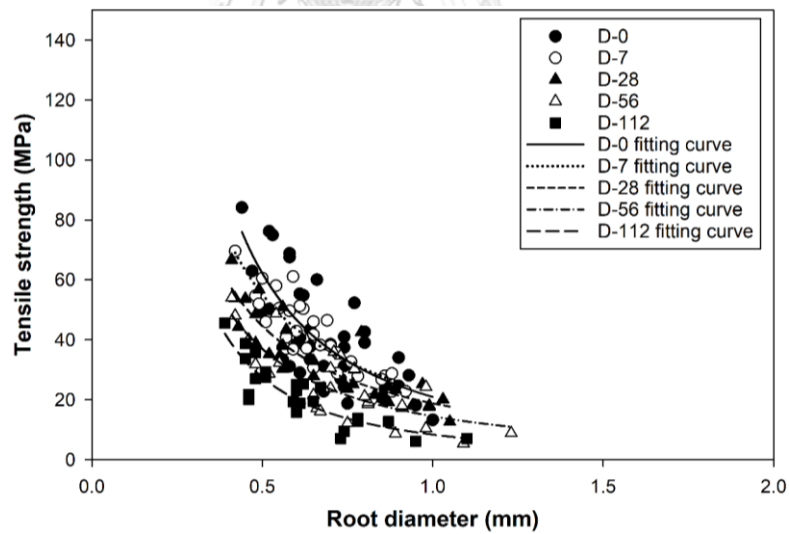
$$T_r = a * d_f^\alpha \quad (5.1)$$

$$E_r = b * d_f^\beta \quad (5.2)$$

where a and b are the scale factor; α and β are the shape factor of the power law.



(a)



(b)

Fig 5. 2. The correlations between tensile strength (T_r) – diameter (d_f) of (a) *C. nemoralis* and (b) *C. zizanioides* subjected to different durations of root decomposition. The equation and R^2 of each fitting are summarised in Table 5. 2.

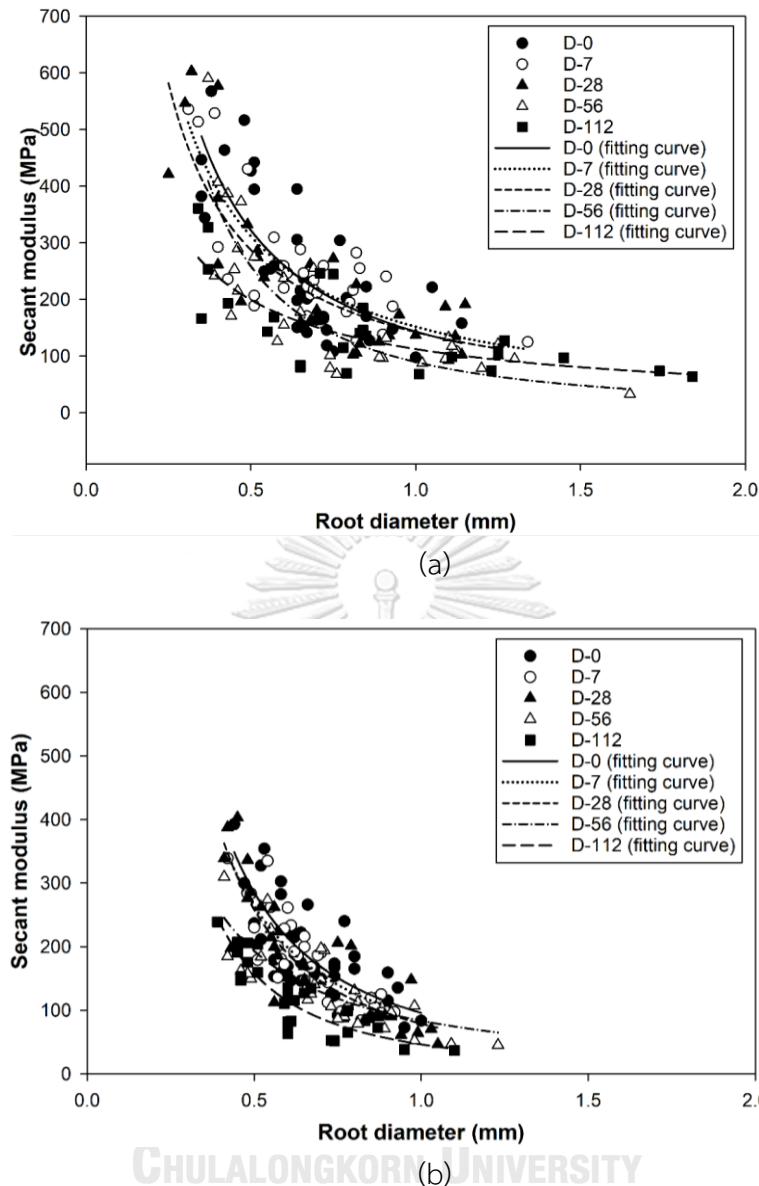


Fig 5. 3. The correlations between secant modulus (E_s) – diameter (d_f) of (a) *C. nemoralis* and (b) *C. zizanioides* subjected to different durations of root decomposition. The equation and R^2 of each fitting are summarised in Table 5. 3.

These factors of each decomposition duration are summarized in Table 5. 2 and Table 5. 3 for the tensile strength and secant modulus, respectively. These correlations have been commonly proposed for vetiver species (Wu et al., 2021). As mentioned in the section 4.4, this negative correlation between root biomechanical properties (i.e., tensile strength and secant modulus) and root diameter could be explained by root anatomy (Chimungu et al., 2015), cellulose and lignin content (Genet et al., 2005; Zhang et al., 2014) and root moisture (Wu et al., 2021). Careful

inspections of the fitted curves and the fitting parameters suggest that the root decomposition did not substantially affect the shape the correlations in both cases. Indeed, the shape factors (α and β), as summarised in Table 5. 2 and Table 5. 3 have minimal variability, compared with the scale factors (a , b) which showed consistent reduction with the decomposition duration. This means that the root decomposition caused a downward shift of the correlation. This finding suggests that the root decomposition did not substantially affect the diameter dependency of the two biomechanical properties.

Table 5. 2. Summary of the fitting parameters (a and α), R^2 value and p -value of the power correlation ($T_r = a*d_f^\alpha$) between tensile strength (T_r) and root diameter (d_f) of the *C. nemoralis* and *C. zizanioides*.

Species	Treatment	n	a	α	R^2	p -value
<i>C. nemoralis</i>	D-0	37	26.1	-1.129	0.56	<0.05
	D-7	33	29.86	-0.909	0.74	<0.05
	D-28	31	25.98	-0.985	0.86	<0.05
	D-56	30	14.88	-1.203	0.42	<0.05
	D-112	25	15.15	-0.7	0.39	<0.05
<i>C. zizanioides</i>	D-0	40	20.09	-1.577	0.55	<0.05
	D-7	34	21.46	-1.381	0.76	<0.05
	D-28	32	18.63	-1.261	0.8	<0.05
	D-56	27	12.73	-1.567	0.65	<0.05
	D-112	27	7.83	-1.815	0.75	<0.05

Table 5. 3. Summary of the fitting parameters (b and β), R^2 value and p -value of the power correlation ($E_s = b*d_f^\beta$) between secant modulus (E_s) and root diameter (d_f) of the *C. nemoralis* and the *C. zizanioides*.

Species	Treatment	n	b	β	R^2	p -value
<i>C. nemoralis</i>	D-0	37	133.41	-1.21	0.6	<0.05
	D-7	33	152.82	-0.98	0.69	<0.05
	D-28	31	134.37	-1.04	0.72	<0.05
	D-56	30	100.1	-1.25	0.69	<0.05
	D-112	25	109.6	-0.75	0.56	<0.05
<i>C. zizanioides</i>	D-0	40	94.59	-1.54	0.61	<0.05
	D-7	34	83.7	-1.66	0.75	<0.05
	D-28	32	71.86	-1.82	0.78	<0.05
	D-56	27	72.55	-1.44	0.6	<0.05
	D-112	27	42.56	-1.86	0.76	<0.05

5.4. Deterioration of mechanical reinforcement of decomposing roots of *C. nemoralis* and *C. zizanioides* species

Following root decomposition (D-7, D-28, D-56 and D-112), the shape of the stress-displacement curves remained similar in each case, displaying a similar strain-hardening behaviour to the fallow case without approaching any plateau (Fig 5. 4). However, this study highlighted the significant influence of root decomposition due to herbicide application on the shearing behaviour of root-reinforced soils (p -value<0.05;). Indeed, there was an evident downward shift of the entire curves, resulting in a drop of the shear stress at any displacement. The same phenomena occurred for all confinements and both species. The initial stiffness of soil reinforced by decomposing roots also dropped, especially under small and moderate confinements. Despite of the strength drop, after 112 days of root decomposition, the ultimate shear stress (at 10 mm displacement) of soils reinforced by decomposing roots remained higher than that of the fallow case.

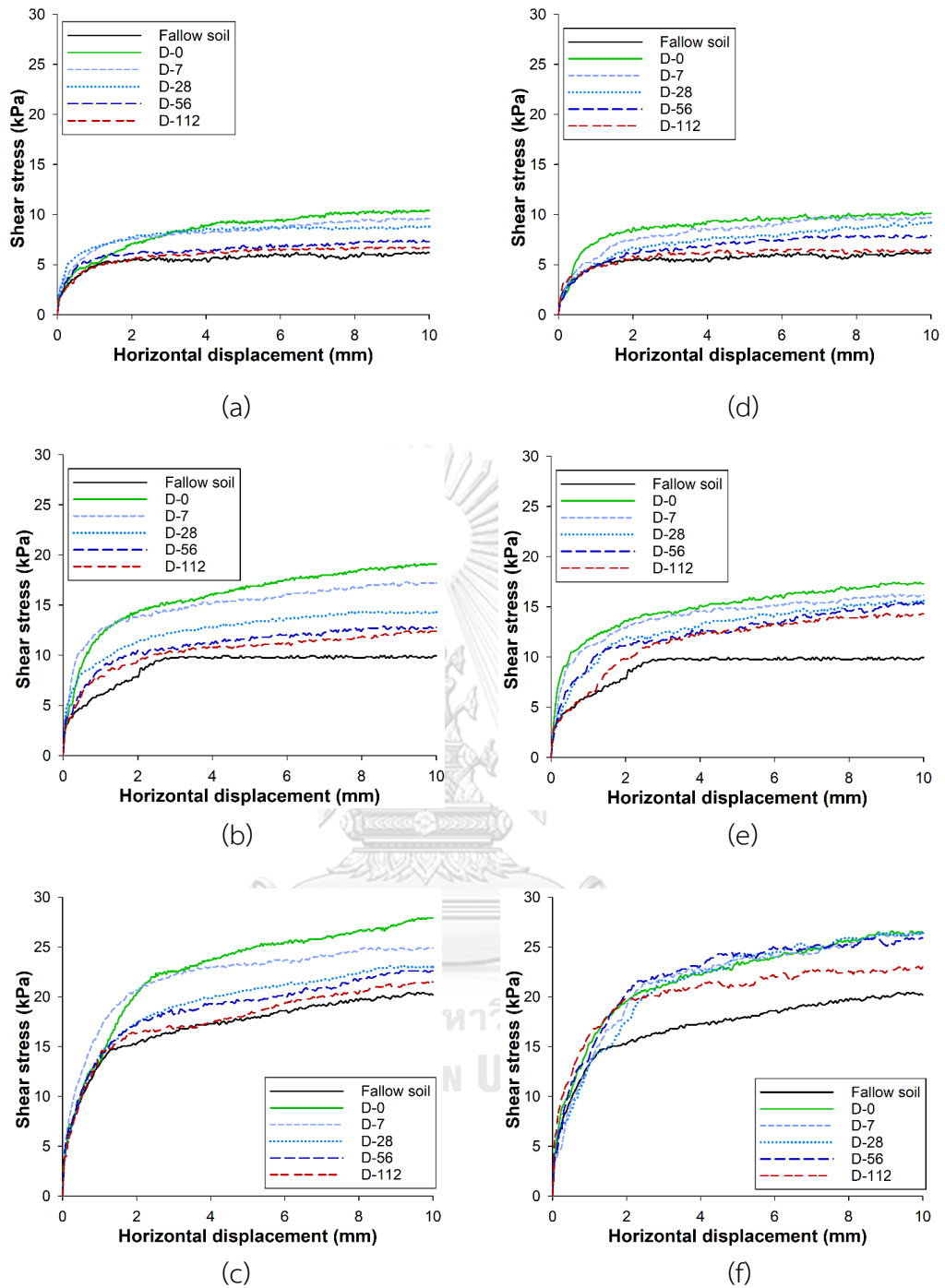
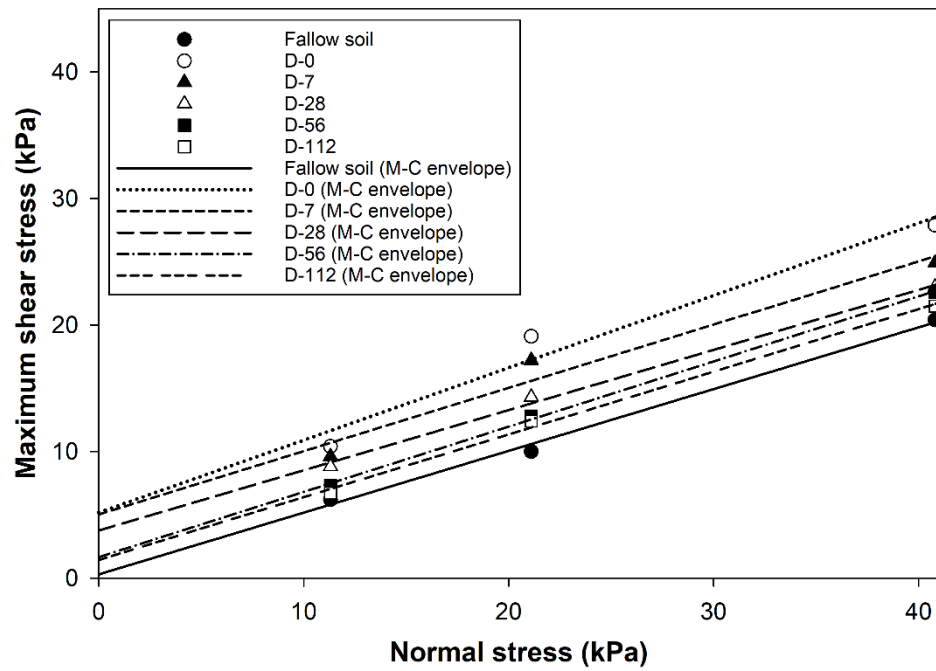
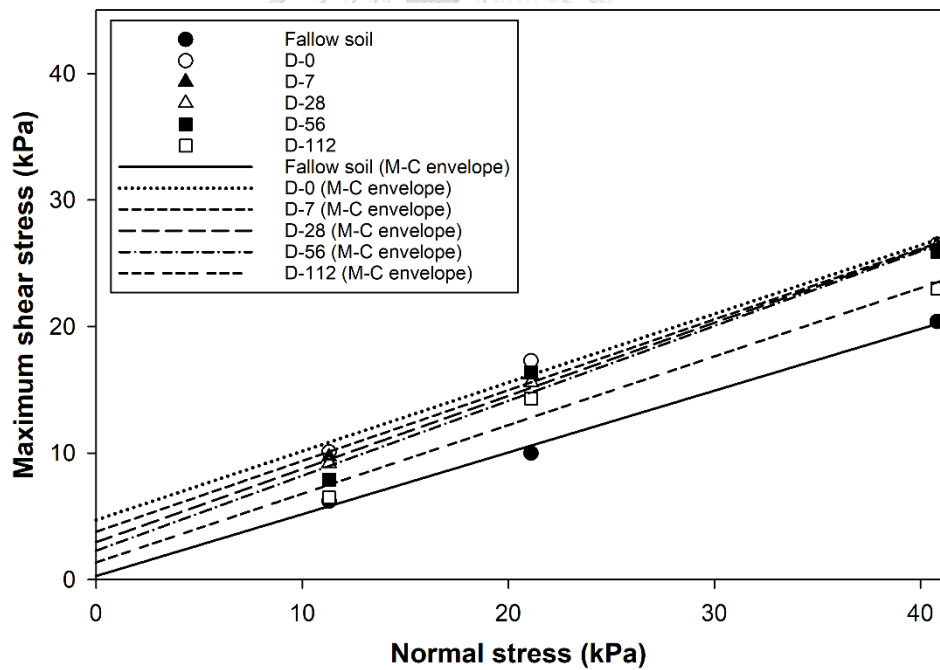


Fig 5. 4. Shear stress-displacement curves of fallow soil and soil reinforced by roots of *C. nemoralis* and *C. zizanioides* subjected to different durations of root decomposition under confining stress of (a) and (d) 11.3 kPa, (b) and (e) 21.1 kPa, (c) and (f) 40.8 kPa.

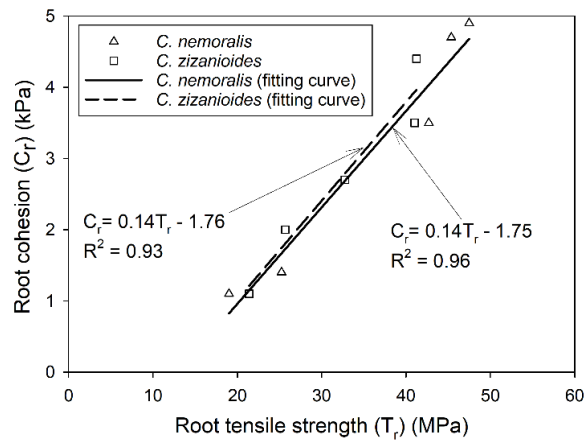


(a)

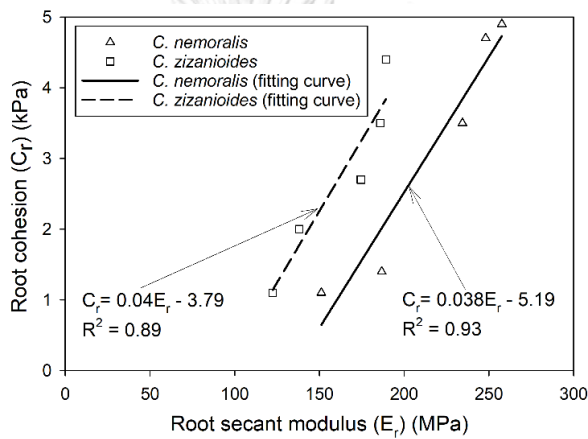


(b)

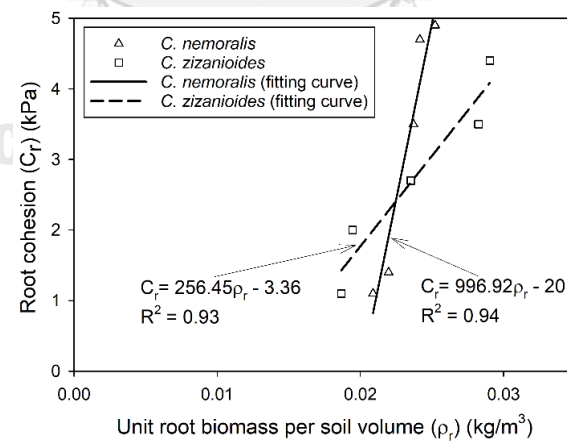
Fig 5. 5. Derived Mohr-Coulomb failure envelopes for the fallow soil and the soils reinforced by the roots of (a) *C. nemoralis* and (b) *C. zizanioides*



(a)



(b)



(c)

Fig 5. 6. Correlations between root cohesion and (a) root tensile strength, (b) secant modulus, (c) unit root biomass per soil volume of *C. nemoralis* and *C. zizanioides* species.

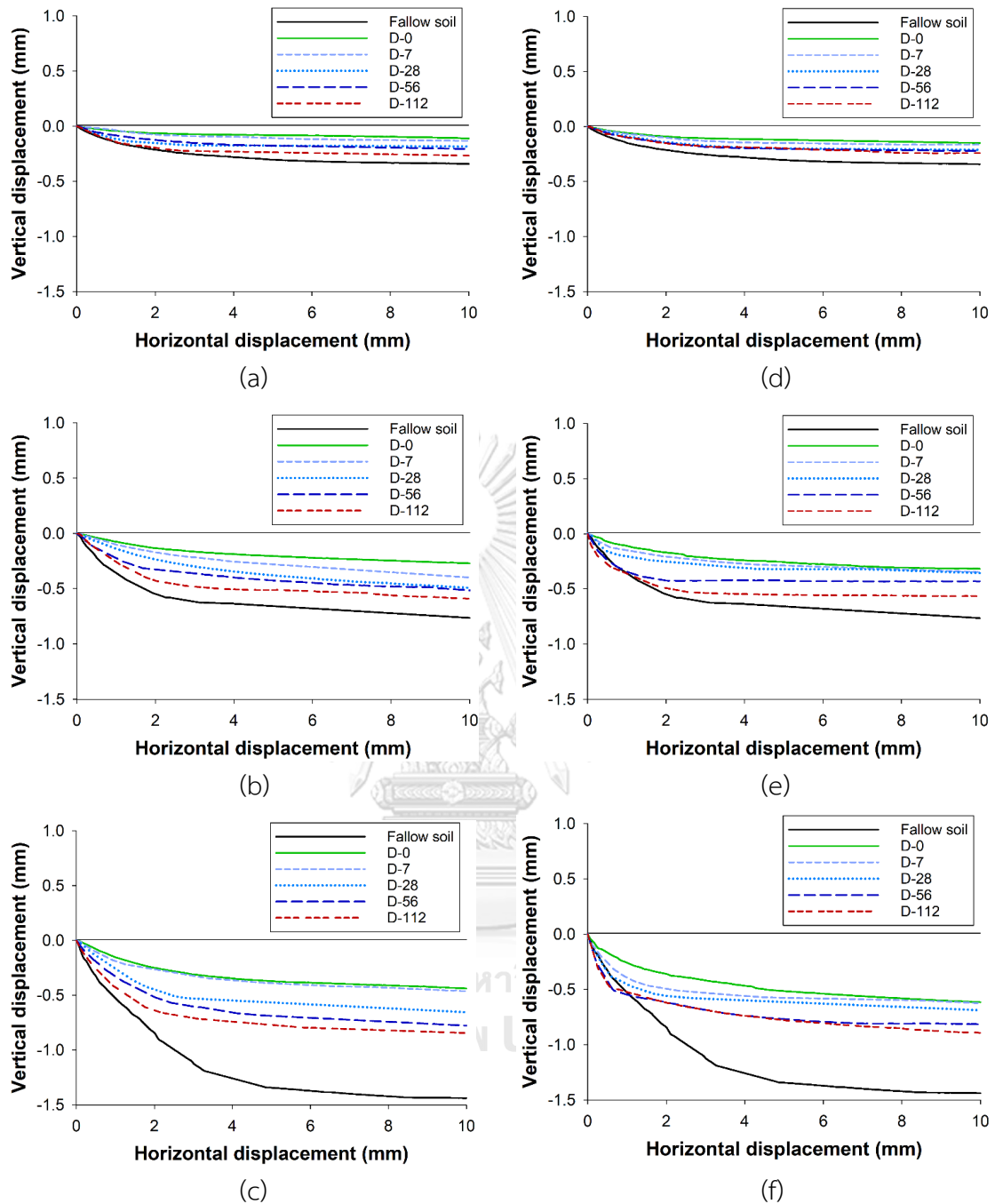


Fig 5. 7. Vertical displacement-horizontal displacement curves of fallow soil and soil reinforced by roots of *C. nemoralis* and *C. zizanioides* subjected to different durations of root decomposition under confining stress of (a) and (d) 11.3 kPa, (b) and (e) 21.1 kPa, (c) and (f) 40.8 kPa.

Relying on the Mohr-Coulomb failure envelopes as shown in Fig 5. 5, the main influence was found in the reduction of root cohesion of both *C. nemoralis* and *C. zizanioides* species. The C_r of both species significantly reduced (comparing to D-0)

after 112 days since herbicide application (p -value <0.05) (Fig 5. 1 and Table 5. 4). Indeed, the root decomposition reduced the C_r of the soils reinforced by *C. nemoralis* and *C. zizanioides* substantially by 77.6% (i.e., from 4.9 kPa to 1.1 kPa) and 75% (i.e., from 4.4 kPa to 1.1 kPa), respectively, after 112 days of decomposition. As highlighted by several studies (e.g., [Ziemer \(1981\)](#), [Vergani et al. \(2016\)](#) and [Zhu et al. \(2019\)](#)), the decline in C_r could be attributed to the reduction in root tensile strength, modulus, root biomass upon root decomposition. Indeed, based on the correlation given in Fig 5. 6, the reduction of C_r of *C. nemoralis* and *C. zizanioides* could be explained by the reduction of tensile strength (96% and 93%), secant modulus (93% and 89%) and, unit root biomass per soil volume (94% and 93%). It can be seen that the rate of the decline of root cohesion for the case of *C. nemoralis* was faster than that of *C. zizanioides* (Fig 5. 1). Again, this could be explained by the biomechanical properties of *C. nemoralis* species reduced at a rate that was faster than those of *C. zizanioides* species due to the root decomposition. Indeed, after 112 days, when compared with the control (i.e., D-0), the mean tensile strength, secant modulus and breakage strain reduced by 60%, 41.4% and 35% (for *C. nemoralis* species) and by 48.1%, 35.3% and, 18.2% (for *C. zizanioides* species), respectively. The root reinforcement of two vetiver species reduced following the negative exponential function with time (Fig 5. 8). This trend was mostly proposed to predict the reduction of root strength/force in the literature ([O'loughlin and Watson, 1979](#); [Vergani et al., 2016](#)). In addition, at the end of the root decomposition (i.e., 112 days), a minimum C_r (1.1 kPa) was found for both species, but it was slightly above the value for the fallow soil. It means that the protective function to vegetated slope of two vetiver species is still remained after 112 days since herbicide application. Therefore, the residual root reinforcement should be used for designing the vegetated slope to eliminate the effect of root decomposition. The reduction rates of C_r following root decomposition of the *C. nemoralis* and *C. zizanioides* species in our study (0.034 kPa/day and 0.03 kPa/day) were greater than those of *S. setchuensis* reported in [Zhu et al. \(2019\)](#) (0.017 kPa/day). The difference in the reduction rate could be explained by the differences in root biomechanical

properties (i.e., tensile strength, secant modulus) between herbaceous (this study) and woody species (Zhu et al., 2019).

By contrast, root decomposition introduced minimal changes in the peak friction angle for the entire period of root decomposition (i.e., $< 4.6^\circ$; Table 5. 4 and Fig 5. 5). Indeed, the roots in the direct shear box were predominantly orientated vertically and thus largely perpendicularly to the shear plane applied. Following the stress path of direct shearing, the roots in this case however were not in the most optimal orientation to mobilise the roots' tensile properties and the interface friction (Karimzadeh et al., 2021). The major mechanism of root reinforcement, in this case, is through apparent soil bonding (i.e., via C_c) due to the root tangling of the soil particles.

Table 5. 4. Summary of the results of the direct shear test for the fallow soil and soils reinforced by the *C. nemoralis* and the *C. zizanioides*.

Treatments		Soil strength parameters	
		c (kPa)	ϕ ($^\circ$)
Bare soil		0.3	26
Soil reinforced by <i>C. nemoralis</i>	D-0	5.2	29.8
	D-7	5	26.6
	D-28	3.8	24.6
	D-56	1.7	27.3
	D-112	1.4	26.4
Soil reinforced by <i>C. zizanioides</i>	D-0	4.7	28.5
	D-7	3.8	29.2
	D-28	3	30
	D-56	2.3	30.6
	D-112	1.4	26.4

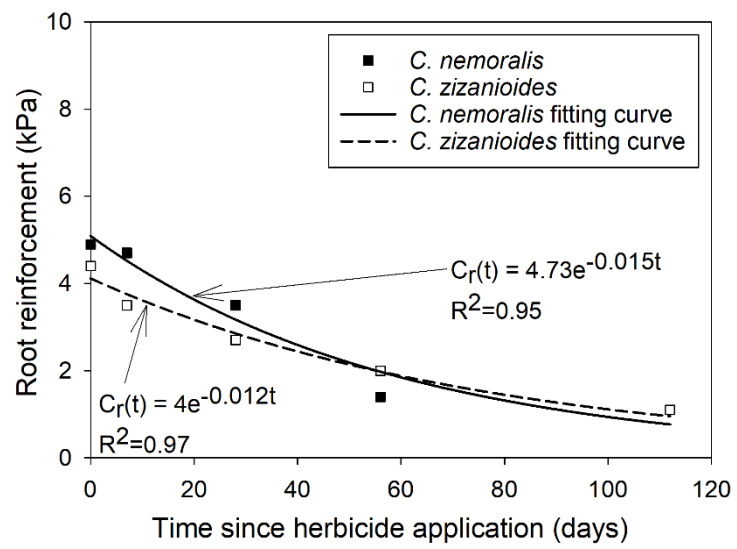
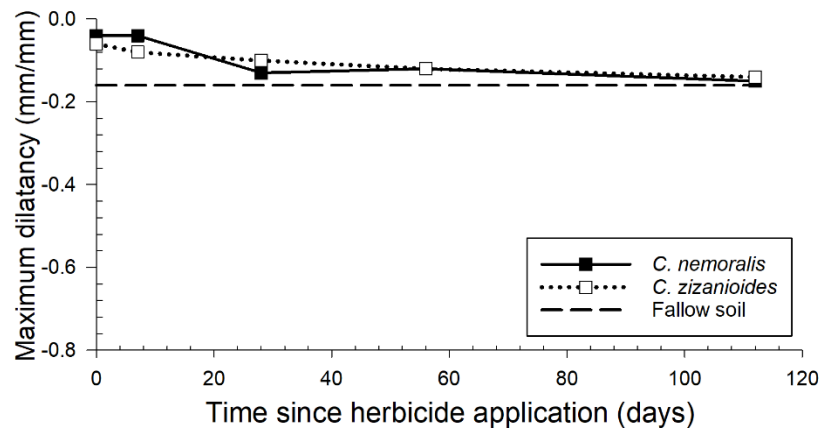
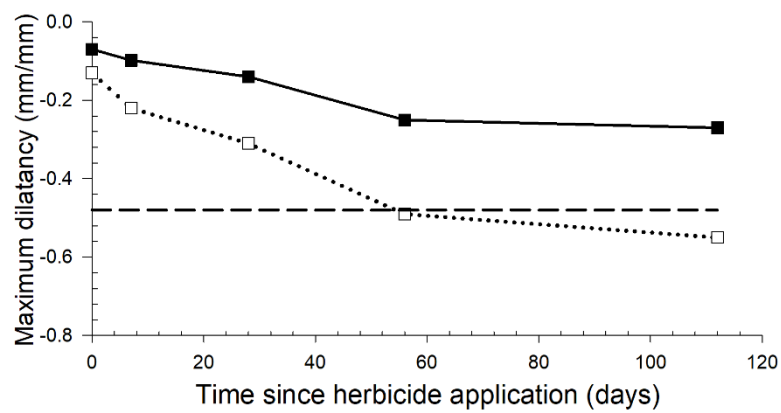


Fig 5. 8. Variation of root reinforcement during the decomposition

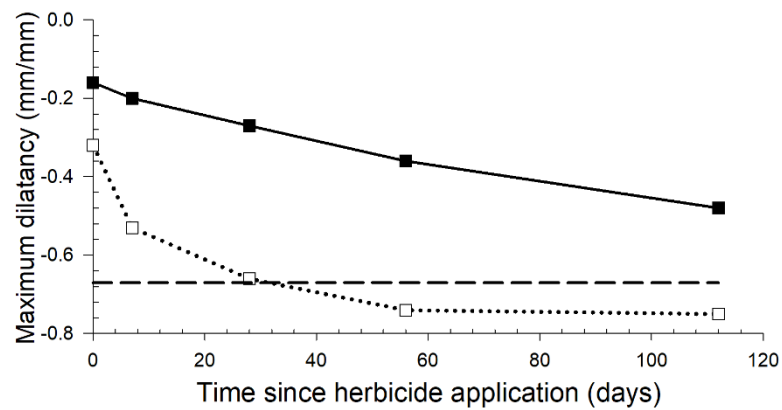




(a)



(b)



(c)

Fig 5. 9. Variation of maximum dilatancy of fallow soil and soil reinforced by *C. nemoralis* and *C. zizanioides* species subjected to different durations of root decomposition under confining stress of (a) and (d) 11.3 kPa, (b) and (e) 21.1 kPa, (c) and (f) 40.8 kPa

Comparing vertical displacement-horizontal displacement curves, we found that soil reinforced by decomposed roots became more contractive with increasing duration of root decomposition (Fig 5. 7). Indeed, consistently, the maximum dilatancy of soil reinforced by decomposed root reduced with time of decomposition (Fig 5. 9). For instance, when compared to the control treatment (D-0) under confining pressure of 40.8 kPa, the maximum dilatancy of soil reinforced by *C. nemoralis* and *C. zizanioides* roots reduced by 200% (from -0.16 to -0.48 mm/mm) and 134.3% (from -0.32 to -0.67 mm/mm), respectively. The phenomenon could be attributable to the reduction of root diameter and root biomass upon decomposition (Fig 5. 1). As root diameters reduced following decomposition, the soil pore space, which was initially occupied by fresh roots (D-0), would be returned, making soil 'feel' apparently looser (Ni et al., 2019). This soil-root interaction would increase the soil porosity and then be more susceptible to soil instability (Ni et al., 2018; Shao et al., 2017). The continual reduction of the maximum dilatancy implies the reduced abilities of the decomposing roots to mobilise their biomechanical strength to enhance the soil strength (Fig 5. 1 and Fig 5. 4). It was noteworthy that, under moderate (i.e., 21.1 kPa) and high (i.e., 40.8 kPa) confinements, the maximum dilatancy of *C. zizanioides* species declined more rapidly than those of *C. nemoralis* species. Indeed, *C. zizanioides* had a higher reduction rate of unit dry root biomass per soil volume than *C. nemoralis* (Fig 5. 1). Importantly, the maximum dilatancy of *C. zizanioides*, after 56 days of root decomposition, dropped below the level of the fallow soil case, at the confining pressures of 21.1 and 40.8 kPa (Fig 5. 8). These observations partially explain why the respective reinforced soils (for the case of D-112; Fig 5. 4) required higher shear displacement to mobilise the shear stress at any displacement. Effects of roots on soil dilatancy are crucial to be quantified to gain insights into the mobilisation of root biomechanical properties to the enhancement of soil shear strength, but this phenomenon has rarely been reported and discussed except Mahannopkul and Jotisankasa (2019b) and Yildiz et al. (2018). Given the lack of data and comparison, we suggest more emphasis of the measurements of the root-induced soil dilatancy in future work. Indeed, vertical displacement upon shearing,

hence the maximum dilatancy (and its relationship with shear stress), are readily available following the conventional procedures of a direct shear testing.

5.5. Concluding remarks

The biomechanical properties (i.e., tensile strength, Young's modulus, secant modulus, and breakage strain) and mechanical reinforcement of decomposing roots of two contrasting vetiver species, *C. nemoralis* and *C. zizanioides* subjected to different durations of decomposition following herbicide application were measured from a series of laboratory uniaxial tensile strength tests and direct shear tests. The following conclusions may be drawn:

Both species demonstrated significant reduction of root tensile strength, secant modulus and breakage strain with the duration of root decomposition. *C. nemoralis* displayed greater drops of these biomechanical properties and took less duration to drop below 50% of the initial values compared with *C. zizanioides*.

Both species consistently displayed significant negative power law correlations between root diameter and root tensile strength (R^2 varied from 0.39 to 0.86; p -value <0.05) and between root diameter and root secant modulus (R^2 varied from 0.56 to 0.78; p -value <0.05). Following root decomposition, the shapes of these correlations remained largely similar, but the correlations shifted downward as the duration of root decomposition increased.

Despite the enhancement of soil shear strength due to the presence of roots, root decomposition significantly reduced the root cohesion with increasing decomposition duration (p -value < 0.05), for both the test species. *C. nemoralis* displayed a greater and quicker loss of root reinforcement than *C. zizanioides* following decomposition. The root cohesion of both species reached about 75% of the original value after 112 days since the herbicide application. Root cohesion can be explained by root strength, root secant modulus and biomass, all with a R^2 of more than 90%. By contrast, the peak friction angle of the reinforced soil, irrespective to the species, showed minimal changes for the entire duration of decomposition tested.

The presence of roots reduced the maximum dilatancy of the soil, but the maximum dilatancy significantly declined with increasing duration of decomposition

following the reductions of root diameter and biomass as root decomposed. Similarly, *C. zizanioides* displayed a greater and quicker reduction of the maximum dilatancy compared with *C. nemoralis*. The root-induced changes in soil dilatancy have shown to affect the shear displacement required to mobilise the same shear stress, especially at intermediate (21.1 kPa) and high (40.8 kPa) confinements.



Chapter 6: Root reinforcement estimation and stability analysis of slope reinforced by decomposing roots

6.1. Introduction

In this chapter, the root reinforcement (C_r) of decomposing roots of *C. nemoralis* and *C. zizanioides* species was estimated using the Wu's model (WWM) (Wu et al., 1979) and the extended Root Bundle Model (RBMw) (Schwarz et al., 2013) coupled with the modified Wu-Waldron Model (WWM) (Gray and Leiser, 1983). The input parameters include root biomechanical properties (i.e., tensile strength, secant modulus) and root geometry (i.e., root length, root orientation, and root diameter distribution). The procedure of root reinforcement estimation is described in detail. The root reinforcement obtained from WWM and extended RBMw coupled with modified WWM were presented and compared. In addition, the numerical study was conducted using root reinforcement obtained from extended RBMw to investigate the influence of root reinforcement deterioration following root decomposition on the stability of the vegetated slope. The obtained results at different decomposition duration for two vetiver roots are presented and discussed.

6.2. Root reinforcement estimation

6.2.1. Root reinforcement estimation procedure

To estimate the root reinforcement, the Wu's model and extended Root Bundle Model (RBMw) proposed by Wu et al. (1979) and Schwarz et al. (2013) were adopted in this study, respectively. The Wu's model assumed all roots in the bundle are perpendicular to shear plane and break simultaneously. By contrast, roots in the bundle were supposed be parallel to each other and break progressively in the RBMw. In Wu's model, the reinforcement of root bundle is the summation of root reinforcement of each root in the bundle (Eq. 6.1). The RBMw is the strain-step loading root bundle model that could capture the complete force/strength-displacement curve of a root bundle (Mao, 2022). In addition, coupled with Weibull survival function, the RBMw considers the variability of biomechanical properties (i.e., either tensile force or strength) within a root diameter class (Vergani et al., 2017). The

key parameters in this model are the strength-diameter (T_r-d), secant modulus-diameter (E_s-d), length-diameter (L_r-d) correlations, and the root diameter distribution.

$$C_r = 1.2 \times \sum_1^N T_{r_i} \left(\frac{A_{r_i}}{A_s} \right) \quad (6.1)$$

where N is root number in the bundle, T_{r_i} and A_{r_i} are tensile strength and area of i^{th} root, and A_s is soil area.

The Fig 6. 1 illustrates in detail the procedure of root reinforcement estimation using RBMw coupled with the modified WWM. The root biomechanical properties (i.e., tensile strength and secant modulus) obtained from the laboratory were used to calibrate the parameters of T_r-d and E_s-d power-law function as following equations:

$$T_r = T_0 d^\alpha \quad (6.2)$$

$$E_s = E_0 d^\beta \quad (6.3)$$

where F_0 , and E_0 are the scale factor and α and β are shape factor of power law equations. Afterward, the calibrated T_r-d and E_s-d correlations were used to determine the Weibull survival function, which is governed by the shape (ω) and scale (λ) factor as shown in the Eq. 6.4. It is noteworthy that the survival function is widely used to present the failure probability of complex system (Schwarz et al., 2013). In the RBMw, Schwarz et al. (2013) hypothesised that survival probability of roots is a function of the normalized displacement (Δx^*) (Eq. 6.5).

$$S(\Delta x^*) = \exp \left[- \left(\frac{\Delta x^*}{\lambda} \right)^\omega \right] \quad (6.4)$$

$$\Delta x^*(d) = \frac{\Delta x_{\max}^{meas}}{\Delta x_{\max}^{fit}(d)} \quad (6.5)$$

$$\Delta x_{\max}^{fit}(d) = \frac{L_0 T_0}{r E_0} d^{\alpha+\gamma-\beta} \quad (6.6)$$

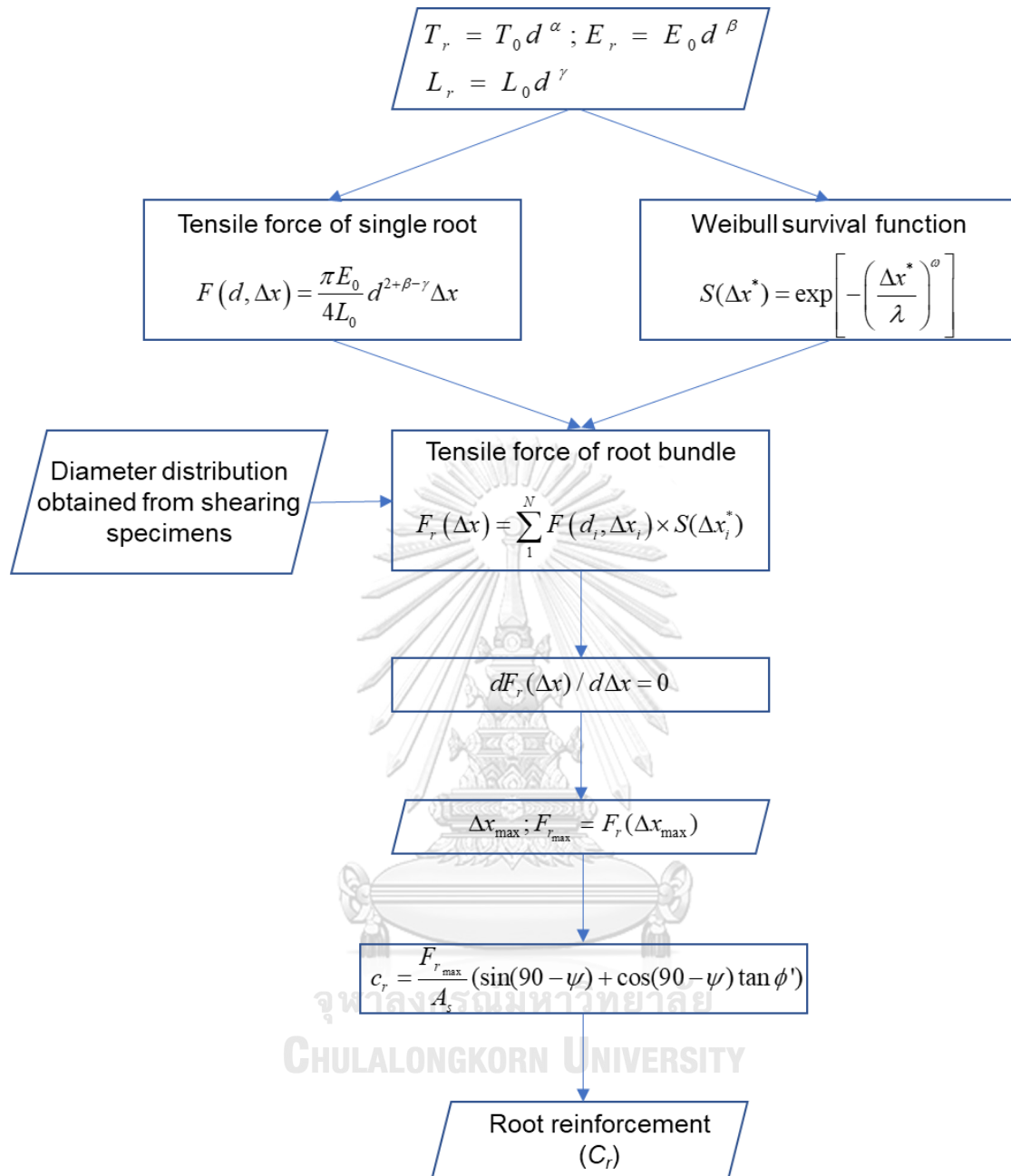


Fig 6. 1. Root reinforcement estimation workflow

In this model, roots in the bundle were considered as the linear-elastic fibres, well anchored into the soil, parallel to each other and break progressively (Schwarz et al., 2013). Thus, the tensile force of a single root can be determined as a function of displacement (Eq. 6.7).

$$F(d, \Delta x) = \frac{r\pi E_0}{4L_0} d^{2+\beta-\gamma} \Delta x, F(d, \Delta x) < F_{\max}(d) \quad (6.7)$$

By summing the force of a single root ($F(d, \Delta x)$) multiplied by the Weibull survival function ($S(\Delta x^*)$), the tensile force ($F_r(\Delta x)$) can be obtained as follows:

$$F_r(\Delta x) = \sum_1^N F(d_i, \Delta x_i) \times S(\Delta x_i^*) \quad (6.8)$$

where N is the number of roots in the root bundle and d_i is diameter of the i^{th} root in the bundle. By substituting the root diameter distribution into the Eq. 6.8, the tensile force of root bundle become to the function of the displacement (Δx). Thus, the displacement at ultimate bundle tensile force (Δx_{max}) can be obtained by finding the solution of $dF_r(\Delta x)/d(\Delta x) = 0$. Then, the maximum tensile force of the root bundle ($F_{r_{\text{max}}}$) is equal to $F_r(\Delta x_{\text{max}})$.

It is noteworthy that the obtained $F_{r_{\text{max}}}$ is known as the lateral root reinforced or pull-out force. To obtain the shear reinforcement of root bundle, which cross the shear plane, the orientation (i) of root bundle is therefore introduced. The modified Wu-Waldron Model (WWM), which proposed by [Gray and Leiser \(1983\)](#), was adopted to estimate maximum shear reinforcement of the root bundle (C_r) as follows:

$$C_r = \frac{F_{r_{\text{max}}}}{A_s} (\sin(90 - \psi) + \cos(90 - \psi) \tan \phi') \quad (6.9)$$

$$\psi = \tan^{-1} \left[\frac{1}{\frac{\Delta x}{Z} + \frac{1}{(\tan^{-1} i)}} \right] \quad (6.10)$$

A_s is soil area (0.01 m²), Δx is shear displacement (m), Z is thickness of shear zone (2 m) and, i is root initial orientation (49.78° and 50.6° for *C. nemoralis* and *C. zizanioides* species, respectively). The root reinforcement estimation was implemented in a MATLAB code.

6.2.2. Calibration of root parameters, Weibull survival function and root diameter distribution

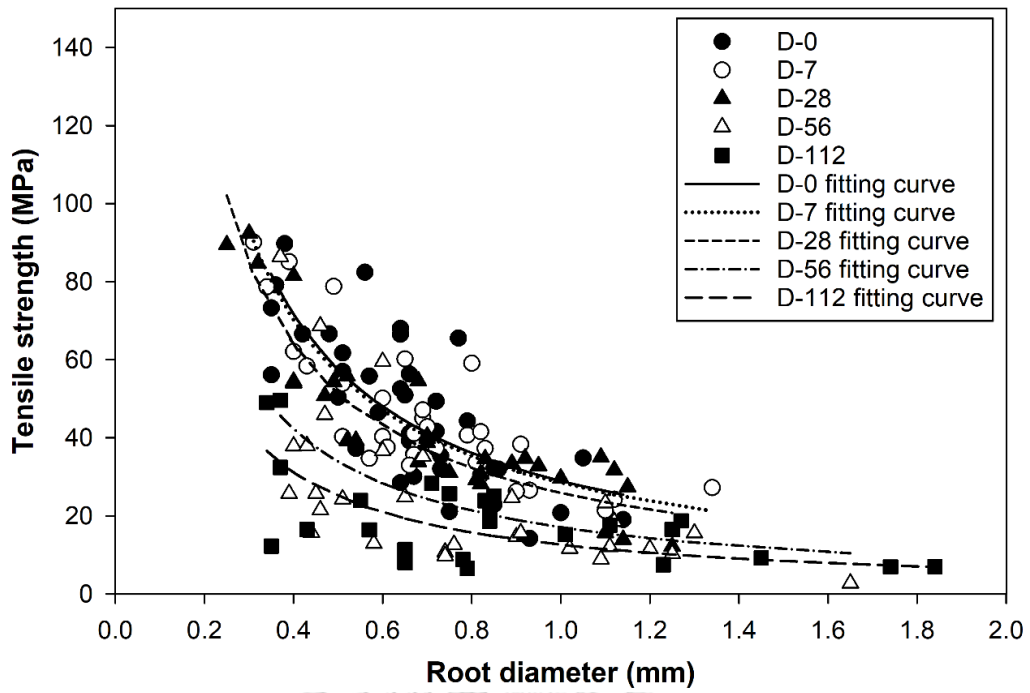
The data from the tensile test of *C. nemoralis* and *C. zizanioides* roots were used to establish the correlations between root diameter and root biomechanical properties (i.e., tensile strength and secant modulus). As discussed in the section 5.3, the root decomposition did not influence on the shape factor (α and β) of T_r-d_f and E_s-d_f

correlations of the two vetiver species. In addition, root secant modulus is linearly correlated to root tensile strength (Eq. 3.3). To make a fair estimation, the shape factor of these correlations was fixed at -0.99 and -1.52 for the treatments of *C. nemoralis* and *C. zizanioides* roots, respectively. The scale (α) and shape factors (T_0 and E_0) of these correlations for the treatments of two vetiver species are summarized in the Table 6. 1. The Fig 6. 2 and Fig 6. 3 show the strength-diameter and secant modulus-diameter correlations of *C. nemoralis* and *C. zizanioides*, respectively. The R^2 value of these correlations reduced not much when the shape factors were fixed. Therefore, it is reasonable to refitting the correlations between root diameter and root biomechanical properties. Another important input parameter in RBMw is the correlation between root length and diameter (L_r-d_f). Unfortunately, root length of two vetiver species was not measured in this study. Therefore, the assumed correlation of root length and diameter for *Panicum virgatum* roots (i.e., grass species) in [Cohen et al. \(2011\)](#) is adopted in this study. The shape (γ) and scale (L_0) factor of length-diameter correlation are 0.7 and 0.4 m, respectively.

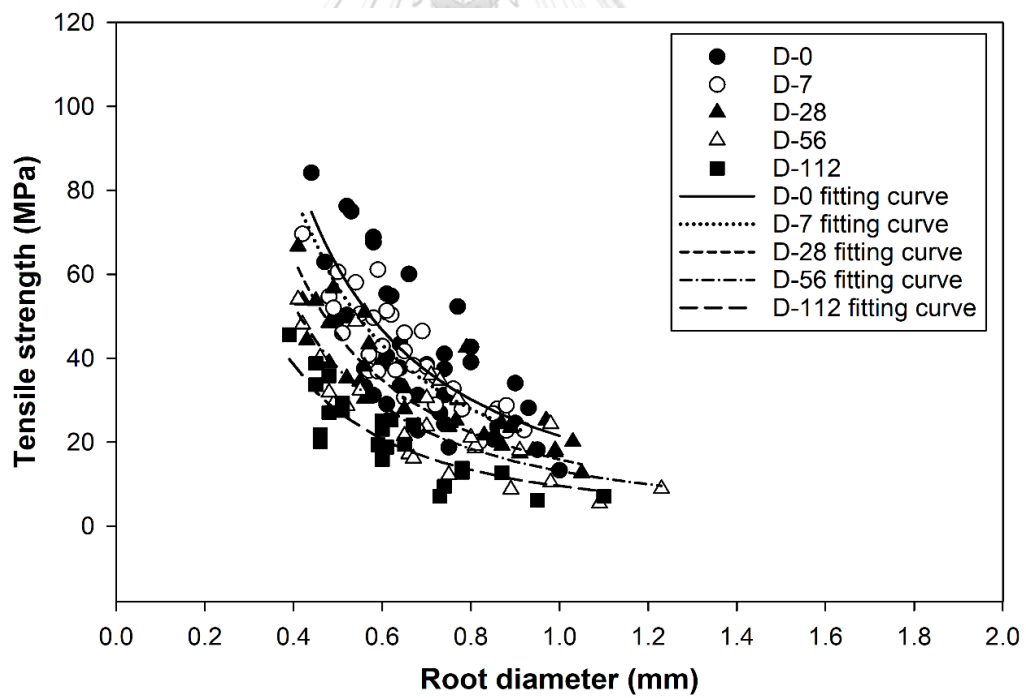
With the calibrated root biomechanical parameters (i.e., T_0 , E_0 , L_0 , α and γ), it is possible to calibrate the Weibull survival function. The relationship between survival probability and normalized displacement of *C. nemoralis* and *C. zizanioides* roots at different decomposition period is illustrated in the Fig 6. 4 and Fig 6. 5, respectively. In addition, the calibrated parameters of Weibull survival function (ω and λ) are reported in the Table 6. 2. The results indicate that Weibull survival function is suitable for capturing the variability of root biomechanical properties within the diameter class for the two vetiver species. Indeed, the R^2 values of the fitting curves were relatively high, which varied from 0.9 to 0.98. In general, the root decomposition introduced the reduction of shape coefficient (ω) for two vetiver species. Indeed, the shape coefficients of control treatment (D-0) were almost double the value of decomposed root treatment after 112 days since herbicide application (D-112; refers to Table 6. 2). This indicates that for the same root diameter, decomposing roots highlighted a higher variability in root tensile strength than that of the growing roots. The similar phenomenon was reported in [Vergani et al. \(2017\)](#) for decomposed roots of *Pinus sylvestris* species.

Table 6. 1. Summary of scale (T_0 and E_0) and shape (α) factors of T_r -d, and E_s -d of *C. nemoralis* and *C. zizanioides* species.

Species	Treatment	α	$T_r = T_0 d^\alpha$		$E_s = E_0 d^\alpha$	
			T_0	R^2	E_0	R^2
<i>C. nemoralis</i>	D-0		28.96	0.54	160.8	0.58
	D-7		28.35	0.73	156.66	0.69
	D-28	-0.99	25.88	0.85	145.32	0.72
	D-56		17.03	0.41	128.49	0.64
	D-112		12.6	0.37	100.84	0.54
<i>C. zizanioides</i>	D-0		21.49	0.55	98.58	0.61
	D-7		19.86	0.74	91.48	0.75
	D-28	-1.52	15.86	0.77	89.05	0.77
	D-56		13.1	0.65	69.56	0.57
	D-112		9.51	0.74	54.59	0.75

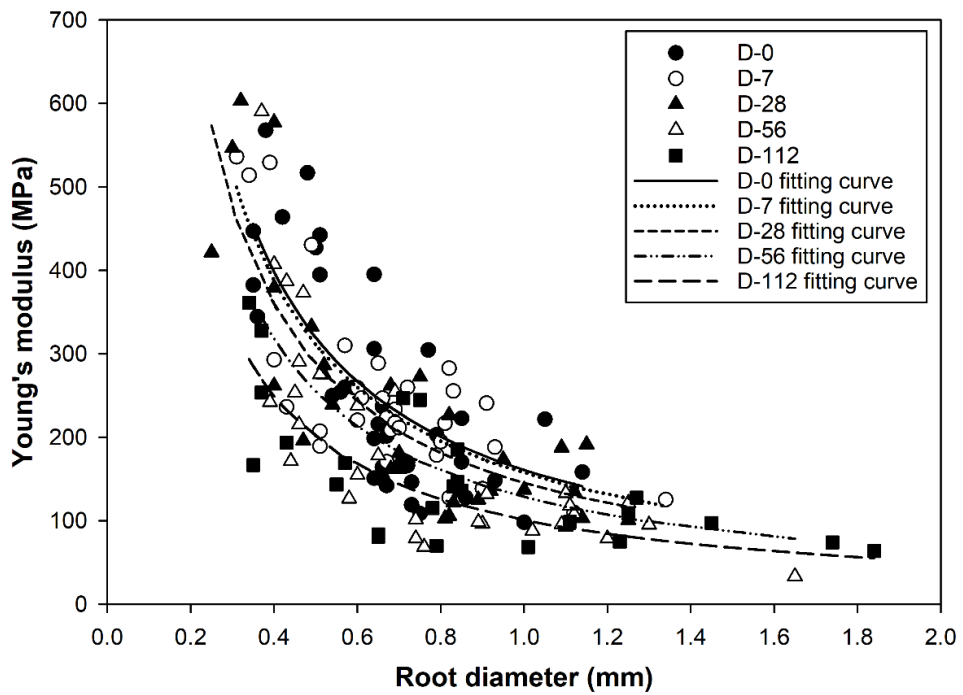


(a)

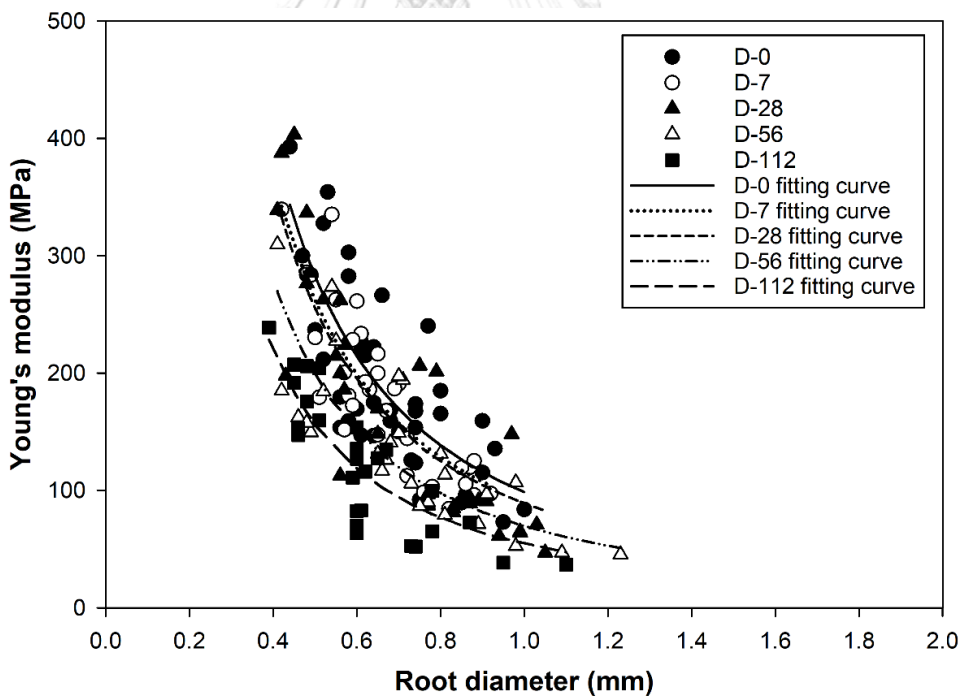


(b)

Fig 6. 2. Tensile strength-diameter correlations (T_r - d) of (a) *C. nemoralis* and (b) *C. zizanioides* species (shape factor a is fixed).



(a)



(b)

Fig 6. 3. Secant modulus-diameter correlations (E_s - d) of (a) *C. nemoralis* and (b) *C. zizanioides* species (shape factor b is fixed).

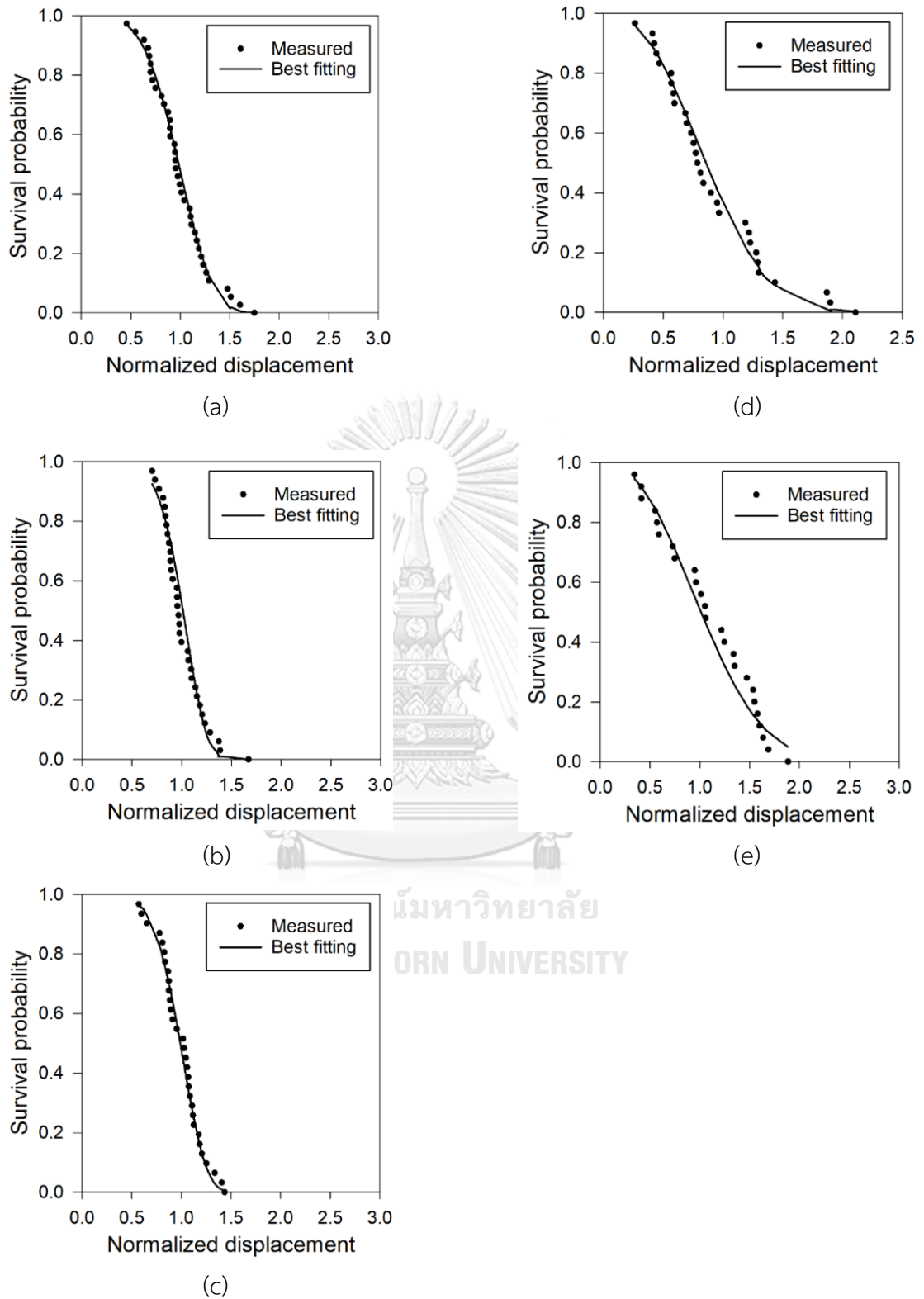


Fig 6. 4. Survival probability of *C. nemoralis* decomposed roots at 0, 7, 28, 56 and, 112 days since herbicide application

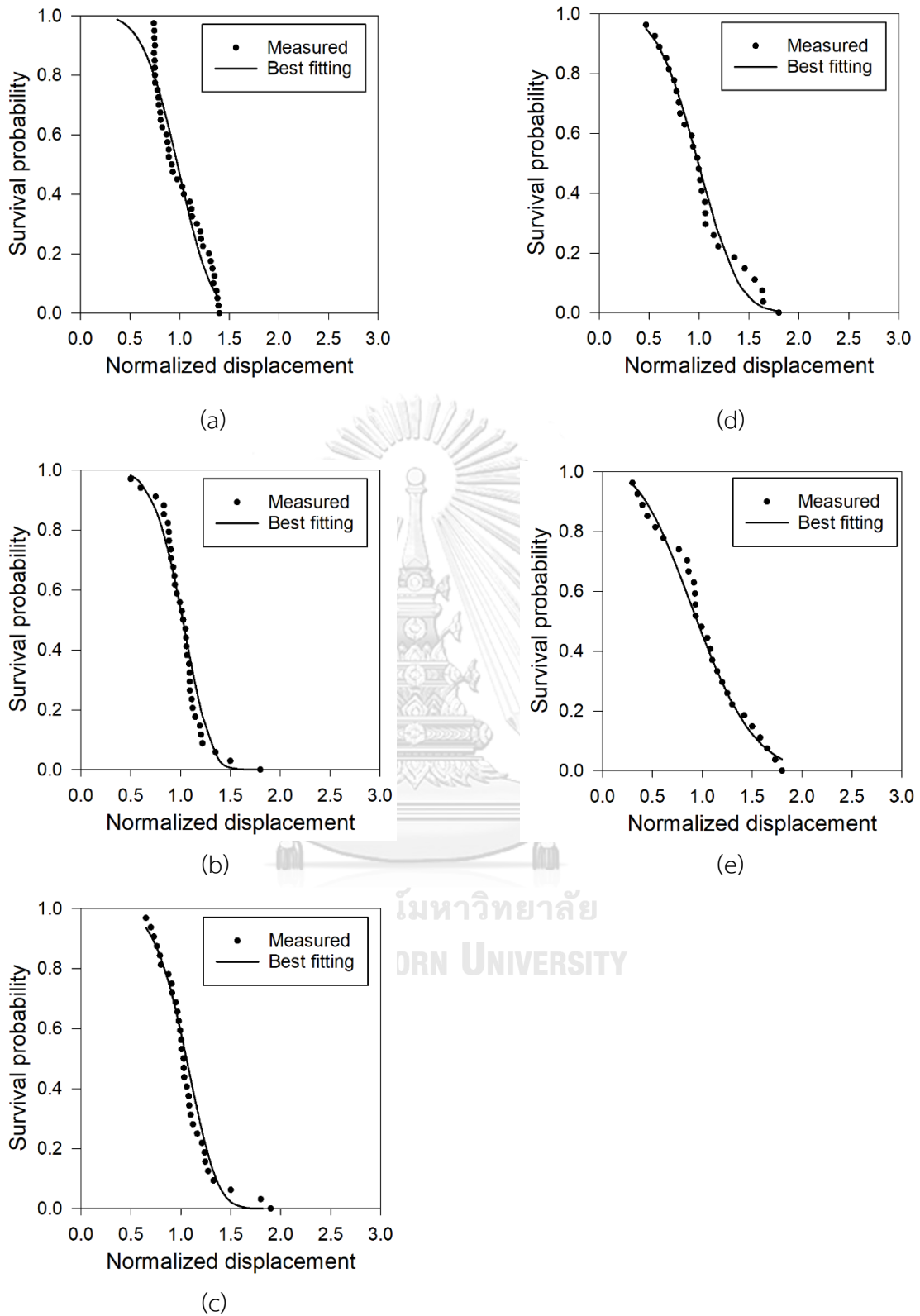


Fig 6. 5. Survival probability of *C. zizanioides* decomposed roots at 0, 7, 28, 56 and, 112 days since herbicide application.

Table 6. 2 Summary of shape (ω) and scale (λ) factors of Weibull survival function for *C. nemoralis* and *C. zizanioides* roots.

Species	Treatment	λ	ω	R ²
<i>C. nemoralis</i>	D-0	1.1	4.07	0.98
	D-7	1.1	6.0	0.94
	D-28	1.1	5.29	0.97
	D-56	1.0	2.4	0.97
	D-112	1.1	2.36	0.93
<i>C. zizanioides</i>	D-0	1.1	4.11	0.9
	D-7	1.1	5.13	0.95
	D-28	1.1	4.85	0.94
	D-56	1.1	3.5	0.97
	D-112	1.1	2.42	0.95

Root diameter distribution is considered an essential parameter in RBMw, which significantly influences root reinforcement. In this study, the root diameter distribution was obtained from the shearing specimens. As discussed in the section 5.4, the root diameter of two vetiver species was significantly reduced due to the root decomposition. It is noted that the shearing specimens were collected from different soil columns for different decomposition treatments. Thus, the change in root number over the decomposition duration cannot be observed. To make a fair estimation, the change in root number was ignored in this study. The root diameter distribution was derived from fresh root (D-0) data and mean root diameter reduction. The fresh root diameter distribution of *C. nemoralis* and *C. zizanioides* species Fig 4. 6.

6.2.3. Estimated reinforcement of decomposing roots

The Fig 6. 6 and Fig 6. 7 show the simulated using the RBMw and measured shear stress-strain curve over 10 mm of displacement of soil reinforced by *C. nemoralis* and *C. zizanioides* roots, respectively. Considering the control treatments (D-0), the RBMw underestimated the contribution of *C. nemoralis* and *C. zizanioides* to soil strength. This could be explained by the use of secant modulus, which obtained at the failure strain, to estimate the root reinforcement in RBMw. In addition, roots are

considered as linear fibers in the RBMw. Therefore, in the RBMw, roots could be mobilised their strength at the larger strain than the roots in soil.

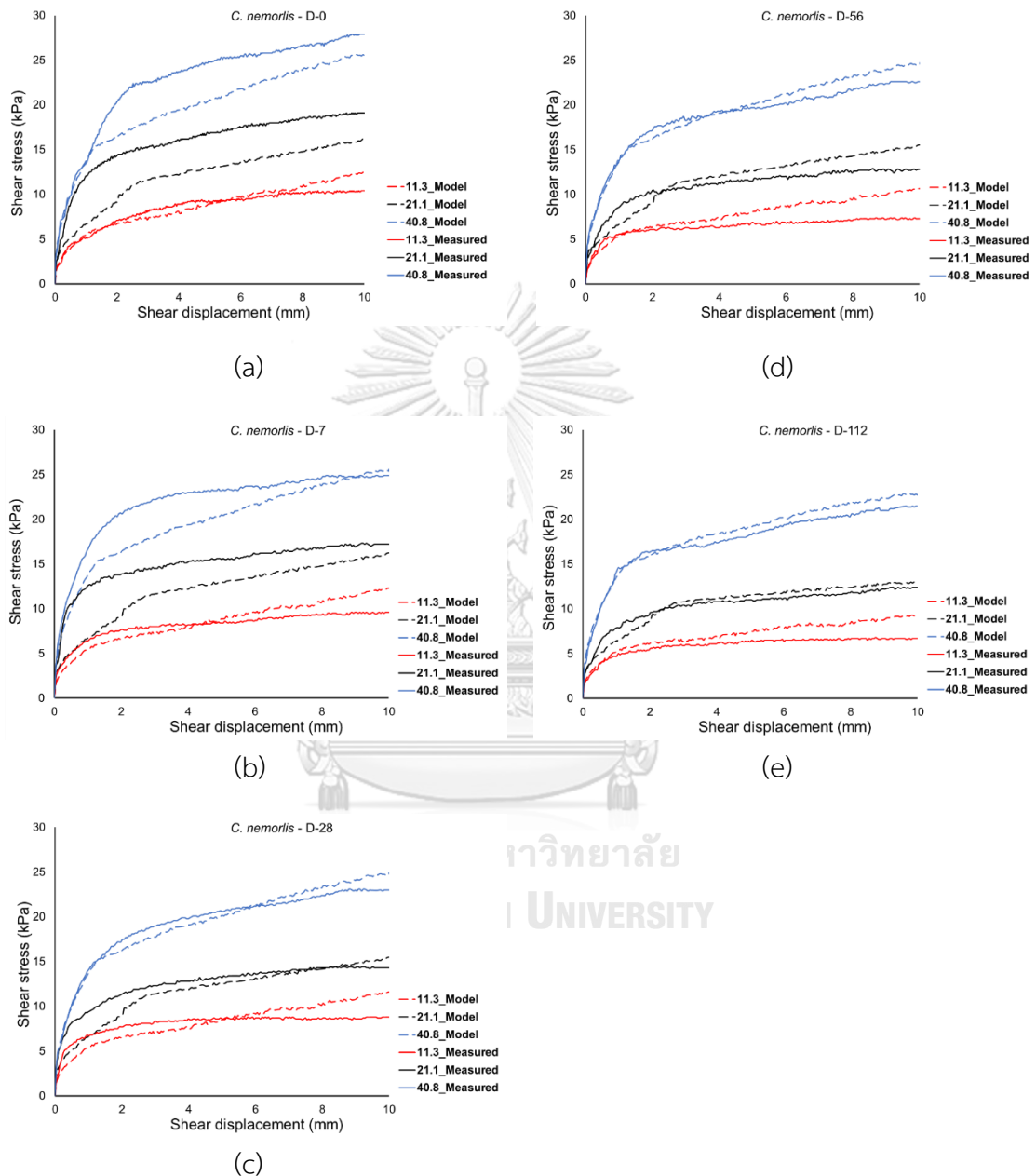


Fig 6. 6. Simulated and experiment shear stress-strain curve of soil reinforced by *C. nemoralis*

By contrast, in the decomposing treatments, RBMw highlighted the overestimation of root reinforcement. Indeed, the estimated reinforcement is 2.2 and 1.2 times higher than the measured reinforcement of decomposing roots at 112 days since herbicide

application of *C. nemoralis* and *C. zizanioides* species, respectively. This could be attributed to the assumption that all roots tend to break rather than pull-out in the RBMw. Whereas failure mechanisms of reinforced soil changed from break to pull-out over the root decomposition as stated in Zhu et al. (2019). Generally, the root reinforcement obtained from RBMw was not much different with the measured reinforcement.

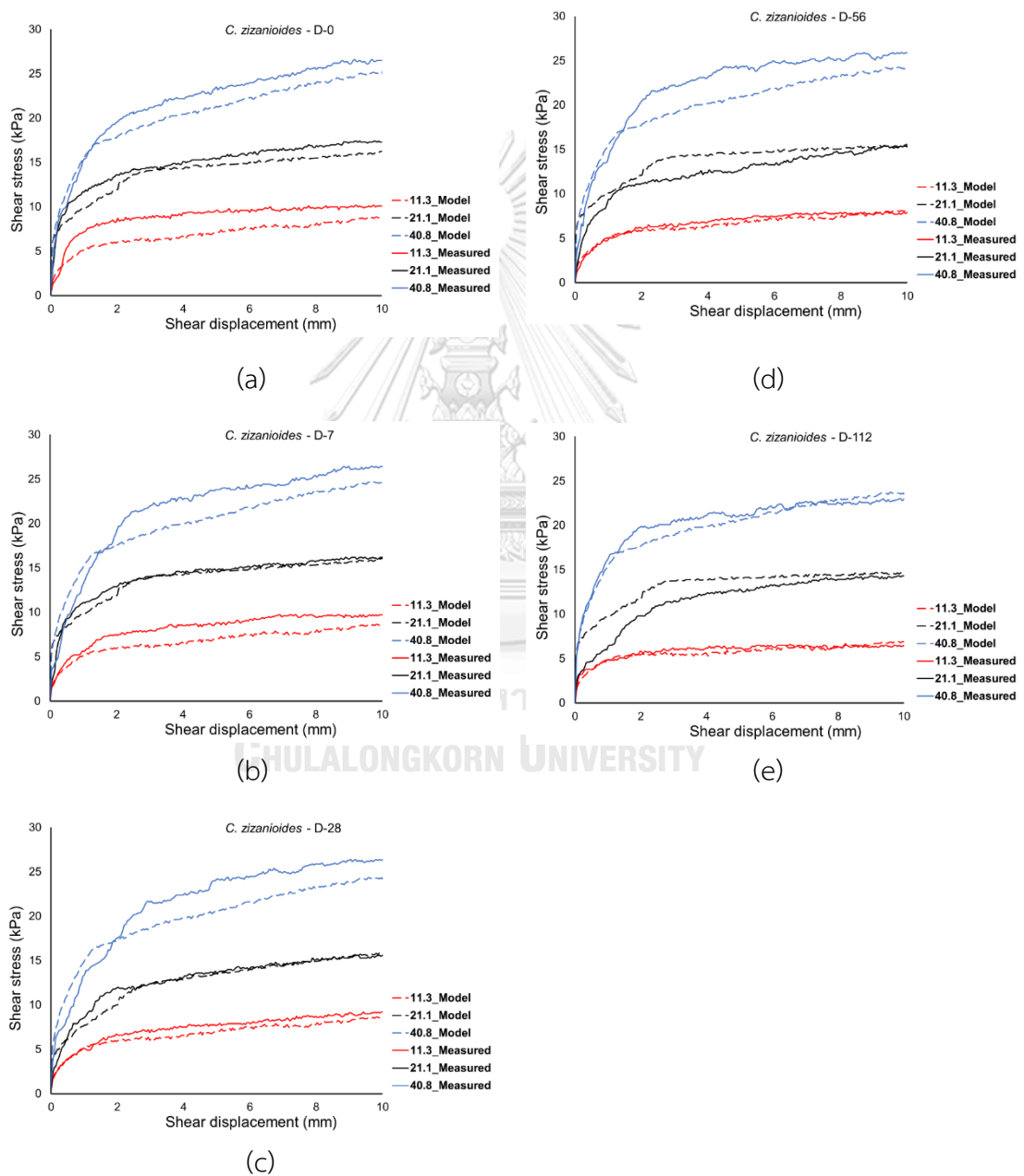


Fig 6. 7. Simulated and experiment shear stress-strain curve of soil reinforced by *C. zizanioides*.

The maximum simulated root reinforcement of two vetiver species over decomposition duration using RBMw coupled with modified WWM, and Wu's model are summarized in Table 6. 3. The maximum root reinforcement obtained from Wu's model is significantly higher than those of RBMw (p -value<0.05). Indeed, considering the control treatment (D-0), the simulated reinforcement of the two vetiver roots using Wu's model is almost 4 times higher than that obtained from RBMw. This could be attributed to the assumption in Wu's model that all roots in the bundle break at the same time and do not depend on displacement. Indeed, the Wu's model cannot predict the displacement at maximum reinforcement, which can be estimated using RBMw.

Table 6. 3. Simulated maximum displacement and maximum root reinforcement (mean and standard error (SE)) of *C. nemoralis* and *C. zizanioides* treatments using RBMw and Wu's model

Species	Treatment	Root bundle model (RBMw)				Wu's Model (kPa)	
		Cr (kPa)		Δx_{max} (mm)		Cr (kPa)	
		Mean	SE	Mean	SE	Mean	SE
<i>C. nemoralis</i>	D-0	27.90	2.40	87.54	0.10	117.73	7.44
	D-7	25.76	2.44	85.66	1.68	114.34	7.22
	D-28	22.19	1.94	77.17	1.47	94.42	5.96
	D-56	10.37	0.78	45.45	5.05	60.49	3.82
	D-112	7.96	0.58	45.45	5.05	42.35	2.67
<i>C. zizanioides</i>	D-0	12.06	1.42	65.65	2.92	44.98	5.27
	D-7	11.80	1.40	65.00	2.89	41.07	4.81
	D-28	8.33	0.99	52.20	1.70	29.94	3.51
	D-56	6.00	0.75	52.19	1.69	24.11	2.82
	D-112	3.76	0.64	47.13	1.68	17.22	2.02

Although there was a difference between simulated reinforcement (i.e., obtained from RBMw) and measured reinforcement, this difference was not much. In addition, considering root reinforcement reduction rate (i.e., which are commonly based on the difference between control and decomposed treatment), the choice of root

reinforcement model is less of importance (Vergani et al., 2014). The root reinforcement estimation, however, should be done with a caution. In this study, the maximum estimated root reinforcement, which obtained from RBMw coupled with modified WWM, were used as the input parameter in vegetated slope stability analysis to estimate the effects of root decomposition on vegetated slope stability. The estimation using RBMw coupled with modified WWM showed a significant reduction in maximum root reinforcement after 112 days since herbicide applications for the two vetiver species (p -value <0.05). This result is consistent with those reported in Vergani et al. (2017), who adopted the same root reinforcement model (i.e., RBMw) to investigate the reduction in root reinforcement of after 4 years since the forest fire. Similar to the direct shear test result, the maximum estimated reinforcement of *C. nemoralis* and *C. zizanioides* species significantly reduced by time follow the exponential function as shown in the Eqs. 6.11 and 6.12, respectively.

$$C_r(t) = 27.25e^{-0.012t}; p\text{-value} < 0.05, R^2 = 0.94 \quad (6.11)$$

$$C_r(t) = 11.86e^{-0.011t}; p\text{-value} < 0.05, R^2 = 0.98 \quad (6.12)$$

where $C_r(t)$ is the maximum root reinforcement at t days after herbicide application. The estimated results show that root reinforcement of *C. nemoralis* reduced faster than those of *C. zizanioides* species. Indeed, the root reinforcement reduction rate of *C. nemoralis* (0.18 kPa/day) is 2.4 times higher than that of *C. zizanioides* species (0.07 kPa/day). This is consistent with the tensile strength and secant modulus of the two vetiver species, which significantly govern the root reinforcement. In addition, the displacement at maximum reinforcement of the two vetiver species reduced as root decomposition. This could be explained by the reduction in the secant modulus of the two vetiver species as discussed in section 5.2.

6.3. Numerical analysis to estimate the influence of root decomposition on vegetated slope stability

6.3.1. Theoretical framework

a. Unsaturated-saturated seepage analysis

The water flow in unsaturated-saturated soil is governed by Darcy's law, which has been proposed by Richrds (1931) (Eq. 6.13).

$$\frac{\partial}{\partial x} \left[k_x \frac{\partial h}{\partial x} \right] + \frac{\partial}{\partial y} \left[k_y \frac{\partial h}{\partial y} \right] + Q = \frac{\partial \theta}{\partial t} \quad (6.13)$$

where k_x , k_y : permeability function in x-, y-direction, respectively; h : total hydraulic head; θ : volumetric moisture content; t : time; Q : applied boundary flux. To solve the Eq. 6.13, the Finite Element Method (FEM) was used in SEEP/W software. The pore water pressure distribution obtained from transient seepage analysis then was used as input parameters in SLOPE/W to estimate the stability of the vegetated slope.

For SWCC derivation, this study adopted the equation proposed by Fredlund and Xing (1994) as follows:

$$\theta_w = \theta_s C(\psi) \left\{ \frac{1}{\left[\ln \left(e + \left(\frac{u_a - u_w}{a} \right)^n \right) \right]^m} \right\} \quad (6.14)$$

where $C(\psi)$ is the correction function and defined as:

$$C(\psi) = 1 - \frac{\ln \left[1 + \frac{(u_a - u_w)}{(u_a - u_w)_r} \right]}{\ln \left[1 + \frac{10^6}{(u_a - u_w)_r} \right]} \quad (6.15)$$

where $C(\psi) = 1$ as recommended by Leong and Rahardjo (1997), θ_w is volumetric water content, θ_s is saturated volumetric water content, a is fitting parameter related to the air-entry value of the soil (kPa), n is fitting parameter related to the SWCC slope, m is fitting parameter related to the residual water content, e is natural number (2.7182), $(u_a - u_w)$ is matric suction (kPa), $(u_a - u_w)_r$ is residual

matric suction corresponding to residual water content (kPa), u_a is pore-air pressure (kPa), u_w is pore-water pressure (kPa). Meanwhile, the permeability function of soil was derived by the Eq. 6.16, which was proposed by [Leong and Rahardjo \(1997\)](#):

$$k_w = k_s \left(\frac{\theta_w}{\theta_s} \right)^p \quad (6.16)$$

where k_w is coefficient of permeability with respect to water for unsaturated soil, k_s is saturated coefficient of permeability and p is fitting parameter corresponding to the permeability function slope.

b. Vegetated slope stability analysis

The stability of vegetated slope was estimated relied on the factor of safety (FS), which is defined as ratio between available shear strength to shear stress along the potential failure surface. The FS can be expressed as

$$FS = \frac{\sum_i^n \tau_f l_i}{\sum_i^n W_i \sin \beta_i} \quad (6.17)$$

Where n is the total number of slices, i is slice index, l_i the length of slice, W_i is the weight of each slice per unit base area and β_i is the slice base inclination, τ_f is the shear strength. For the vegetated slope under unsaturated-saturated condition, the shear strength is given by

$$\tau_f = C_r + c' + (\sigma - u_a) \tan \phi' + (u_a - u_w) \tan \phi^b \quad (6.18)$$

Where C_r is root reinforcement (i.e., root cohesion); c' and ϕ' are effective cohesion and internal friction angle of soil, respectively; $\sigma - u_a$ is effective normal stress; $u_a - u_w$ is matric suction; u_a is pore-air pressure; u_w is pore-water pressure; ϕ^b angle indicating the rate of increase in shear strength relative to the matric suction. Finally, the FS of vegetated slope under unsaturated-saturated condition can be defined as:

$$FS = \frac{\sum \left[(c' + C_r) l R + N R \tan \phi' - u_w l \frac{\tan \phi^b}{\tan \phi'} R \tan \phi' - u_a l \left(1 - \frac{\tan \phi^b}{\tan \phi'} \right) R \tan \phi' \right]}{\sum W \sin \beta} \quad (6.19)$$

where N is normal force at base of slices and defined as:

$$N = \frac{W - \frac{c'l \sin \beta}{FS} + u_a \frac{l \sin \beta}{FS} (\tan \phi' - \tan \phi^b) + u_w \frac{l \sin \beta}{FS} \tan \phi^b}{m_\beta} \quad (6.20)$$

$$m_\beta = \cos \beta + \frac{\sin \beta \tan \phi'}{FS} \quad (6.21)$$

where: R is radius for a circular surface.

In this study, the Bishop's simplified method was adopted in SLOPE/W software to estimate the FS of vegetated slope.

6.3.2. Geometry, boundary conditions and soil properties

Table 6. 4. Summary key properties of residual soil

Parameter		Value	Unit
Physical property	Unit weight (γ_s)	20	kN/m ³
Mechanical property	Effective soil cohesion (c')	10	kPa
	Effective friction angle (ϕ')	26	degree
Hydraulic property	Saturated hydraulic conductivity (k_s)	10^{-5}	m/s
	Rate of increase in shear strength cause by matric suction (ϕ^b)	26	degree
SWCC parameters	Saturated volumetric moisture content (θ_s)	0.45	
	Fitting parameters	a	50 kPa
		m and n	1

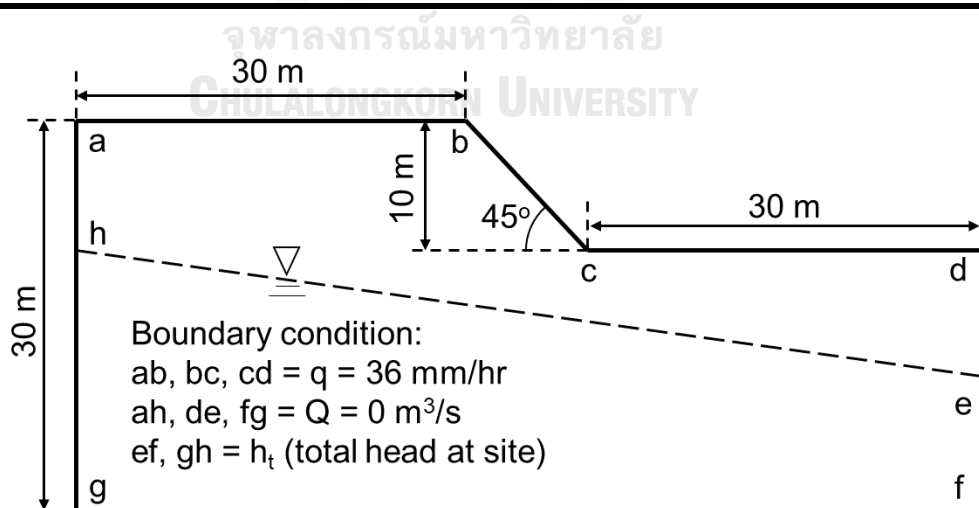


Fig 6. 8. Slope geometry and boundary conditions (adopted from Rahardjo et al. (2007))

In this study, a hypothetical unsaturated slope was adopted from [Rahardjo et al. \(2007\)](#) as shown in Fig 6. 8. The adopted slope geometry and boundary conditions are given the Fig 6. 8. In detail, the ground water table was set at 5 m below the slope toe and inclined at 7° to horizontal to archive an initial pore-water pressure in the unsaturated slope. To avoid the generation of unrealistic pore-water pressure in rainfall, the maximum negative pore-water pressure was set to be -75 kPa. This limit was adopted based on the measured data of negative pore-water pressure at several site in Singapore ([Rahardjo et al., 2000](#)). The rainfall intensity of 36 mm/hr was used in this study. The seepage analysis was performed for 24 hours. The physical, shear and hydraulic properties of fine-grained silty soil are summarized in Table 6. 4. It is noteworthy that the influence of root decomposition on soil hydraulic properties was ignored.

6.3.3. Transient seepage analysis result

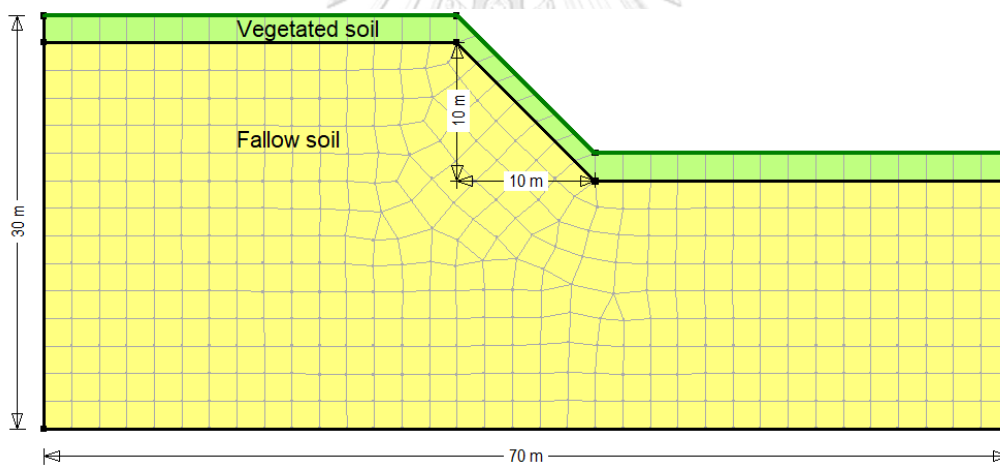


Fig 6. 9. Full-scale finite element model of hypothetical slope

The transient seepage analysis was conducted using SEEP/W software. The full-scale finite element model of hypothetical slope was depicted in Fig 6. 9. The Fig 6. 10 a and b show the pore-water pressure distribution in the bare slope before and after 24 hours rainfall with intensity of 36 mm/hr, respectively. After 24 hours of rainfall, the ground water table rises up to middle of the slope, with the maximum negative pore-water pressure is -18.8 kPa (Fig 6. 10b). This is consistent with those reported in [Rahardjo et al. \(2007\)](#). In this study, it is assumed that the presence of roots does not influence on the hydraulic properties of the bare slope. Thus, the simulated pore-

water pressure then was used as an input parameter in SLOPE/W to determine the factor of safety (FS) for both bare slope and vegetated slope.

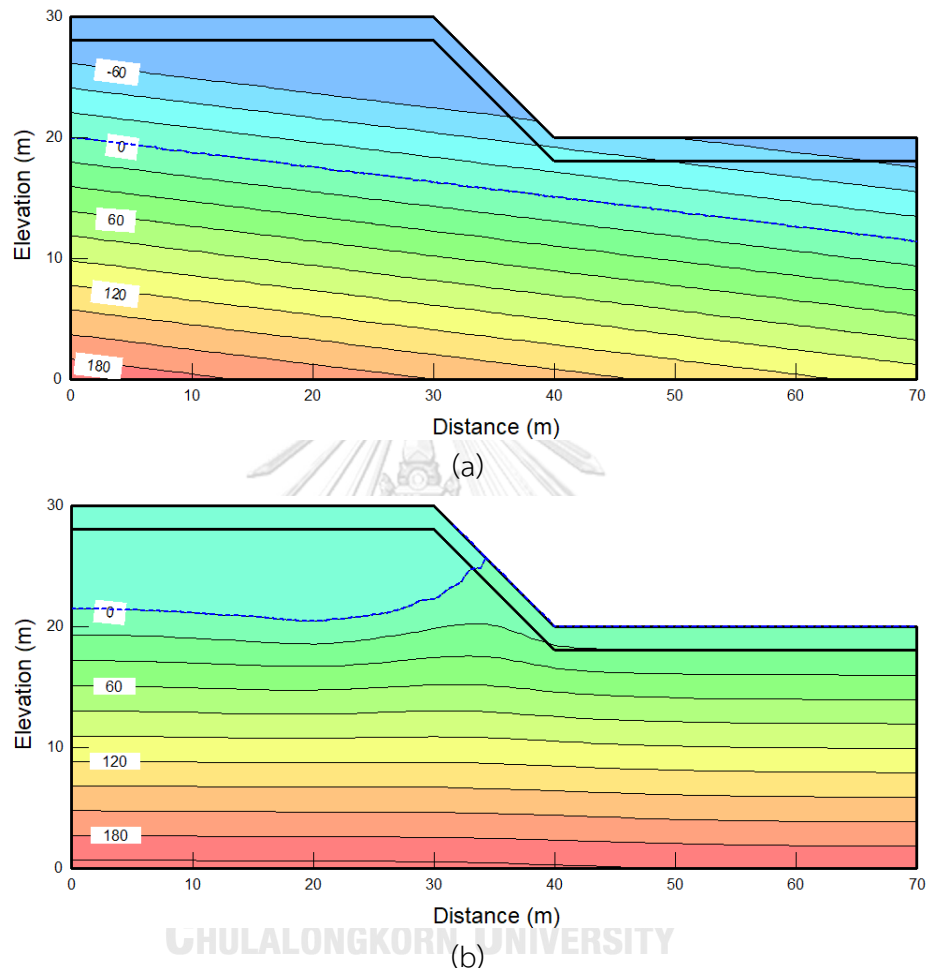


Fig 6. 10. Pore water distribution (a) before and (b) after rainfall with intensity of 36 mm/h

6.3.4. Influence of root decomposition on vegetated slope stability

In this study, SLOPE/W was used to evaluate the decomposition influences of *C. nemoralis* and *C. zizanioides* roots on slope stability through the FS value. The Limit Equilibrium Method (LEM) was adopted in this study. The six scenarios were considered for slope stability analysis: (1): bare slope; (2): slope reinforced by growing root (D-0); (3), (4), (5), and (6): slope reinforced by decomposed roots after 7, 28, 56, and 112 days since herbicide application (D-7, D-28, D-56 and D-112), respectively.

The failure surface of bare slope and slope reinforced by growing roots of *C. nemoralis* and *C. zizanioides* species after 24 hours of rainfall are shown in Fig 6. 11. After 24 hours rainfall with intensity of 36 mm/hr, the FS of the bare slope was reduced by 52.8%, from 2.16 to 1.02. Although the FS value was significantly reduced, the bare slope remained stable after 24 hours of rainfall with an intensity of 36 mm/hr. The reduction in FS of bare slope could be attributed to the reduction in suction and the water table mounding (Rahardjo et al., 2007). The FS value of 1.02 (i.e., lowest FS of bare slope at the 24th hour of rainfall duration) was used as the benchmark for estimating the influence of root decomposition on vegetated slope stability. The presence of growing roots of *C. nemoralis* and *C. zizanioides* species improves the stability of the vegetated slope (Fig 6. 11a, and b). Indeed, compared to bare slope, the FS value of slope reinforced by growing roots of *C. nemoralis* and *C. zizanioides* species increased up to 26.5% (from 1.02 to 1.29) and 12% (1.02 to 1.15), respectively. The FS increase of the *C. nemoralis* and *C. zizanioides* roots in this study (i.e., 26.5% and 12%) was lower than that those of *C. zizanioides* roots (i.e., 75%) reported in Nguyen et al. (2018). The difference in FS increase could be explained by the difference in failure mechanism of slope in this study and Nguyen et al. (2018). Indeed, the slope failure mechanism in Nguyen et al. (2018) was classified as shallow failure, which failure above 1 m in depth. Whereas the failure slip surface of slope in this study located at the depth of 4.5 m. Due to the failure surface located very deep (i.e., more than 2m of root zone), the number of slices that considered cohesion of vegetated soil to estimate FS is less than that considered cohesion of bare soil. In addition, this study assumed that root cohesion fully distributes over the 2m of the root zone, which is in contrast to real cases where vetiver species are grown in the hedges (i.e., each hedge 1m apart). Therefore, the slip surface between each hedge was omitted. These explain why the FS slightly change due to the presence of two vetiver species. The *C. nemoralis* species highlighted the greater protective function than *C. zizanioides* species, which is widely utilised for slope stabilisation (Truong et al., 2008). Therefore, *C. nemoralis* species could be considered as an alternative species to *C. zizanioides* species in soil bioengineering for slope stabilisation.

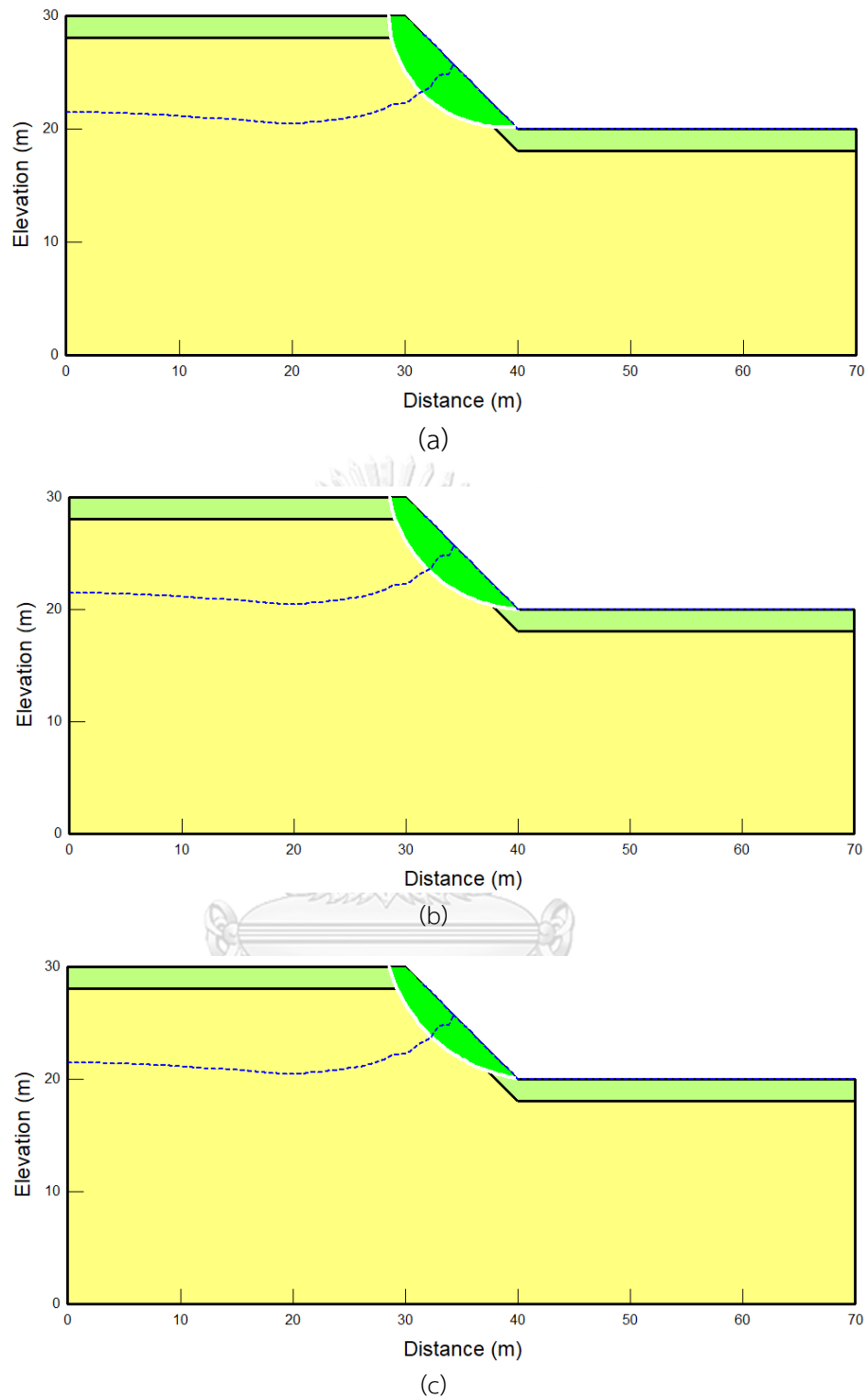


Fig 6. 11. Failure surface of (a) bare slope and slope reinforced by growing roots of (b) *C. nemoralis* and (c) *C. zizanioides* species after 24 hours of rainfall (the worst case)

Considering the slope reinforced by decomposed roots scenarios, the simulated FS significantly decreased with time since herbicide applications (p -value <0.05 ; Fig 6. 12

and Fig A. 2 and Fig A. 3). Indeed, compared to growing roots cases (D-0), the FS value of slope reinforced by decomposed roots (D-112) of *C. nemoralis* and *C. zizanioides* species reduced by 14.2% and 7.3%, respectively. This can be a consequence of the reduction in root reinforcement due to root decomposition. As root decomposition, the protective function of *C. nemoralis* and *C. zizanioides* roots to slope stability was diminished. Consequently, after the two vetiver species die off due to herbicide application, the vegetated slope will be more susceptible to climate change, such as heavy rainfall, which could trigger slope instability. Therefore, the herbicide or any techniques should be applied carefully for land conversion, especially in the mountainous areas which are susceptible to slope instability. Also, this study is expected to provide more insight into the understanding of temporal variation of root protective function after the herbicide application.

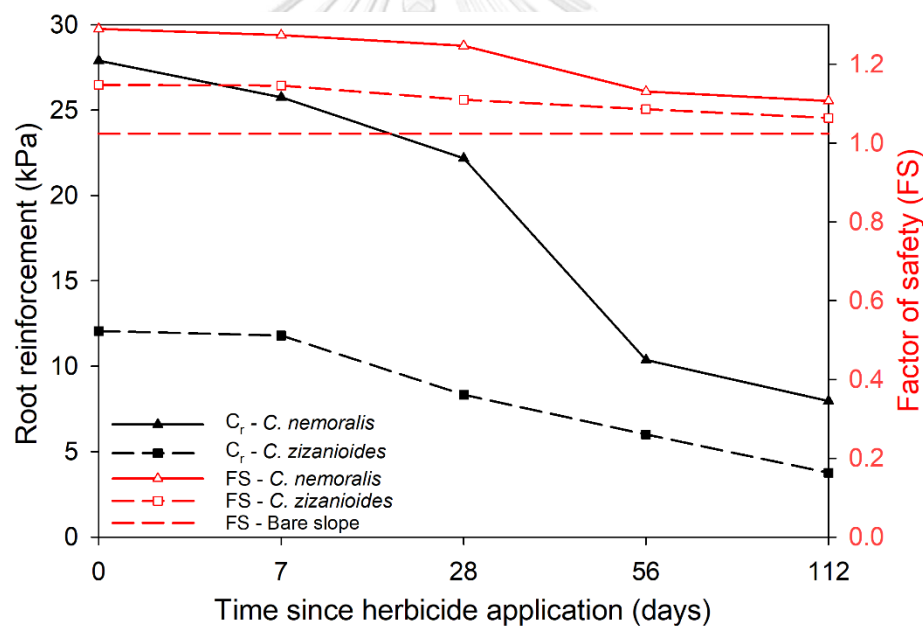


Fig 6. 12. Simulated root reinforcement and factor of safety (FS) of slope reinforced by decomposed roots of *C. nemoralis* and *C. zizanioides* species.

6.4. Conclusive remarks

Using the two well-known root reinforcement models (i.e., Wu's model and RBMw), the root mechanical reinforcement was estimated from the root morphological traits (i.e., diameter distribution, root length-diameter correlation, root orientation) and root biomechanical properties (i.e., tensile strength and secant modulus). In addition,

the simulated root reinforcement was used to investigate the influence of root decomposition on vegetated slope stability. The following conclusion can be drawn:

The reduction of Weibull shape coefficients indicated that the biomechanical properties of decomposing roots (i.e., tensile strength and modulus) are more variable than those of growing roots. Thus, the RBMw, which uses the Weibull survival function to capture the variability in root biomechanical properties, could be more appropriate for estimating the reinforcement of decomposing roots.

For all cases, the Wu's model provided the estimated reinforcement greater than those estimated by RBMw. Compared to laboratory or field testing, the RBMw provides some major advantage as: (1) the variation of root amount presented in soil matrix can be controlled; (2) root reinforcement can be estimated at the higher shear displacement, where roots fully mobilise their strength. The estimated results highlighted the significant reduction in contribution of *C. nemoralis* and *C. zizanioides* roots over the root decomposition as found in the laboratory investigation.

The result obtained from numerical modelling indicated that the presence of both *C. nemoralis* and *C. zizanioides* roots significantly enhance the stability of fallow slope. However, the protective function of *C. nemoralis* and *C. zizanioides* roots declined after herbicide application. Thus, the application of herbicide for land conversion should be done with caution, especially in the mountainous areas, where are more susceptible to slope instability.

Chapter 7: Conclusion and recommendation

7.1. Conclusion

In this study, a series of laboratory testing was conducted to measure the morphological traits (i.e., RAR_s , root diameter, root orientation), root biomechanical properties (i.e., tensile strength, secant modulus, initial modulus, breakage strain) and root mechanical reinforcement of two contrasting vetiver species, including *C. nemoralis* and *C. zizanioides* species. In addition, the temporal variation of root biomechanical properties and mechanical reinforcement was investigated in the laboratory. Besides that, the root reinforcement was estimated using the existing root reinforcement models (i.e., Wu's model and RBMw). Finally, the influence of root decomposition on stability of vegetated slope was estimated using numerical modelling (i.e., SEEP/W and SLOPE/W). The following conclusions can be drawn:

The comprehensive dataset of morphological traits, biomechanical properties, mechanical reinforcement of growing roots of the two vetiver species are presented. These two species highlighted the significant difference in terms of root diameter, root breakage strain and modulus (i.e., secant and initial modulus). Both species consistently displayed significant negative power law correlations between root diameter and root biomechanical properties (i.e., tensile strength, secant and initial modulus) ($p\text{-value} < 0.05$).

This study is the first to use a rhizobox for observing root morphological traits and to identify a correlation between root orientation and diameter. This finding provides new insights into root orientation, which is an important yet often overlooked parameter in the evaluation of existing root reinforcement models.

Under the same growth conditions, the contribution of *C. nemoralis* and *C. zizanioides* roots to soil shear strength in terms of cohesion is similar. Thus, it is suggested that the *C. nemoralis* species shares similar soil reinforcement effects to the *C. zizanioides* species, which has been widely used in soil bioengineering practice. Furthermore, this study is expected to be a milestone for promoting vetiver species (i.e., especially *C. nemoralis* species) for soil bioengineering in Southeast Asian countries, which are greatly impacted by global climate change.

This study demonstrated the significant reduction in root tensile strength, secant modulus, breakage strain of two contrasting vetiver species due to herbicide application. *C. nemoralis* species highlighted the greater reduction rate of biomechanical properties than those of *C. zizanioides* species. In addition, root decomposition did not show the influence on the shape of the diameter-strength and diameter-secant modulus correlations, but these correlations shifted downward as the duration of root decomposition increased.

The laboratory results demonstrated that the root decomposition following herbicide application highlighted the significant influence on shear behaviour of vegetated soil. Shear strength (i.e., cohesion) and maximum dilatancy of soil reinforced by both two vetiver species significantly reduced with increasing duration of root decomposition.

Similar to the laboratory results, the simulation using the RBMw highlighted the significantly deterioration of root reinforcement after 112 days since herbicide application. In addition, the simulated shear displacement, which obtained at the ultimate root reinforcement, significantly reduced with increasing duration of root decomposition.

The numerical modelling results demonstrated the improvement of slope stability due to the presence of *C. nemoralis* and *C. zizanioides* roots. However, this protective function of both *C. nemoralis* and *C. zizanioides* roots was reduced with increasing duration of root decomposition following herbicide application. Thus, the application of herbicide for land conversion should be done with caution, especially in the mountainous areas, where are more susceptible to slope instability.

7.2. Recommendation

This study is a semi-controlled experiment, which is effective in making fairer and quantitative comparisons of the biomechanical properties of roots and the root reinforcement between the two selected species. However, extrapolating our test results to the field conditions requires careful examination. Future work should be performed to further evaluate our laboratory findings. In particular, further studies should determine how the roots of the two species in the open field can be affected in terms of growth rate and root orientation. Future research should also investigate

the effects of growth conditions, such as growth media, water, and nutrient availability, on the biomechanical properties, morphological traits, and mechanical reinforcement of roots.

This study demonstrated the significance of the effects of root decomposition (following herbicide application) on the variations of both the root biomechanical properties and root reinforcement of two vetiver species over a decomposition period of up to 112 days (i.e., more than 3 months). This study suggests future work to investigate how root decomposition may change the root anatomy and root chemical components (e.g., cellulose and lignin) in order to explain and provide greater insights into the variations of the root biomechanical properties and as well as the root cohesion. This study encourages future biomechanical test results to include root Young's modulus and root secant modulus, which have been considered importance to better describe the soil-root interaction and to aid the formulation of future root reinforcement models. We also recommend to pay more attention on the maximum dilatancy introduced by (decomposing) roots, which have important implication to the soil's ability to mobilise the shear stress to resist shearing.

This study highlighted the significant variation in root biomechanical properties, especially for the decomposing roots. This could result in the variation of root mechanical reinforcement. However, the vegetated slope stability analysis was performed using the LEM in SLOPE/W, which cannot capture the variation of root reinforcement. In addition, this study assumed reinforcement of roots distribute uniformly in the soil matrix. Thus, this study suggests the future works to perform vegetated slope stability analysis using probabilistic method, which can capture the spatial variation of root reinforcement.

REFERENCES

- Ali, F. H., & Osman, N. (2008). Shear strength of a soil containing vegetation roots. *Soils and Foundations*, 48(4), 587-596. doi:<https://doi.org/10.3208/sandf.48.587>
- Ammann, M., Böll, A., Rickli, C., Speck, T., & Holdenrieder, O. (2009). Significance of tree root decomposition for shallow landslides. *For Snow Landsc Res*, 82(79-94), 79.
- ASTM-2487. (2011). Standard Practice for Classification of Soils for Engineering Purposes (Unified Soil Classification System). In. West Conshohocken, Pennsylvania, U.S.A: ASTM International.
- ASTM-D3080/D3080M. (2011). Standard test method for direct shear test of soils under consolidated drained conditions. In. West Conshohocken, Pennsylvania, U.S.A: ASTM International.
- Badhon, F. F., Islam, M. S., Islam, M., Arif, M., & Uddin, Z. (2021). A simple approach for estimating contribution of vetiver roots in shear strength of a soil-root system. *Innovative Infrastructure Solutions*, 6(2), 1-13. doi:<https://doi.org/10.1007/s41062-021-00469-1>.
- Bischetti, G. B., Chiaradia, E. A., Simonato, T., Speziali, B., Vitali, B., Vullo, P., & Zocco, A. (2005). Root strength and root area ratio of forest species in Lombardy (Northern Italy). In *Eco-and ground bio-engineering: The use of vegetation to improve slope stability* (pp. 31-41): Springer.https://doi.org/10.1007/978-1-4020-5593-5_4.
- Bishop, D. M., & Stevens, M. E. (1964). Landslides on logged areas in southeast Alaska. *US Forest Service research paper NOR;-1*.
- Boldrin, D., Leung, A. K., & Bengough, A. (2017). Root biomechanical properties during establishment of woody perennials. *Ecological Engineering*, 109, 196-206. doi:<https://doi.org/10.1016/j.ecoleng.2017.05.002>
- Boldrin, D., Leung, A. K., & Bengough, A. G. (2018). Effects of root dehydration on biomechanical properties of woody roots of *Ulex europaeus*. *Plant and soil*, 431(1), 347-369. doi:<https://doi.org/10.1007/s11104-018-3766-7>
- Boonyanuphap, J. (2013). Cost-benefit analysis of vetiver system-based rehabilitation

- measures for landslide-damaged mountainous agricultural lands in the lower Northern Thailand. *Natural hazards*, 69(1), 599-629.
- Bordoni, M., Vercesi, A., Maerker, M., Ganimede, C., Reguzzi, M., Capelli, E., . . . Gagnarli, E. (2019). Effects of vineyard soil management on the characteristics of soils and roots in the lower Oltrepò Apennines (Lombardy, Italy). *Science of The Total Environment*, 693, 133390. doi:<https://doi.org/10.1016/j.scitotenv.2019.07.196>.
- Chimungu, J. G., Loades, K. W., & Lynch, J. P. (2015). Root anatomical phenes predict root penetration ability and biomechanical properties in maize (*Zea mays*). *Journal of Experimental Botany*, 66(11), 3151-3162. doi:<https://doi.org/10.1093/jxb/erv121>.
- Chok, Y., Jaksa, M., Kaggwa, W., & Griffiths, D. (2015). Assessing the influence of root reinforcement on slope stability by finite elements. *International Journal of Geo-Engineering*, 6(1), 1-13. doi:<https://doi.org/10.1186/s40703-015-0012-5>.
- Clements, D. R., Benoit, D. L., Murphy, S. D., & Swanton, C. J. (1996). Tillage effects on weed seed return and seedbank composition. *Weed science*, 44(2), 314-322. doi:<https://doi.org/10.1017/s0043174500093942>.
- Cohen, D., Schwarz, M., & Or, D. (2011). An analytical fiber bundle model for pullout mechanics of root bundles. *Journal of Geophysical Research: Earth Surface*, 116(F3). doi:<https://doi.org/10.1029/2010jf001886>
- Coppin, N. J., & Richards, I. G. (1990). *Use of vegetation in civil engineering*: Ciria Butterworths.
- Council, N. R. (1993). *Vetiver Grass: A Thin Green Line Against Erosion*: National Academy Press, Washington, DC.<https://doi.org/10.17226/2077>.
- De Baets, S., Poesen, J., Reubens, B., Wemans, K., De Baerdemaeker, J., & Muys, B. (2008). Root tensile strength and root distribution of typical Mediterranean plant species and their contribution to soil shear strength. *Plant and soil*, 305(1-2), 207-226. doi:<https://doi.org/10.1007/s11104-018-3636-3>.
- Diambra, A., Ibraim, E., Wood, D. M., & Russell, A. (2010). Fibre reinforced sands: experiments and modelling. *Geotextiles and geomembranes*, 28(3), 238-250. doi:<https://doi.org/10.1002/nag.2142>.
- Docker, B., & Hubble, T. (2008). Quantifying root-reinforcement of river bank soils by

- four Australian tree species. *Geomorphology*, 100(3-4), 401-418. doi:<https://doi.org/10.1016/j.geomorph.2008.01.009>.
- Donjadee, S., Clemente, R., Tingsanchali, T., & Chinnarasri, C. (2010). Effects of vertical hedge interval of vetiver grass on erosion on steep agricultural lands. *Land Degradation & Development*, 21(3), 219-227. doi:<https://doi.org/10.1002/ldr.900>.
- Dumlao, M. R., Ramananarivo, S., Goyal, V., DeJong, J. T., Waller, J., & Silk, W. K. (2015). The role of root development of *Avena fatua* in conferring soil strength. *American journal of botany*, 102(7), 1050-1060. doi:<https://doi.org/10.3732/ajb.1500028>
- Eab, K. H., Likitlersuang, S., & Takahashi, A. (2015). Laboratory and modelling investigation of root-reinforced system for slope stabilisation. *Soils and Foundations*, 55(5), 1270-1281. doi:<https://doi.org/10.1016/j.sandf.2015.09.025>.
- Fahlen, A. (2002). Mixed tree-vegetative barrier designs: experiences from project works in northern Vietnam. *Land Degradation & Development*, 13(4), 307-329. doi:<https://doi.org/10.1002/ldr.508>.
- FAO. (2021). *FAOSTAT* (database). Retrieved from <https://www.fao.org/faostat/en/#home>
- Fowze, J., Bergado, D., Soralump, S., Voottipreux, P., & Dechasakulsom, M. (2012). Rain-triggered landslide hazards and mitigation measures in Thailand: From research to practice. *Geotextiles and geomembranes*, 30, 50-64.
- Fredlund, D. G., & Xing, A. (1994). Equations for the soil-water characteristic curve. *Canadian Geotechnical Journal*, 31(4), 521-532. doi:<https://doi.org/10.1139/t94-061>.
- Genet, M., Stokes, A., Salin, F., Mickovski, S. B., Fourcaud, T., Dumail, J.-F., & Van Beek, R. (2005). The influence of cellulose content on tensile strength in tree roots. *Plant and soil*, 278(1-2), 1-9. doi:<https://doi.org/10.1007/s11104-005-8768-6>.
- Gray, D., & Leiser, A. (1983). *Biotechnical Slope Protection and Erosion Protection*. In: Van Nostrand Reinhold & Co., New York.
- Gray, D. H., & Ohashi, H. (1983). Mechanics of fiber reinforcement in sand. *Journal of Geotechnical Engineering*, 109(3), 335-353. doi:<https://doi.org/10.1016/0148->

[9062\(83\)91273-1](https://doi.org/10.1016/j.scitotenv.2020.141128)

- Grima, N., Edwards, D., Edwards, F., Petley, D., & Fisher, B. (2020). Landslides in the Andes: Forests can provide cost-effective landslide regulation services. *Science of The Total Environment*, 745, 141128. doi:<https://doi.org/10.1016/j.scitotenv.2020.141128>.
- Hengchaovanich, D. (1998). Vetiver for Slope Stabilization and Erosion Control. *China Vetiver Network, Nanjing*.
- Houlbrooke, D., Thom, E., Chapman, R., & McLay, C. (1997). A study of the effects of soil bulk density on root and shoot growth of different ryegrass lines. *New Zealand Journal of Agricultural Research*, 40(4), 429-435. doi:<https://doi.org/10.1080/00288233.1997.9513265>
- Islam, M., Arifuzzaman, N., & Nasrin, S. (2010). *In-situ shear strength of vetiver grass rooted soil*. Paper presented at the Bangladesh Geo. Conf.: Natural Hazards and Counter Measures in Geotechnical Engg.
- Islam, M. S., Arif, M. Z., Badhon, F. F., Mallick, S., & Islam, T. (2016). Investigation of vetiver root growth in sandy soil. *Proceedings of the BUET-ANWAR ISPAT 1st Bangladesh Civil Engineering SUMMIT*.
- Islam, M. S., & Badhon, F. F. (2020). *A mathematical model for shear strength prediction of vetiver rooted soil*. Paper presented at the Geo-congress 2020: engineering, monitoring, and management of geotechnical infrastructure.
- Johnson, A., & Wilcock, P. (2002). Association between cedar decline and hillslope stability in mountainous regions of southeast Alaska. *Geomorphology*, 46(1-2), 129-142. doi:
[https://doi.org/10.1016/s0169-555x\(02\)00059-4](https://doi.org/10.1016/s0169-555x(02)00059-4)
- Jotisankasa, A., Sirirattanachat, T., Rattana-arekul, C., Mahannopkul, K., & Sopharat, J. (2015). *Engineering characterization of Vetiver system for shallow slope stabilization*. Paper presented at the Proceedings of the 6th International Conference on Vetiver (ICV-6), Danang, Vietnam.
- Kamchoom, V., Boldrin, D., Leung, A. K., Sookkrajang, C., & Likitlersuang, S. (2021). Biomechanical properties of the growing and decaying roots of *Cynodon dactylon*. *Plant and soil*, 1-18. doi:<https://doi.org/10.1007/s11104-021-05207-1>

- Kamchoom, V., & Leung, A. K. (2018). Hydro-mechanical reinforcements of live poles to slope stability. *Soils and Foundations*, 58(6), 1423-1434. doi:<https://doi.org/10.1016/j.sandf.2018.08.003>
- Kamchoom, V., Leung, A. K., & Ng, C. W. W. (2014). Effects of root geometry and transpiration on pull-out resistance. *Géotechnique Letters*, 4(4), 330-336. doi:<https://doi.org/10.1680/geolett.14.00086>
- Karimzadeh, A. A., Kwan Leung, A., & Amini, P. F. (2022). Energy-Based Assessment of Liquefaction Resistance of Rooted Soil. *Journal of Geotechnical and Geoenvironmental Engineering*, 148(1), 06021016. doi:[https://doi.org/10.1061/\(asce\)gt.1943-5606.0002717](https://doi.org/10.1061/(asce)gt.1943-5606.0002717).
- Karimzadeh, A. A., Leung, A. K., Hosseinpour, S., Wu, Z., & Fardad Amini, P. (2021). Monotonic and cyclic behaviour of root-reinforced sand. *Canadian Geotechnical Journal*(ja). doi:<https://doi.org/10.1139/cgj-2020-0626>
- Karrenberg, S., Blaser, S., Kollmann, J., Speck, T., & Edwards, P. (2003). Root anchorage of saplings and cuttings of woody pioneer species in a riparian environment. *Functional ecology*, 170-177. doi:<https://doi.org/10.1046/j.1365-2435.2003.00709.x>.
- Kavian, A., Saleh, I., Habibnejad, M., Brevik, E. C., Jafarian, Z., & Rodrigo-Comino, J. (2018). Effectiveness of vegetative buffer strips at reducing runoff, soil erosion, and nitrate transport during degraded hillslope restoration in northern Iran. *Land Degradation & Development*, 29(9), 3194-3203. doi:<https://doi.org/10.1002/ldr.3051>.
- Kitamura, S. (1968). Field experiment on the uprooting resistance of tree root.
- Komori, D., Rangsiwanichpong, P., Inoue, N., Ono, K., Watanabe, S., & Kazama, S. (2018). Distributed probability of slope failure in Thailand under climate change. *Climate Risk Management*, 20, 126-137.
- Kristo, C., Rahardjo, H., & Satyanaga, A. (2017). Effect of variations in rainfall intensity on slope stability in Singapore. *International soil and water conservation research*, 5(4), 258-264. doi:<https://doi.org/10.1016/j.iswcr.2017.07.001>.
- Leaungvutiviroj, C., Piriyaopin, S., Limtong, P., & Sasaki, K. (2010). Relationships between

- soil microorganisms and nutrient contents of *Vetiveria zizanioides* (L.) Nash and *Vetiveria nemoralis* (A.) Camus in some problem soils from Thailand. *Applied Soil Ecology*, 46(1), 95-102. doi:<https://doi.org/10.1016/j.apsoil.2010.06.007>
- Leknoi, U., & Likitlersuang, S. (2020). Good practice and lesson learned in promoting vetiver as solution for slope stabilisation and erosion control in Thailand. *Land Use Policy*, 99, 105008. doi:<https://doi.org/10.1016/j.landusepol.2020.105008>
- Leong, E. C., & Rahardjo, H. (1997). Review of soil-water characteristic curve equations. *Journal of Geotechnical and Geoenvironmental Engineering*, 123(12), 1106-1117. doi:
[https://doi.org/10.1061/\(asce\)1090-0241\(1997\)123:12\(1106\)](https://doi.org/10.1061/(asce)1090-0241(1997)123:12(1106)).
- Leung, A. K., & Ng, C. W. W. (2013). Analyses of groundwater flow and plant evapotranspiration in a vegetated soil slope. *Canadian Geotechnical Journal*, 50(12), 1204-1218. doi:<https://doi.org/10.1139/cgj-2013-0148>
- Likitlersuang, S., Phan, T. N., Boldrin, D., & Leung, A. K. (2022). Influence of growth media on the biomechanical properties of the fibrous roots of two contrasting vetiver grass species. *Ecological Engineering*, 178, 106574. doi:<https://doi.org/10.1016/j.ecoleng.2022.106574>
- Likitlersuang, S., Takahashi, A., & Eab, K. H. (2017). Modeling of root-reinforced soil slope under rainfall condition. *Engineering Journal*, 21(3), 123-132. doi:<https://doi.org/10.4186/ej.2017.21.3.123>
- Liu, G., Hu, F., Zheng, F., & Zhang, Q. (2019). Effects and mechanisms of erosion control techniques on stairstep cut-slopes. *Science of The Total Environment*, 656, 307-315. doi:<https://doi.org/10.1016/j.scitotenv.2018.11.385>.
- Liu, Y.-J., Wang, T.-W., Cai, C.-F., Li, Z.-X., & Cheng, D.-B. (2014). Effects of vegetation on runoff generation, sediment yield and soil shear strength on road-side slopes under a simulation rainfall test in the Three Gorges Reservoir Area, China. *Science of The Total Environment*, 485, 93-102. doi:<https://doi.org/10.1016/j.scitotenv.2014.03.053>.
- Maffra, C., Sousa, R., Sutili, F., & Pinheiro, R. (2019). The effect of roots on the shear strength of texturally distinct soils. *Floresta e Ambiente*, 26(3). doi:<https://doi.org/10.1590/2179-8087.101817>

- Mahannopkul, K., & Jotisankasa, A. (2019a). Influence of root suction on tensile strength of *Chrysopogon zizanioides* roots and its implication on bioslope stabilization. *Journal of Mountain Science*, 16(2), 275-284. doi:<https://doi.org/10.1007/s11629-018-5134-8>
- Mahannopkul, K., & Jotisankasa, A. (2019b). Influences of root concentration and suction on *Chrysopogon zizanioides* reinforcement of soil. *Soils and Foundations*, 59(2), 500-516. doi:<https://doi.org/10.1016/j.sandf.2018.12.014>
- Mao, Z. (2022). Root reinforcement models: classification, criticism and perspectives. *Plant and soil*, 1-12.
- Mašková, T., & Klimeš, A. (2020). The effect of rhizoboxes on plant growth and root: shoot biomass partitioning. *Frontiers in plant science*, 10, 1693. doi:<https://doi.org/10.3389/fpls.2019.01693>.
- McMichael, B., & Quisenberry, J. (1993). The impact of the soil environment on the growth of root systems. *Environmental and experimental botany*, 33(1), 53-61. doi:[https://doi.org/10.1016/0098-8472\(93\)90055-k](https://doi.org/10.1016/0098-8472(93)90055-k)
- Meijer, G., Bengough, A., Knappett, J., Loades, K., & Nicoll, B. C. (2018). In situ measurement of root reinforcement using corkscrew extraction method. *Canadian Geotechnical Journal*, 55(10), 1372-1390. doi:<https://doi.org/10.1139/cgj-2017-0344>.
- Mickovski, S., & Van Beek, L. (2009). Root morphology and effects on soil reinforcement and slope stability of young vetiver (*Vetiveria zizanioides*) plants grown in semi-arid climate. *Plant and soil*, 324(1-2), 43-56. doi:<https://doi.org/10.1007/s11104-009-0130-y>.
- Morin, S., Coquillé, N., Éon, M., Budzinski, H., Parlanti, É., & Stachowski-Haberkorn, S. (2021). Dissolved organic matter modulates the impact of herbicides on a freshwater alga: A laboratory study of a three-way interaction. *Science of The Total Environment*, 782, 146881. doi:<https://doi.org/10.1016/j.scitotenv.2021.146881>
- Nguyen, T. S., Likitlersuang, S., & Jotisankasa, A. (2018). Stability analysis of vegetated residual soil slope in Thailand under rainfall conditions. *Environmental Geotechnics*, 7(5), 338-349. doi:<https://doi.org/10.1680/jenge.17.00025>.

- Nguyen, T. S., Likitlersuang, S., & Jotisankasa, A. (2020). Stability analysis of vegetated residual soil slope in Thailand under rainfall conditions. *Environmental Geotechnics*, 7(5), 338-349. doi:<https://doi.org/10.1680/jenge.17.00025>
- Ni, J., Leung, A. K., & Ng, C. W. W. (2019). Modelling effects of root growth and decay on soil water retention and permeability. *Canadian Geotechnical Journal*, 56(7), 1049-1055. doi:<https://doi.org/10.1139/cgj-2018-0402>.
- Ni, J., Leung, A. K., Ng, C. W. W., & Shao, W. (2018). Modelling hydro-mechanical reinforcements of plants to slope stability. *Computers and Geotechnics*, 95, 99-109. doi:<https://doi.org/10.1016/j.compgeo.2017.09.001>.
- Noorasyikin, M., & Zainab, M. (2016). *A tensile strength of Bermuda grass and Vetiver grass in terms of root reinforcement ability toward soil slope stabilization*. Paper presented at the IOP conference series: materials science and engineering.
- O'loughlin, C., & Watson, A. (1979). Root-wood strength deterioration in radiata pine after clearfelling. *NZJ For. Sci*, 9(3), 284-293.
- Parish, S. (1990). A review of non-chemical weed control techniques. *Biological Agriculture & Horticulture*, 7(2), 117-137. doi:<https://doi.org/10.1080/01448765.1990.9754540>.
- Phan, T. N., Likitlersuang, S., Kamchoom, V., & Leung, A. K. (2021). Root biomechanical properties of *Chrysopogon zizanioides* and *Chrysopogon nemoralis* for soil reinforcement and slope stabilisation. *Land Degradation & Development*, 1-13. doi:<https://doi.org/10.1002/ldr.4063>.
- Pollen, N., & Simon, A. (2005). Estimating the mechanical effects of riparian vegetation on stream bank stability using a fiber bundle model. *Water Resources Research*, 41(7). doi:<https://doi.org/10.1029/2004wr003801>
- Pollen, N., Simon, A., & Collison, A. (2004). Advances in assessing the mechanical and hydrologic effects of riparian vegetation on streambank stability. *Riparian vegetation and fluvial geomorphology*, 8, 125-139. doi:<https://doi.org/10.1029/008wsa10>.
- Preti, F. (2013). Forest protection and protection forest: Tree root degradation over hydrological shallow landslides triggering. *Ecological Engineering*, 61, 633-645.

doi: <https://doi.org/10.1016/j.ecoleng.2012.11.009>.

- Priyadharshini, J., & Seran, T. (2010). Paddy husk ash as a source of potassium for growth and yield of cowpea (*Vigna unguiculata* L.). *Journal of Agricultural Sciences*, 4(2), 67. doi:<https://doi.org/10.4038/jas.v4i2.1646>.
- Rahardjo, H., Leong, E. C., Deutscher, M. S., Gasmu, J. M., & Tang, S. (2000). Rainfall-induced slope failures. *Geotechnical engineering monograph*, 3, 86.
- Rahardjo, H., Ong, T., Rezaur, R., & Leong, E. C. (2007). Factors controlling instability of homogeneous soil slopes under rainfall. *Journal of Geotechnical and Geoenvironmental Engineering*, 133(12), 1532-1543. doi:[https://doi.org/10.1061/\(asce\)1090-0241\(2007\)133:12\(1532\)](https://doi.org/10.1061/(asce)1090-0241(2007)133:12(1532)).
- Rey, F., Bifulco, C., Bischetti, G. B., Bourrier, F., De Cesare, G., Florineth, F., . . . Phillips, C. (2019). Soil and water bioengineering: Practice and research needs for reconciling natural hazard control and ecological restoration. *Science of The Total Environment*, 648, 1210-1218. doi:<https://doi.org/10.1016/j.scitotenv.2018.08.217>.
- Richrds, L. (1931). Capillary conduction of liquids through porous medium. *Physics*, 1, 318-333.
- Sapbamrer, R. (2018). Pesticide use, poisoning, and knowledge and unsafe occupational practices in Thailand. *New solutions: a journal of environmental and occupational health policy*, 28(2), 283-302. doi:<https://doi.org/10.1177/1048291118759311>.
- Schwarz, M., Cohen, D., & Or, D. (2010). Root-soil mechanical interactions during pullout and failure of root bundles. *Journal of Geophysical Research: Earth Surface*, 115(F4). doi:<https://doi.org/10.1029/2009jf001603>
- Schwarz, M., Giadrossich, F., & Cohen, D. (2013). Modeling root reinforcement using a root-failure Weibull survival function. *Hydrology & Earth System Sciences*, 17(11). doi:<https://doi.org/10.5194/hess-17-4367-2013>
- Shao, W., Ni, J., Leung, A. K., Su, Y., & Ng, C. W. W. (2017). Analysis of plant root-induced preferential flow and pore-water pressure variation by a dual-permeability model. *Canadian Geotechnical Journal*, 54(11), 1537-1552.

doi:<https://doi.org/10.1139/cgj-2016-0629>.

- Sidle, R. C., Ziegler, A. D., Negishi, J. N., Nik, A. R., Siew, R., & Turkelboom, F. (2005). Erosion processes in steep terrain—Truths, myths, and uncertainties related to forest management in Southeast Asia. *Forest Ecology and Management*, 224(1-2), 199-225. doi:<https://doi.org/10.1016/j.foreco.2005.12.019>
- Silver, W. L., & Miya, R. K. (2001). Global patterns in root decomposition: comparisons of climate and litter quality effects. *Oecologia*, 129(3), 407-419. doi:<https://doi.org/10.1007/s004420100740>.
- Soralump, S. (2010). Rainfall-triggered landslide: from research to mitigation practice in Thailand. *Geotechnical Engineering*, 41(1), 39.
- Stokes, A., Atger, C., Bengough, A. G., Fourcaud, T., & Sidle, R. C. (2009). Desirable plant root traits for protecting natural and engineered slopes against landslides. *Plant and soil*, 324(1-2), 1-30. doi:<https://doi.org/10.1007/s11104-009-0159-y>.
- Teerawattanasuk, C., Maneecharoen, J., Bergado, D. T., Voottipruex, P., & Le, G. L. (2014). Root strength measurements of vetiver and ruzi grasses. *Lowland Technology International*, 16(2), 71-80. doi:https://doi.org/10.14247/lti.16.2_71
- Thomas, R. E., & Pollen-Bankhead, N. (2010). Modeling root-reinforcement with a fiber-bundle model and Monte Carlo simulation. *Ecological Engineering*, 36(1), 47-61. doi:<https://doi.org/10.1016/j.ecoleng.2009.09.008>
- Tosi, M. (2007). Root tensile strength relationships and their slope stability implications of three shrub species in the Northern Apennines (Italy). *Geomorphology*, 87(4), 268-283. doi:<https://doi.org/10.1016/j.geomorph.2006.09.019>
- Truong, P., & Loch, R. (2004). *Vetiver system for erosion and sediment control*. Paper presented at the Proceeding of 13th international soil conservation organization conference.
- Truong, P., Tan, V. T., & Elise, P. (2008). *The vetiver system for slope stabilization, an Engineer's handbook*: The Vetiver Network International.
- USDA. (1951). Soil Textural Triangle. In.
- Vergani, C., Chiaradia, E., Bassanelli, C., & Bischetti, G. (2014). Root strength and density decay after felling in a Silver Fir-Norway Spruce stand in the Italian Alps. *Plant and soil*, 377(1), 63-81. doi:<https://doi.org/10.1007/s11104-013-1860-4>

- Vergani, C., Schwarz, M., Soldati, M., Corda, A., Giadrossich, F., Chiaradia, E. A., . . . Bassanelli, C. (2016). Root reinforcement dynamics in subalpine spruce forests following timber harvest: a case study in Canton Schwyz, Switzerland. *Catena*, *143*, 275-288. doi:<https://doi.org/10.1016/j.catena.2016.03.038>
- Vergani, C., Werlen, M., Conedera, M., Cohen, D., & Schwarz, M. (2017). Investigation of root reinforcement decay after a forest fire in a Scots pine (*Pinus sylvestris*) protection forest. *Forest Ecology and Management*, *400*, 339-352. doi:<https://doi.org/10.1016/j.foreco.2017.06.005>
- Voottipruex, P., Bergado, D., Mairaeng, W., Chucheepsakul, S., & Modmoltin, C. (2008). Soil reinforcement with combination roots system: A case study of vetiver grass and *Acacia Mangium* Willd. *Lowland Technology International*, *10*(2, Dec), 56-67.
- Waidmann, S., Sarkel, E., & Kleine-Vehn, J. (2020). Same same, but different: growth responses of primary and lateral roots. *Journal of Experimental Botany*, *71*(8), 2397-2411. doi:<https://doi.org/10.1093/jxb/eraa027>
- Waldron, L. (1977). The shear resistance of root-permeated homogeneous and stratified soil. *Soil Science Society of America Journal*, *41*(5), 843-849.
- Wang, G.-y., Huang, Y.-g., Li, R.-f., Chang, J.-m., & Fu, J.-l. (2020). Influence of vetiver root on strength of expansive soil-experimental study. *PLoS One*, *15*(12), e0244818. doi:<https://doi.org/10.1371/journal.pone.0244818>.
- Wasino, R., Likitlersuang, S., & Janjaroen, D. (2019). The performance of vetivers (*Chrysopogon zizanioides* and *Chrysopogon nemoralis*) on heavy metals phytoremediation. *International journal of phytoremediation*, *21*(7), 624-633. doi:<https://doi.org/10.1080/15226514.2018.1546275>
- Watson, A., Phillips, C., & Marden, M. (1999). Root strength, growth, and rates of decay: root reinforcement changes of two tree species and their contribution to slope stability. *Plant and soil*, *217*(1), 39-47. doi:https://doi.org/10.1007/978-94-017-3469-1_4
- Wongwichit, D., Siriwong, W., & Robson, M. G. (2012). Herbicide exposure to maize farmers in Northern Thailand: knowledge, attitude, and practices. *Journal of Medicine and Medical Sciences*, *3*(1), 034-038.

- Wood, D. M., Diambra, A., & Ibraim, E. (2016). Fibres and soils: a route towards modelling of root-soil systems. *Soils and Foundations*, 56(5), 765-778. doi:<https://doi.org/10.1016/j.sandf.2016.08.003>.
- Wu, T. H., McKinnell III, W. P., & Swanston, D. N. (1979). Strength of tree roots and landslides on Prince of Wales Island, Alaska. *Canadian Geotechnical Journal*, 16(1), 19-33. doi:<https://doi.org/10.1139/t79-003>
- Wu, Z., Leung, A., Boldrin, D., & Ganesan, S. (2021). Variability in root biomechanics of *Chrysopogon zizanioides* for soil eco-engineering solutions. *Science of The Total Environment*, 145943. doi:<https://doi.org/10.1016/j.scitotenv.2021.145943>.
- Yildiz, A., Graf, F., Rickli, C., & Springman, S. M. (2018). Determination of the shearing behaviour of root-permeated soils with a large-scale direct shear apparatus. *Catena*, 166, 98-113. doi:<https://doi.org/10.1016/j.catena.2018.03.022>.
- Zaimes, G. N., Tardio, G., Iakovoglou, V., Gimenez, M., Garcia-Rodriguez, J. L., & Sangalli, P. (2019). New tools and approaches to promote soil and water bioengineering in the Mediterranean. *Science of The Total Environment*, 693, 133677. doi:<https://doi.org/10.1016/j.scitotenv.2019.133677>.
- Zegeye, A. D., Langendoen, E. J., Tilahun, S. A., Mekuria, W., Poesen, J., & Steenhuis, T. S. (2018). Root reinforcement to soils provided by common Ethiopian highland plants for gully erosion control. *Ecohydrology*, 11(6), e1940. doi:<https://doi.org/10.1002/eco.1940>.
- Zhang, C.-B., Chen, L.-H., & Jiang, J. (2014). Why fine tree roots are stronger than thicker roots: The role of cellulose and lignin in relation to slope stability. *Geomorphology*, 206, 196-202. doi:<https://doi.org/10.1016/j.geomorph.2013.09.024>.
- Zhu, J., Wang, Y., Wang, Y., Mao, Z., & Langendoen, E. J. (2019). How does root biodegradation after plant felling change root reinforcement to soil? *Plant and soil*, 446(1), 211-227. doi:<https://doi.org/10.1007/s11104-019-04345-x>
- Ziemer, R. (1981). *Roots and the stability of forested slopes*. Paper presented at the In: Timothy RH Davies and Andrew J. Pearce (eds). Proceedings of the International Symposium on Erosion and Sediment Transport in Pacific Rim Steeplands, 1981 January 25-31, Christchurch, NZ Int. Assn. Hydrol. Sci. Pub. No. 132: 343-361.

Ziemer, R., & Swanston, D. (1977). Root strength changes after logging in southeast Alaska [*Tsuga heterophylla*, *Picea sitchensis*, logging damage]. *USDA Forest Service Research Note PNW (USA)*. no. 306.



APPENDIX

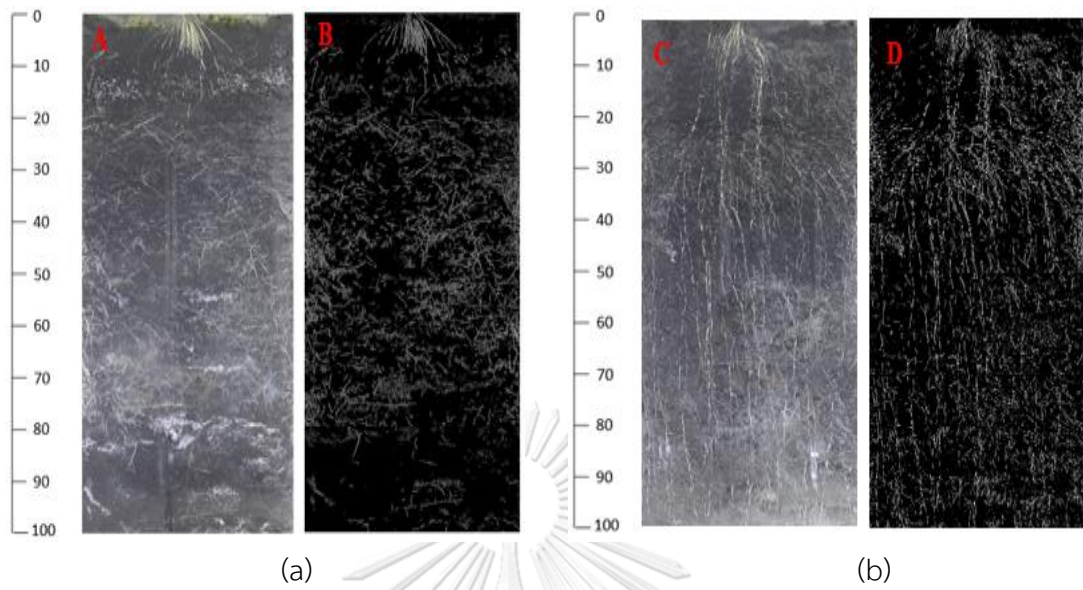


Fig A. 1. The RGB and grey scale image of root system of (a) *C. nemoralis* and (b) *C. zizanioides* species

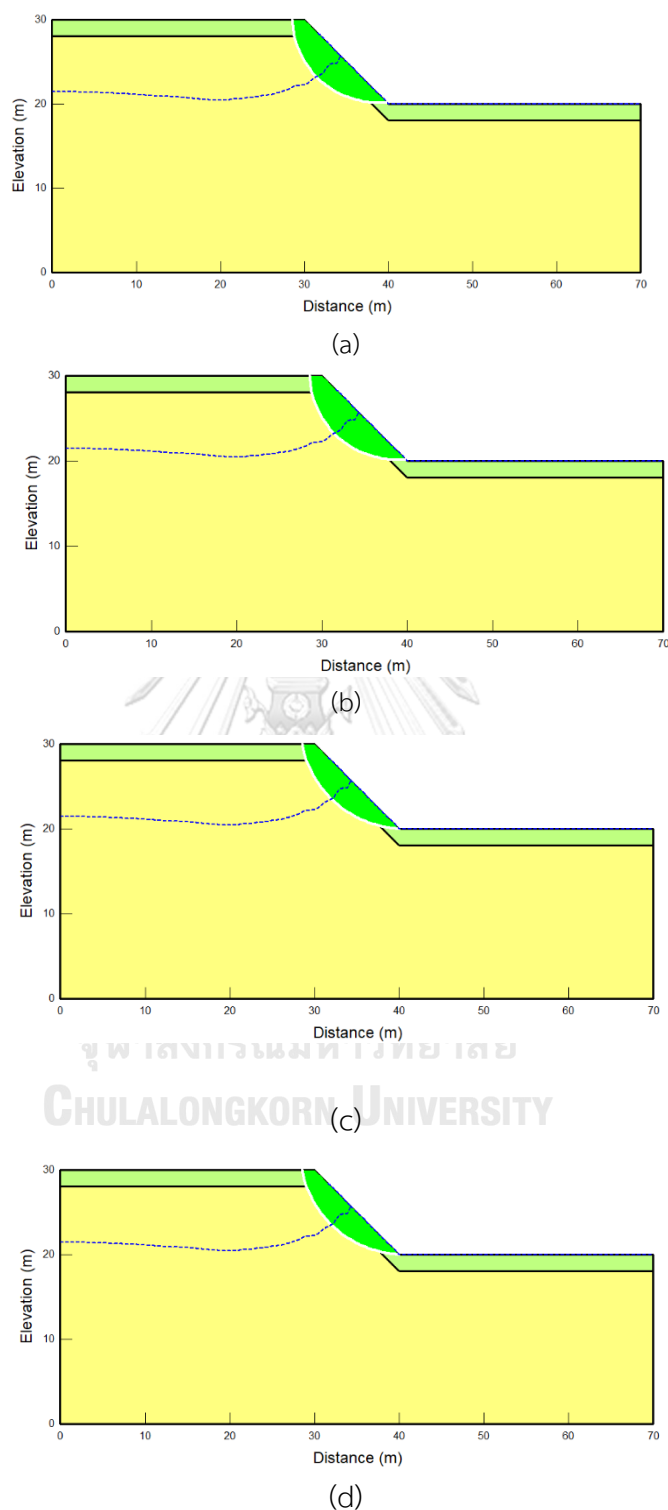


Fig A. 2. Failure surface after 24 hours of rainfall (the worst case) of slope reinforced by decomposed root of *C. nemoralis* species after (a) 7 days, (b) 28 days, (c) 56 days and (d) 112 days since herbicide application

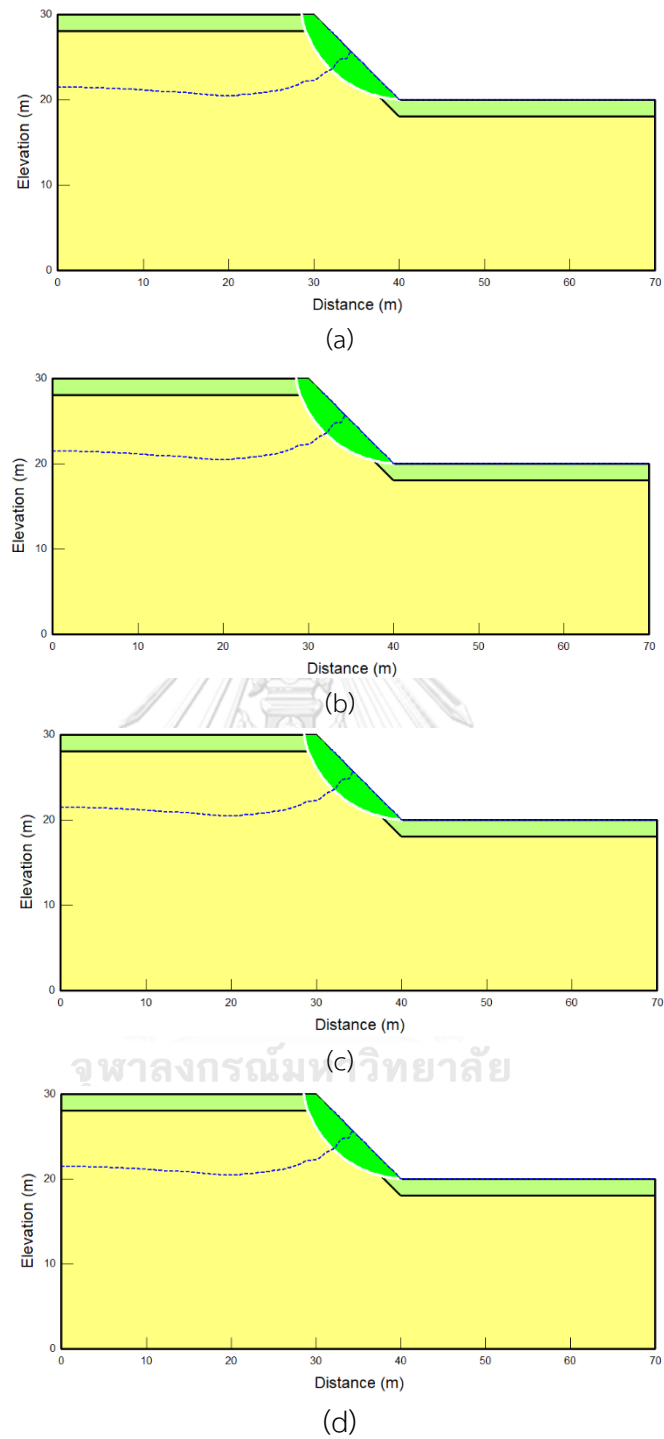


Fig A. 3. Failure surface after 24 hours of rainfall (the worst case) of slope reinforced by decomposed root of *C. zizanioides* species after (a) 7 days, (b) 28 days, (c) 56 days and (d) 112 days since herbicide application

VITA

NAME	Trung Nghia Phan
DATE OF BIRTH	30 September 1994
PLACE OF BIRTH	Ben Tre Province, Vietnam
INSTITUTIONS ATTENDED	Ho Chi Minh City University of Technology (HCMUT), Vietnam Chulalongkorn University (CU), Thailand
PUBLICATION	Root biomechanical properties of <i>Chrysopogon zizanioides</i> and <i>Chrysopogon nemoralis</i> for soil reinforcement and slope stabilisation. Influence of growth media on the biomechanical properties of the fibrous roots of two contrasting vetiver grass species. Characterization of Stationary and Nonstationary Random Fields with Different Copulas on Undrained Shear Strength of Soils: Probabilistic Analysis of Embankment Stability on Soft Ground. Influence of copula approaches on reliability analysis of slope stability using random adaptive finite element limit analysis.
AWARD RECEIVED	Best Paper Award